

Report No. UT-09.14

STRUCTURAL CONCRETE DESIGN AND CURING INVESTIGATION

Prepared For:

Utah Department of Transportation
Research Division

Submitted by:

Utah State University
Department of Civil and Environmental
Engineering

Authored by:

Paul Barr
Marv Halling
Shane Boone
Jeffery Bailey
Raul Toca
Franklan Angomas

July 30, 2009

DISCLAIMER:

The authors alone are responsible for the preparation and accuracy of the information, data, analysis, discussions, recommendations, and conclusions presented herein. The contents do not necessarily reflect the views, opinions, endorsements, or policies of the Utah Department of Transportation and the US Department of Transportation. The Utah Department of Transportation makes no representation or warranty of any kind, and assumes no liability therefore.

Technical Report Documentation Page

1. Project No. UT-09.14	2. Government Accession No.	3. Recipient's Catalog No.	
4. Title and Subtitle Structural Concrete Design and Curing Investigation		5. Report Date July 30, 2009	
		6. Performing Organization Code	
7. Author(s) Paul J. Barr, Marv Halling, Shane Boone, Jeffery Bailey, Raul Toca and Franklin Angomas		8. Performing Organization Report No. UTCM 09-14	
9. Performing Organization Name and Address Utah State University Department of Civil and Environmental Engineering Logan, UT 84322-4110		10. Work Unit No. (TRAIS) JOB/PROJ: 5H06029h	
		11. Contract or Grant No. 06-9057	
12. Sponsoring Agency Name and Address Utah Department of Transportation 4501 South 2700 West Salt Lake City, Utah 84114-8410		13. Type of Report and Period Covered Final Report 07/07 – 07/09	
		14. Sponsoring Agency Code PIC No. N/A	
15. Supplementary Notes Prepared in cooperation with the Utah Department of Transportation or U.S. Department of Transportation, Federal Highway Administration			
16. Abstract <p>Bridge deck replacement is costly. UDOT has had a mixed experience in the performance of these bridge decks. According to Linford and Reaveley (2004) 70 out of the 71 bridges that were investigated along I-15 had some type of cracking very within a few years after completion. However, some bridges decks built prior to the I-15 project have performed well with minimal problems.</p> <p>This research focused on the investigation of deck cracking as a function of the mix design and curing conditions. It is believed by some that reductions in the shrinkage of the concrete deck mix by as little as 20% would reduce the concrete bridge deck cracking significantly. For this research, this reduction in shrinkage was sought through adjustments in the mix design or better curing practices.</p>			
17. Key Word concrete, bridge design, bridge deck, mix design, durability, shrinkage, freeze thaw		18. Distribution Statement Public distribution	
19. Security Classif. (of this report) Unclassified	20. Security Classif. (of this page) Unclassified	21. No. of Pages 143	22. Price n/a

ACKNOWLEDGEMENTS

The authors express sincere appreciation to Daniel Hsiao of the Utah Department of Transportation research division for his guidance throughout the project. We would also like to thank Boyd Wheeler, Tim Biel and John Butterfield who were part of the technical activity committee.

EXECUTIVE SUMMARY

Bridge deck replacement is costly. UDOT has had a mixed experience in the performance of these bridge decks. According to Linford and Reaveley (2004) 70 out of the 71 bridges that were investigated along I-15 had some type of cracking very within a few years after completion. However, some bridges decks built prior to the I-15 project have performed well with minimal problems.

This research focused on the investigation of deck cracking as a function of the mix design and curing conditions. It is believed by some that reductions in the shrinkage of the concrete deck mix by as little as 20% would reduce the concrete bridge deck cracking significantly. For this research, this reduction in shrinkage was sought through adjustments in the mix design or better curing practices. Obtaining this objective involved a literature review of previous research, documenting the curing practices and performing material tests of three bridges within the state of Utah that represented different regions. The final goal of the research was to improve upon the deck concrete mix design and current curing practices for future bridge decks.

Investigation of UDOT's Current Curing and Mix Design Practices

As the initial focus of this research, three bridges that were scheduled to have a deck replacement were selected. The three bridges represented the three UDOT regions that have the largest volume of bridge work, namely Regions 1 through 3. The three bridges will be referred to as the Logan Canyon Bridge, the Sandy Bridge and the Provo Canyon Bridge. The Logan Canyon Bridge and the Sandy Bridge superstructures were designed as simply supported, reinforced concrete bridge decks supported on precast, prestressed concrete girders. The Provo Canyon Bridge superstructure was a multispan, reinforced concrete bridge deck supported on steel I-girders. For each of the bridges, concrete samples were taken at the time of casting and curing practices were observed.

Six material tests were performed on each of the deck samples. Each of the material tests were performed in accordance to ASTM standards. The six tests include: concrete compressive strength (ASTM C31 and C39), split tensile strength tests (ASTM C496), modulus of elasticity (ASTM 469), shrinkage (ASTM C157), freeze-thaw resistance (ASTM C666) and chloride-ion penetration (ASTM C1202). The select following results were obtained for the Logan Canyon Bridge, Sandy Bridge and Provo Canyon Bridge respectively:

- The 28-day tensile capacity of the three sampled bridges was 210 psi, 330 psi and 240 psi respectively. Each of these measured values were lower than the estimated calculated tensile capacity of $7.5 \cdot f_c^{.5}$. This result can be an indication of the cause of early bridge deck cracking. The 56-day tensile capacities were 240 psi, 430 psi and 310 psi respectively.
- After 116 days of testing, the average shrinkage strain for the three concrete mixes was 540×10^{-6} , 970×10^{-6} and 690×10^{-6} . These measured values are higher than the predicted

values in the AASHTO Specifications and may also be an indication of the cause of deck cracking.

- None of the three bridge decks that were observed after casting were most cured for the required 14 days. All decks were cover after casting and kept moist initially, but after as few as three days the decks were allowed to dry out. The moist cure for the Region 1 bridge was all but eliminated after 5 days. Similarly, the curing of the Region 2 and Region 3 bridges after 6 and 8 days respectively.

Investigation of Proposed Mix Designs

Three proposed mix designs were evaluated after discussions with UDOT. The mix designs include a reduction of the fly ash replacement content to 15%, an increase in the fly ash replacement content to 25% and a self consolidating high performance mix that was developed by Eagle Precast. The following are some of the highlighted research findings:

- After 118 days of testing, the average shrinkage strain for the three proposed concrete mixes was 440.2×10^{-6} , 567.2×10^{-6} and 572.2×10^{-6} for the Eagle precast mix, the 669 mix and the representative 668 mix. In comparison, each one of the proposed mix designs had a smaller shrinkage strain than the previously mentioned concrete mixes. This reduction in the shrinkage properties can be an advantageous property when trying to reduce deck cracking.
- Chloride Ion penetration test showed that the total charge passed through the Eagle precast concrete specimens was 230.8 coulombs, for the 669 Bridge deck concrete specimens was 681.2 coulombs and for the 668 Bridge deck concrete was 832.6 coulombs. Having all three concrete samples very low chloride ion permeability.

Recommendations

Based on the research findings, it is the recommendations of the researchers to implement the following:

- Enforce a more rigorous inspection program to ensure that bridge decks are properly cured for 14 days after casting. It is believed that the current UDOT requirements are adequate but are not be enforced.
- Consider reducing the fly ash replacement requirement from 20% to 15%. While the recommendation is based on a single bridge finding, the lower fly ash reduced the shrinkage strain and produced comparable freeze-thaw durability and chloride ion penetration results.
- Continue the implementation of precast deck panels. The self-consolidating concrete that was used at Eagle Precast to fabricate the tested deck panels showed material properties that were by far more advantageous than the current UDOT mix design. If the in service condition of these bridge decks can be adequately maintained, this alternative is advantageous both in terms of user costs as well as structural behavior.

Table of Contents

ACKNOWLEDGEMENTS	iv
EXECUTIVE SUMMARY	v
1.0 INTRODUCTION	1
2.4 DEVELOPMENT OF AN OPTIMAL HIGH-PERFORMANCE CONCRETE MIXTURE FOR TENNESSEE BRIDGE DECKS (Salem and Burdette 2004)	14
2.5 DEVELOPING HIGH-PERFORMANCE CONCRETE MIX FOR NEW YORK STATE BRIDGE DECKS (Streeter 1999)	16
2.6 COMPARISON OF VARIOUS STATE DECK MIX DESIGNS	20
3.0 INVESTIGATION OF EXISTING MIX DESIGN ON REPRESENTATIVE BRIDGES	23
3.1. The First Dam Bridge (At the mouth of Logan Canyon)	23
3.1.1. Deck Mix Design	25
3.2 Sandy Bridge	26
3.2.1 Deck Mix Design	27
3.3 Provo Canyon Bridge	29
4.1. Compressive Strength	33
4.1.1 Characteristics and Proportions of Materials	33
4.1.1.1 Water-cement ratio	33
4.1.1.2. Air Entrainment	34
4.1.1.3. Cement Type	35
4.1.1.5. Admixtures	36
4.1.2 Curing Conditions	36
4.1.2.1. Time	36
4.1.2.2 Humidity	37
4.1.3 Testing parameters	37
4.1.3.1 Specimen Parameters	37
4.1.3.2 Loading Conditions	38
4.2. Tensile Strength	42
4.3. Elastic Modulus of Elasticity	47
.....	52
4.4. Shrinkage	54
4.4.1. Cement Factor	54
4.4.2. Aggregate Properties	54
4.4.3. Water Content	54
4.4.4. Type of Cement	55
4.4.5 Curing and Storage	55
4.4.6 Size Effects	55
4.5 Freeze/Thaw	61
4.6 Chloride Ion Penetration	65
5.1 Compressive Strength	73
5.1.1 Selection and Proportioning of the Materials	73
5.1.1.1 Cement Type	73
5.1.1.2 Water/Cement Ratio	76
5.1.1.3 Aggregates	76
5.1.1.4 Admixtures	77
5.1.2 Curing Conditions	78

5.1.3 Test Specifications	79
5.2 Modulus of Elasticity	82
5.3 Shrinkage	87
5.4 Freeze & Thaw	89
5.5 Chloride Ion Penetration	94
6.0 CONCLUSION	99
6.1 Test Results for Current UDOT Mix Design	99
6.2 Summary of Current Curing Practices	101
6.3 Test Results for Variations to UDOT Mix Design	102
REFERENCES	103
APPENDIX A	104
APPENDIX B	107

Table of Figures

Figure 3-3 Deck Placement	28
Figure 3-4 Reinforcing Steel (Provo Canyon Bridge)	29
Figure 4-5 Vibration of Concrete Specimens, onsite at Sandy Bridge	38
Figure 4-6 Compressive Strength Test	39
Figure 4-7 Compressive Strength vs. Time Results for Three Bridges	42
Figure 4-8 Tensile Strength Test	43
Figure 4-9 Tensile Strength vs. Time Results for Three Bridges	47
Figure 4-10 Modulus of Elasticity Test	49
Figure 4-11 Modulus of Elasticity vs. Time Results for Three Bridges	52
Figure 4-12 Experimental and ACI Modulus of Elasticity Comparison (First Dam Bridge)	52
Figure 4-13 Experimental and ACI Modulus of Elasticity Comparison (Sandy Bridge)	53
Figure 4-14 Experimental and ACI Modulus of Elasticity Comparison (Provo Canyon Bridge)	53
Figure 4-15 Shrinkage Test	56
Figure 4-16 Strain vs. Time	61
Figure 4-17 Concrete Specimens placed in Freeze-Thaw Machine.....	62
Figure 4-18 Chloride-Ion Penetration Test	67

List of Tables

Table 2-1 Characteristics of the Various Mix Designs	7
Table 2-2 Proposed Mix Designs	9
Table 2-3 Proposed HPC Mix and Standard Mix Designs	11
Table 2-4 Deck Mix Proportions	12
Table 2-5 Concrete Deck Test Results	13
Table 2-6 Proportions of the Five Concrete Mixes.....	15
Table 2-7 Concrete Mixtures.....	18
Table 2-8 Proportions of Concrete Mixes.....	19
Table 2-9 Class HP Specification Requirements	20
Table 2.10 Comparison of Various State Mix Designs	21
Table 3-1 Bridge Deck Concrete Quantities (Logan Canyon Bridge).....	25
Table 3-2 Target and Actual Mix Design Weights.....	26
Table 3-3 Sandy Bridge Deck Mix Design.....	28
Table 3-4 Provo Canyon Deck Mix Design.....	30
Table 4-5 First Dam Bridge Compressive Strength Test Results	40
Table 4-6 Sandy Bridge Compressive Strength Test Results	40
Table 4-7 Provo Canyon Bridge Compressive Strength Test Results	41
Table 4-8 First Dam Bridge Tensile Strength Test Results	44
Table 4-9 Sandy Bridge Tensile Strength Test Results	45
Table 4-10 Provo Canyon Bridge Tensile Strength Test Results	46
Table 4-11 First Dam Bridge Modulus of Elasticity	50
Table 4-12 Sandy Bridge Modulus of Elasticity.....	50
Table 4-13 Provo Canyon Modulus of Elasticity	51
Table 4-14 Shrinkage Test Recordings.....	57
Table 4-15 Length Change Calculations	58
Table 4-16 Strain (10^{-6})	59
Table 5-17 Summary of Performed Tests.....	72
Table 5-18 Classification of Portland Cement (ASTM 150).....	75
Table 5-19 Mix Designs	78
Table 5-20 Eagle Precast Compressive Strength Test Results.....	80
Table 5-21 669 Bridge Deck Compressive Strength Test Results.....	80
Table 5-22 668 Bridge Deck Compressive Strength Test Results.....	81
Table 5-23 Eagle Precast Sample Modulus of Elasticity.....	84
Table 5-24 669 Bridge Deck Sample Modulus of Elasticity	84
Table 5-25 668 Bridge Deck Sample Modulus of Elasticity	84

Table 5-26 Strain of 669 Bridge Deck Samples in $\mu\epsilon$	88
Table 5-27 Strain of 668 Bridge Deck Samples in $\mu\epsilon$	88
Table 5-28 Fundamental Transverse Natural Frequencies	92
Table 5-29 Relative Dynamic Modulus of Elasticity.....	93
Table 5-30 Durability Factors.....	94
Table 5-31 Recorded Current Readings.....	97
Table 5-32 Charge Passed Through the Specimens (coulombs).....	97
Table 5-33 Chloride Ion Permeability Based on Charged Passed	97

Appendix B: Table of Figures

Figure B. 1 M.O.E First Dam Bridge Day 3	107
Figure B. 2 M.O.E First Dam Bridge Day 3	108
Figure B. 3 M.O.E First Dam Bridge Day 7	108
Figure B. 4 M.O.E First Dam Bridge Day 7	109
Figure B. 5 M.O.E First Dam Bridge Day 14	109
Figure B. 6 M.O.E First Dam Bridge Day 14	110
Figure B. 7 M.O.E First Dam Bridge Day 28	110
Figure B. 8 M.O.E First Dam Bridge Day 28	111
Figure B. 9 M.O.E First Dam Bridge Day 56	111
Figure B. 10 M.O.E First Dam Bridge Day 56	112
Figure B. 11 M.O.E Sandy Bridge Day 1	112
Figure B. 12 M.O.E Sandy Bridge Day 1	113
Figure B. 13 M.O.E Sandy Bridge Day 3	113
Figure B. 14 M.O.E Sandy Bridge Day 3	114
Figure B. 15 M.O.E Sandy Bridge Day 7	114
Figure B. 16 M.O.E Sandy Bridge Day 7	115
Figure B. 17 M.O.E Sandy Bridge Day 14	115
Figure B. 18 M.O.E Sandy Bridge Day 14	116
Figure B. 19 M.O.E Sandy Bridge Day 28	116
Figure B. 20 M.O.E Sandy Bridge Day 28	117
Figure B. 21 M.O.E Sandy Bridge Day 56	117
Figure B. 22 M.O.E Provo Canyon Bridge Day 1	118
Figure B. 23 M.O.E Provo Canyon Bridge Day 1	118
Figure B. 24 M.O.E Provo Canyon Bridge Day 3	119
Figure B. 25 M.O.E Provo Canyon Bridge Day 3	119
Figure B. 26 M.O.E Provo Canyon Bridge Day 7	120
Figure B. 27 M.O.E Provo Canyon Bridge Day 7	120
Figure B. 28 M.O.E Provo Canyon Bridge Day 14	121
Figure B. 29 M.O.E Provo Canyon Bridge Day 14	121
Figure B. 30 M.O.E Provo Canyon Bridge Day 28	122
Figure B. 31 M.O.E Provo Canyon Bridge Day 28	122
Figure B. 32 M.O.E Provo Canyon Bridge Day 56	123

1.0 INTRODUCTION

In the past, concrete design specifications focused primarily on the strength characteristics of concrete. However, mainly because of environmental mechanisms that affect its integrity, concrete is now designed also bearing in mind durability issues. Climatic conditions in the form of temperature fluctuations and ambient moisture, as well as exposure conditions in the form of aggressive chemicals, have become as serious a concern as mechanical conditions and initial cost. This, in part, because of the increasing repair and replacement costs of structures as a consequence of material failure. This has completely changed the notion about what “good” concrete means, and has promoted the engineering of concrete to a point in which its direct performance can be manipulated by its designer. Ultimately, the type of structure we are dealing with, the environmental conditions to which the structure will be exposed, and the types of loads it is expected to withstand will dictate the ultimate concrete design.

Bridge concrete decks are certainly not exempt to the aforementioned concerns, and those in Utah are especially not an exception. Utah is characterized by extreme and varying climatic conditions, which exposes bridges to freeze-thawing cycles and to constant application of deicing salts, resulting in some deterioration. This poses durability concerns that must be addressed. As a result, the concrete mixes are being designed to override this problem, and hence improve the life span of the bridges.

In an attempt to relate the field conditions to the experimental test results, standard laboratory tests are performed on the mixes. These estimate the concrete performance characteristics of the mix, which are in turn measured against a set of concrete performance criteria, the final objective being the estimation of the long-term durability and strength of the concrete decks.

This project presents 6 laboratory tests that will measure the strength and durability characteristics of the concrete decks of 3 Utah bridges, and therefore, the overall performance of the concrete mixes used to construct them. Chapter 2 provides a literature review of previous

research. In Chapters 3 and 4 the three bridges are described as well as the material test results. A summary of the conclusions are provided in Chapter 5.

2.0 LITERATURE REVIEW

The issue of developing concretes of sufficient strength and durability varies for locations possessing different climatic and material availability characteristics. This results in the development of different design mixes, according to the location we are in, giving us a chance to learn from previous experiences. This is why, in this section, we will take a look at the tested strength and durability of concrete mixes from other states.

2.1 INFLUENCE OF FLY ASH ON THE SULFATE RESISTANCE OF CONCRETE (Tikalsky and Carrasquillo 1992)

The sulfate resistance of concrete containing fly ash was investigated in a laboratory study in which concrete specimens were continuously soaked in a 10 percent sodium sulfate solution for 18 months. Eighteen fly ashes and two other pozzolans were used as a partial replacement for Type II Portland cement in a standard 4000 Psi mix design. In addition to the effects of fly ash composition on the sulfate resistance of concrete, the study investigated the effects of the level of fly ash replacement, slump, air content, cement type, and moist curing time. Failure of the concrete was determined by an average expansion of four specimens greater than 0.5 percent of the specimen's original length.

Sulfate attack occurs when the cementitious matrix of the paste in concrete is corroded through the formation of the crystalline compounds ettringite ($C_6AS_3H_{32}$) and gypsum (CSH_2). Tricalcium Aluminate (C_3A) is the reactive aluminate compound that contributes to the expansive reactions associated with ettringite formation. This is the reason why among the principal methods used to prevent sulfate attack are the replacement of Type I Portland cement (possessing between 8 and 12 percent of tricalcium aluminate) with a Type II (less than 8 percent) or V (less than 5 percent) Portland Cement. Another method is to introduce a pozzolan such as fly ash into the concrete mixture.

Fly ash has a positive effect on long-term durability of concrete exposed to sulfate environments by contributing chemically and physically to the properties of concrete, by the means of two mechanisms: the “dilution effect” and the “pozzolanic effect”. The “dilution effect” is simply the reduction of C_3A by replacing a portion of the Portland cement with fly ash, causing a decrease in the total C_3A by as much as 30 percent by weight of the cementitious material. The “pozzolanic effect” is the pozzolanic reaction between fly ash and calcium hydroxide, a byproduct of Portland cement hydration that results in the formation of a refined calcium silicate hydrate binder matrix. As a result of this, concrete becomes less permeable and the excess calcium is consumed, becoming unavailable to the formation of ettringite or gypsum compounds.

This research study showed that there is a relation between the comparison of fly ash and the sulfate resistance of concrete. What separates a fly ash that decreases the sulfate resistance of concrete to one that increases it, are two factors: the calcium oxide content of the fly ash and the calcium aluminate composition of the amorphous phase of the fly ash. Minor changes in the physical properties of the concrete due to the addition of fly ash provided no significant additional sulfate resistance to the concrete.

The testing procedure at hand was one whose purpose was to evaluate the performance of a particular concrete mixture as a function of the performance of a known control mixture. In this study, the control mixture was a type II Portland cement (6.0 percent C_3A) with a 28 day compressive strength in excess of 4050 psi. These properties are considered suitable for moderate sulfate exposure conditions and represent the most common solution to potential sulfate attack in concrete highway structures.

The effect of fly ash content on the sulfate resistance of concrete was studied using nine fly ashes at a 25, 35, and 45 percent replacement for Type II Portland cement. Low-calcium ASTM Class F fly ashes are shown to have excellent sulfate resistance in both expansion and cracking, whereas high-calcium ASTM Class C fly ashes showed increased susceptibility to cracking and expansion with an increase in fly ash content.

Of the major chemical compounds found in fly ash, only the calcium oxide content provided a positive indication of the sulfate resistance of concrete containing fly ash.

The mineralogical composition of fly ashes that resulted in concrete with increased sulfate resistance was restricted to a few inert minerals such as mullite, quartz, ferrite spinel, and some evidence of hematite. Fly ashes which contributed to a decrease in sulfate resistance of concrete typically contained lesser quantities of these inert minerals and significant amounts of reactive crystalline phases such as anhydrite, lime, periclase, sodalites, and tricalcium aluminate.

Minor physical changes in the paste structure due to reduced water-cement ratio, improved curing conditions, and increased air content did not substantially increase the sulfate resistance of concrete containing fly ash.

As a result of all this, this research program showed that compositional effects of fly ash dominate over physical effects of fly ash on the sulfate resistance of concrete.

2.2 DEVELOPMENT OF OPTIMAL CONCRETE MIX DESIGNS FOR BRIDGE DECKS (Xi et al. 2001)

This study was conducted because Field inspections and a recent study report ("Cracking in Bridge Decks: Causes and Mitigation", CDOT Report 99-8) showed that the cracking problem of bridge decks in Colorado has not been completely solved, and there is a need to further improve the concrete mix designs currently used in Colorado for concrete bridge decks.

Four different tests were selected for characterizing the mechanical and durability properties of concrete;

- **Compressive strength tests.** These were performed at 3 days, 7 days, 28 days, and 56 days. Two 4" x 8" cylinders were used for each test day.

- **Rapid chloride permeability test (ASTM C 1202, AASHTO T277 “Electrical Indication of Concrete’s Ability to Resist Chloride Ion Penetration”).** These were performed at 28 days and 56 days. 4” x 2” cylinders were used for each of the test days.

- **Crack resistance test (or ring test, AASHTO PP34-98 “Standard Practice for Estimating the Crack Tendency of Concrete”).** Two concrete rings of 6” in height with an outer diameter of 18” and inner diameter of 12” were made for each concrete mix. After one day of curing under room temperature, the molds were removed and the concrete rings were placed in the lab (temperature = 72°F and relative humidity = 35%) until the first crack was observed. The cracks were monitored by unaided eye as well as by a zoom.

- **Drying shrinkage test (ASTM C-157 “Standard Test Method for Length Change of Hardened Hydraulic-cement Mortar and Concrete”).** Two concrete prisms of 3” x 3” x 12” were made and after 7 days of curing in a fog room at 68°F, 100% Relative Humidity), the prisms were removed and placed in the lab (temperature 72°F and relative humidity 35%). Shortening of the prisms due to drying shrinkage was then measured. This test was only performed for some concrete mixes.

The project consisted of two phases. There were 18 mix designs formulated in the Phase I study in order to single out some good mix designs satisfying the selected strength and durability requirements. The second phase of the study consisted of a “fine-tuning” of the mixes selected from the Phase I and finalization of the mix designs to be used in the field.

The recommended concrete mixes were characterized by good workability, proper air content, adequate strength, low chloride permeability, and low drying shrinkage potential.

In the Phase I study, the following parameters were selected for the concrete mixes:

- **Slump** = 3 to 4 inches
- **Maximum size of aggregate** = 3/4 inch
- **Compressive strength** = 4500 psi
- **Air content** = 6.5 %

The cement content (WC), water-cement ratio (w/c) and fly ash content (Wfa) were selected as experimental parameters:

Three w/c were tested: 0.37, 0.41, and 0.45.

Three W_C were tested: 450, 485, and 515 lb/yd³.

Two different Wfa were used in the project: 20% and 25% of the cement content.

The objective of the Phase I study was to identify the optimal concrete mix design in terms of moderate compressive strength, low chloride permeability, and high crack resistance.

Conclusions that can be made based on the results of the Phase I of our study were the following:

1. The ratio of water to cementitious materials has the most significant effect on rapid chloride permeability. Permeability was found to be almost proportional to the w/(c+m) ratios at 28d or 56d.
2. The increase of fly ash content from 20% to 25% of the cement content does not significantly affect the permeability.
3. Permeability is not correlated to slump, because the apparent correlation between the two is due to the water/cementitious ratio.
4. Permeability is correlated to the compressive strength. When the permeability is high, the strength is low. However, the permeability is not significantly reduced by the increased strength caused by the increase in cement content from 450 lb/yd³ to 515 lb/yd³.
5. The effect of air content on the compressive strength depends on the level of air entrainment. When the air content is below about 6.3%, the strength is not significantly affected. When the air content is above 6.3%, the strength is low.

6. With an increase of the cement content and thus the strength of concrete, the time for the first cracking to occur is shortened.
7. With the addition of silica fume in 4%, Class F fly ash in 20% of the cement content, and water/cementitious ratio of 0.41 or lower, the 56d chloride permeability can be effectively reduced to below 2,000 Coulombs.

Based on the test results and conclusions derived from the Phase I of the study, the ranges of the concrete design parameters were:

- cement content about 450 to 485 lb/yd³
- w/m about 0.37 to 0.41
- fly ash addition about 20% to 25%
- silica fume 4%

Those mixes having high compressive strengths, low chloride permeability and high crack resistance were selected as the optimal mix designs for the phase II study. These are shown below.

Table 2-1 Characteristics of the Various Mix Designs

	1	2	3	4	5	6	7	8	9	10	11	12	13	14	15	16	17	18
Permeability	▪	▪		▪			▪	▪		▪	▪		▪	▪		▪		
Strength				▪			▪	▪	▪	▪	▪	▪	▪	▪	▪	▪	▪	▪
Cracking	▪	▪	▪	▪	▪	▪	▪	▪										
Selections				▪			▪	▪										

In the phase II study, important influential parameters on concrete properties that had not been examined in Phase I were investigated, including the type of fly ash, curing time, and aggregate gradation.

In addition to the selected mixes from Phase I, more mix designs were incorporated into the Phase II of the study, including two mix designs from Lafarge (the material supplier for the construction project of I-225 & Parker Rd.), and two mixes from CDOT - Class DT, and Class SF.

The conclusions of the phase II portion of the study were the following:

1. Class F fly ash is better than Class C fly ash in improving both the chloride permeability and cracking resistance of concrete.
2. A proper increase in the content of coarse aggregate can improve the permeability, the cracking resistance, and 28-day strength.
3. Increases in the proportion of an intermediate size of gravel did not improve the cracking resistance of concrete, nor the permeability. A larger size and higher proportion of gravel should be used.
4. Longer curing time (12 days) seems to have an unfavorable effect on cracking resistance of concrete, but this needs to be confirmed by a more detailed experimental study.

Considering the overall performance of the mixes during phases I and II, the ranges for the concrete design parameters were determined.

1. Cement content from 465 to 485 lb/yd³;
2. Water/cementitious ratio from 0.37 to 0.41
3. 4% silica fume
4. Class F fly ash from 20% to 25%
5. Curing time of seven days

Based on this, two mix designs are recommended for use in the summer and in the winter, respectively.

In the summer season, Mix II4-4 is preferable. It has a low cement content of 465 lb/yd³ and a high fly ash content of 25 wt. % of cement. The water/cementitious ratio can be slightly increased if necessary to improve workability.

In the winter season, Mix II8 is preferable. It has higher cement content and lower fly ash content than Mix II4-4. In Mix II8, gravel content could be increased to 1780 lb/yd³ and w/c could be slightly reduced. In both mixes, Class F fly ash should be used.

The description of both mixes is shown below.

Table 2-2 Proposed Mix Designs

	Mix II4-4	Mix II8
Cement Content (lb/yd³)	465	485
Fly Ash (lb/yd³) (wt.% of concrete)	F116 (25)	F97 (20)
Silica Fume (lb/yd³) (wt.% of concrete)	18.6 (4)	19.4 (4)
W/(C+M)	0.37	0.41
Sand (lb/yd³)	1231	1398
Gravel (lb/yd³)	1780	1595
HR WR (oz/100 lb. cement)	11.91	11.14
Micro Air (oz/100 lb. cement)	0.54	1.6
Retarder (oz/100 lb. cement)	2.16	3.2
Slump (in.)	6	5.5
Air Content (%)	5.5	8.5
Permeability at 28 days (Coulomb)	3290 2747	2941 3161
Permeability at 56 days (Coulomb)	2528 2005	1393 1609
First Cracking (days)	18	14
	3 Days	3487 2512

Compressive Strength (Psi)	7 Days	4363	3695
	28 Days	5645	4657
	56 Days	5661	5414

2.3 APPLICATION OF HIGH PERFORMANCE CONCRETE (HPC) IN A NEW HAMPSHIRE BRIDGE (Waszczuk and Juliano 1999)

The University of New Hampshire (UNH) performed field and laboratory testing on three different mix proportions as part of this research project. The requirements for the three mixes were: design strength of 41 Mpa; 28-day cylinder strength of 50 Mpa (7200 psi); and a maximum chloride ion permeability of 1000 coulombs at 56 days. Test slabs representing each mix were installed at a UNH bridge deck testing facility, and subjected to heavy truck traffic for a period of six months during the winter season. The mix with the best performance under these conditions was selected for use in future bridge decks.

Once the mix design was approved by NHDOT and prior to placing the deck concrete, a 3.8 m³ (5 yd³) trial placement simulating the actual finishing and curing conditions was carried out. An additional plasticizer was added in order to achieve the desired slump for proper workability. The criteria for the HPC deck concrete mix as well as the criteria for New Hampshire's standard class AA deck concrete mix, are listed below.

Table 2-3 Proposed HPC Mix and Standard Mix Designs

	HPC mix	Standard mix
Cement	Type II	Type II or IP
Silica fume	7.50%	-
w/c	0.38 (max)	0.38 (max)
Air content	6 to 9 percent	5 to 8 percent
28-day cylinder strength, f'_{CR}	50 Mpa (7200 psi)	30 Mpa (4000 psi)
Chloride ion permeability	1000 coulombs (max)	-
Corrosion inhibitor	20 L/m ³ (4 gal/yd ³)	-
Curing procedure	4 day wet cure w/ cotton mats	3 day wet burlap cure

As can be seen, this HPC mix deviates from the New Hampshire's standard class AA mix by requiring 7.5 percent of the total cementitious content to be silica fume. Also, a higher 28-day cylinder strength of 50 Mpa and a limit on the chloride ion permeability of 1000 Coulombs or less was specified. A corrosion inhibitor was necessary due to deviations from NHDOT's standard practice of protecting concrete decks with barrier membrane and an asphalt overlay.

Some difficulty maintaining the required air content and a consistent slump was encountered during the deck placement. A higher dosage of superplasticizer than was used in the trial

placement needed to be added on site in order to achieve the desired workability in the concrete. The deck mix proportions are shown below.

Table 2-4 Deck Mix Proportions

Cement	Ciment Quebec- SF (approx. 8 percent silica fume)	300 kg (660 lb)
Fine aggregate	Sand	540 kg (1190 lb)
Coarse aggregate	No. 67 Stone (19 mm)	823 kg (1815 lb)
Water	114 L (30 gal)	115 kg (253 lb)
Air entrainment	Daravair - 1000	150 mL (5 oz)
Water reducer	WRDA w/ hycol	600 mL (20 oz)
Superplasticizer	Daracem - 100	4.7 L (158 oz)
Corrosion inhibitor	DCI-S	15 L (4 gal)
w/c		0.384

The interaction of the corrosion inhibitor with the other admixtures during the travel time to the site may have contributed to the inconsistent air content and slump results. The modulus of elasticity was lower than expected. Regardless, the average 28-day cylinder strength was will in excess of 50 Mpa (7200 psi) requirement and the results from the 56-day rapid chloride permeability tests performed on deck cores were astounding. Even though the air content of the concrete fell below the specification requirement, the freeze-thaw durability tests performed revealed excellent results after 300 cycles. These results are shown on the following tab

Table 2-5 Concrete Deck Test Results

Test	Target	Results	Test Method
Slump	125 to 180 mm.	75 to 125 mm.	AASHTO T119
	(5 to 7 in.)	(3 to 5 in.)	
Unit weight	-	65.3 to 66.7 kg.	AASHTO
		(144 to 147 lb.)	T121
Air content	6 to 9 percent	4.0 to 5.8 percent	AASHTO T152
w/c	0.38	0.39	-
28-day cylinder	50 Mpa	56.3 to 66.3 Mpa	AASHTO T22
	(7200 psi)	(8163 to 9614 psi)	
Modulus of Elasticity, E	30.6 Gpa	29.0 to 30.0 Gpa	ASTM C 469
	(4.4 x 10 ⁶ psi)	(4.2 to 4.3 x 10 ⁶ psi)	
Chloride ion Permeability	1000	609 to 896	AASHTO T277
	Coulombs	Coulombs	
Freeze-thaw Durability	80 percent	96 to 99 percent	AASHTO T161
Scaling	-	0 to 1	ASTM C 672

Based on these results, the concrete deck will be highly resistant to chloride intrusion and freeze-thaw deterioration and should provide superior long-term service.

2.4 DEVELOPMENT OF AN OPTIMAL HIGH-PERFORMANCE CONCRETE MIXTURE FOR TENNESSEE BRIDGE DECKS (Salem and Burdette 2004)

This paper describes a laboratory investigation of the development of an optimal high-performance concrete (HPC) mixture for Tennessee cast-in place bridge decks. Five types of concrete mixtures were developed by varying the quantity of fly ash, slag, and silica fume, while keeping the water/cementitious ratio constant. The Tennessee Department of Transportation Class D concrete was used as the control mix. The following parameters relevant to bridge deck performance were evaluated:

- Compressive strength, ASTM C 39, at 7 and 28 days.
- Drying shrinkage, ASTM C 157, at 1, 2, 3, 4, 5, 6, 7, 14, 21, 28, 56, and 112 days, after 7 days of water curing.
- Freeze-thaw durability, ASTM C 666 Procedure A, using 76 x 102 x 406 mm. specimens.
- Chloride ion permeability, ASTM C 1202 and AASHTO T 277, 60 volts DC applied at 56 days, and total charge passed during a 6 hour period.

Type I Portland cement, Class C fly ash, ground-granulated blast-furnace slag, and silica fume were all used. In addition to this, two chemical admixtures were also used: high-range water-reducing agent (HRWRA) conforming to ASTM C 494 type A and F and air-entraining agent (AEA) conforming to ASTM C 260. The aggregates used were limestone #57, limestone #7 and natural sand.

The Class D mix (the control mix) did not contain mineral admixtures as cement replacement and its aggregate gradation is typically of a gap-graded aggregate using limestone as the coarse aggregate and natural sand as its fine aggregate. The other four modified mixes are a result of

lowering the cementitious content of the Class D mix by 10%, modifying the gap-gradation to a more densely graded aggregate and the incorporation of fly ash, slag, and silica fume as cement replacements. Mix FA refers to a 25 percent replacement of cement by fly ash; Mix FASF refers to a 20 percent replacement of cement by fly ash and a 5 percent replacement of cement by silica fume. Mix S refers to a 35 percent replacement of cement by slag; Mix SSF refers to a 35 percent replacement of cement by slag and a 5 percent replacement of cement by silica fume. The five mixes are shown in the chart below.

Table 2-6 Proportions of the Five Concrete Mixes

Materials (kg/m³)	Class D	FA	FASF	S	SSF
Cement	368	254	254	220	203
Slag	-	-	-	118	118
Silica Fume	-	-	17	-	17
Fly Ash	-	85	68	-	-
Limestone (#57)	1157	671	671	678	676
Limestone (#7)	-	488	488	493	491
Sand	682	715	714	722	720
Water	147	135	135	135	135
w/cm	0.4	0.4	0.4	0.4	0.4

Results showed that in terms of the 28-day compressive strength of the concrete mixes, all four displayed higher values than the Class D mix, despite the fact that the cementitious content of all four mixes was lower. The reasons for this are the following: (1) since the w/cm ratio was maintained constant, lowering the cementitious material also meant lowering the mixing water content. Lower cement and water content means less cement paste and consequently a higher aggregate content per unit volume; (2) Since the aggregate particles are closer together (because

of less cement paste) there is greater interlocking between the aggregate particles resulting in higher strength; (3) Less cement and water content leads to less bleeding, and thus a higher compressive strength.

The freezing and thawing durability of all mixes, was clearly acceptable. The drying shrinkage, one of the main reasons of cracking in bridge decks, was lower for all of the four mixes with respect to the control mix, which is attributed to the lower cementitious content of the mix. Finally, the chloride ion permeability values were also lower for all of the four mixes, and this is also due to a lower cement paste, which produces less porous material in a given volume of concrete.

TDOT specifications has limiting values that require at least a minimum cementitious material and a maximum w/cm ratio for Class D bridge decks, all to ensure adequate workability, strength, and durability. However, after seeing the results for all four alternative mixes, it can be concluded that this may not be the most effective approach for ensuring the durability of the bridge decks. It can be said that the performance of the bridge decks could be enhanced by substituting the control mix for one of the alternative mixes. Furthermore, it can be concluded by the results that, in general: the cementitious material of a mix can be lowered by using more densely graded aggregates, and that this reduction (while always keeping the w/cm ratio constant) is beneficial to the compressive strength, drying shrinkage and chloride ion permeability of the mix. By replacing the Class D mix to a more densely graded mix, and using 25 percent fly ash as a cement replacement would reduce the drying shrinkage by 25 percent and the chloride ion permeability by 75 percent, making mix FA the most feasible replacement for the Tennessee Class D concrete mix.

2.5 DEVELOPING HIGH-PERFORMANCE CONCRETE MIX FOR NEW YORK STATE BRIDGE DECKS (Streeter 1999)

This paper describes the implementation of a more durable high-performance concrete mixture for bridge decks. Class HP concrete is a modification of New York State's standard Class H

concrete, incorporating two pozzolan substitutions for cement – 20 percent Class F fly ash and 6 percent microsilica.

The most common failure mechanism for New York State bridge decks has been concrete spalling resulting from corrosion of the reinforcement. This is why a concrete mixture that reduced permeability and the potential for cracking was sought.

NYSDOT Class E concrete is the standard bridge deck concrete, with Class H concrete an allowable replacement in pumping placement applications. The latter was the one used as the control mixture. The mixtures tested were: Class E, Class H (Control), Modified Class E, Class HP (Modified Class H), a mixture with improved aggregate-packing characteristics, and a modified NYSDOT microsilica concrete mixture. The concrete mixtures and their proportions are shown below.

Table 2-7 Concrete Mixtures

Mixture Name	Cement kg/m³	Fine aggregate (% total agg.)	Water- Cement Ratio	Air Content %	Slump Range (mm)	Description
NYSDOT Class E	359	35.80	0.44	5-8	75-100	Standard mixture for structural slabs and approach slabs
NYSDOT Class H (Control)	400	40.00	0.42	5-8	75-100	Standard mixture for pumping applications
NYSDOT Class HP (Modified Class H)	296.5	40.00	0.40	5-8	75-100	Trial Mixture
Modified Class E	359	35.80	1.40	5-8	75-100	Trial Mixture
Improved Agg. Packing	278.7	44.50	2.40	5-8	75-100	Trial Mixture
Modified Microsilica	343.4	39.40	3.40	5-8	125-200	Trial Mixture

Table 2-8 Proportions of Concrete Mixes

Material	NYSDOT Class H	NYSDOT Class HP	Modified Class E	Improved Agg. Packing	Modified Microsilica
Water (kg/m³)	167.2	160.1	153.6	149.4	153
Cement (kg/m³)	400.3	296.5	289.4	278.7	343.4
Fine Aggregate (kg/m³)	690.8	680.2	622.7	786.9	664.2
Coarse Aggregate (kg/m³)	1,038.90	1,038.30	1134.4	980.8	1022.9
Class F Fly Ash (kg/m³)	0	80.1	71.2	71.2	46.3
Microsilica (kg/m³)	0	23.7	23.7	23.7	35.6
Air-Entraining Agent (mL/m³)	261	456	437	425	696
Set-Retarding Water Reducer (mL/m³)	1,305	1,305	1,235	1,218	3,608

Five concrete properties were tested: (1) handling and workability, (2) concrete strength gain, (3) permeability, (4) resistance to cracking, and (5) scaling.

Based on the laboratory results the most suitable mixture was selected and then used in a field trial application to further determine the mixture's performance.

The test results showed that all mixes performed better than the control mixture. The rate of strength gain was such that at 14 days each mixture had developed sufficient strength to conform to the current specifications (which permit early loading), chloride-permeability testing showed a reduction for all mixtures of between 70 and 80 percent over the control mixture, cracking-potential testing of the trial mixtures under severe curing conditions in the laboratory resulted in less cracking than Class H exhibits under normal field conditions, and none of the trial mixtures showed any significant signs of scaling. The mixture with the most suitable characteristics was the modified Class H concrete, designated Class HP for high performance.

Results from the field tests showed that Class HP concrete was very user friendly in that it was easily pumped, placed, and finished. Class HP specification requirements are listed below.

Table 2-9 Class HP Specification Requirements

Property	Quantity
Cement content (kg/m³)	300
Fly ash content (kg/m³)	80
Microsilica content (kg/m³)	25
Sand percent total aggregate	40
Water-to-total cementitious content of 405 kg/m³	0.40 maximum
Desired air content (%)	6.5
Allowable air content (%)	5.0-8.0
Desired Slump (mm)	89
Allowable Slump (mm)	75-100
Coarse aggregate gradation	100% passing 37.5 mm. sieve 93-100% passing 25.0 mm. sieve 27-58% passing 12.5 mm. sieve 0-8% passing 6.3 mm. sieve

2.6 COMPARISON OF VARIOUS STATE DECK MIX DESIGNS

Various state DOT mix designs were obtained and compared with the UDOT mix design. Table 2-10 lists the mix design properties of each of these states.

Table 2.10 Comparison of Various State Mix Designs

States	Cement (lb/yd ³)	Course aggregate (lb/yd ³)	Fine aggregate (lb/yd ³)	Fly Ash (lb/yd ³)	Silica fume (lb/yd ³)	w/c ratio	28-d strength (psi)
Arizona	564-658						4000
Colorado	580-640					.38-.42	4500 at 56 days
Delaware	458	1846	1051	247		0.4	
Florida	764	2234	1345	191		0.37	5500
Georgia	734	1918	990			0.38	2245 psi at 6d
Idaho	550			138		0.42	5600
Illinois	630				70	0.31	6950 at 14d
Iowa	457	1669	1393	114		0.50	
Kansas	602	1474	1469			0.44	6680
Kentucky	620.3	40%	36%			0.42	4351.1
Louisiana	306	1900	1176			0.39	5680
Minnesota	836	1385	1374			0.32	
Missouri	729	1785	1078			0.37	8590
Montana	657.4					0.40	4931.3
Nebraska	750			75		0.31	8000 at 56d
New Hampshire	583.2		1775			0.45	
New Mexico	687	1400	1290	172		0.32	7873
New York	505			149	42	0.4	
Oklahoma	559	1710	1272	133		0.4	
Oregon	440	1340	1370		30	0.42	
South Carolina	611	65% to 35% ratio				0.4	4000
South Dakota	585-715	55% minimum				0.45	4000 min
Tennessee	375	2041	1258	125		0.4	4000 min
Texas	382-610			88-131		0.31-0.43	4000
Virginia	560			140		0.45	5000
Washington	660			75		0.39	4000 at 56d
West Virginia	560					0.47	4000
Wisconsin	660	2960			50	0.4	
Wyoming	611					0.45	3750
Utah	520			20%(sub)		0.45	4000
minimum value	306	1340	0.36	75	30	0.31	3750

maximum value	836	2234	1775	247	70	0.50	8590
--------------------------	------------	-------------	-------------	------------	-----------	-------------	-------------

In general, the UDOT mix design strength specifications are near the average of the sampled DOTs. The water-to-cement ratio of 0.40 is also near the typical value. The biggest difference between UDOTs mix design and other states values is in the quantity of fly ash. UDOTs 20% fly ash replacement is larger than most DOTs although not the highest.

3.0 INVESTIGATION OF EXISTING MIX DESIGN ON REPRESENTATIVE BRIDGES

This chapter provides a description of the design characteristics of each of the three tested bridges. Furthermore, the mix design used for each is detailed.

3.1. The First Dam Bridge (At the mouth of Logan Canyon)

The bridge deck on which the testing was performed is located at the mouth of Logan Canyon and allows passage of the Logan River. The bridge deck was placed in two different phases on top of seven pre-cast pre-stressed concrete girders. The formwork was to be removed after the deck was placed.

The total quantity of concrete used in construction of the bridge deck was 370.9 cubic yards. The approach slab on both ends of the bridge is 25 feet in length with a cold joint used to connect the approach slab to the deck itself. The bridge deck is 107' 3/8" in length running east to west, the width of the bridge is 59' 2" running north to south. The deck was designed as an 8 1/2" thick reinforced concrete slab. The deck was placed in two phases due to the staged construction of the bridge; the first phase was 20' 11" in width and the second phase was 38' 3" in width. The bridge deck has a north to south slope and going from north to south slope of 3.48%. The deck reinforcing steel was to have a bottom clearance of one inch and clearance down from the top of the slab of 2 1/2 inches. Even though the girders were pre-cast, reinforcing steel extending from the top of the girders was provided to help connect the slab to the girders as well as the abutment diaphragms. Steel was also provided to connect the deck slab to the barricades.

Ralph L. Wadsworth Construction was onsite to place the concrete at the time the samples were taken. The first section of bridge deck was placed on the 26th of September, 2005. Before the deck was actually cast, the form work and reinforcing steel was secured and inspected by UDOT. This inspection is shown in Figure 3.1.



Figure 3-1 Reinforcing Steel and Form Work (Logan Canyon Bridge)

Steel was inspected for size and location of placement in the bridge deck, along with making sure the proper amount of reinforcing steel was used. Form work was inspected for location and debris. It is required that no debris be allowed inside of the form work.

The concrete was to be placed by bucket and crane where the deck could not be reached by a concrete truck. Upon arrival of the first concrete truck UDOT along with Utah State researchers took representative samples of the concrete for testing. UDOT performed on-site testing for slump, air content, and temperature. Using a vibratory table, USU researchers were able to cast both 4 x 8 inch and 6 x 12 inch cylinders for the material testing. The tested concrete was only sampled from the concrete placed during Phase 1. After casting, the concrete cylinders were allowed to cure in a temperature controlled wet room at Utah State University's Structural Engineering Laboratory. The bridge deck concrete quantities are as follows:

Table 3-1 Bridge Deck Concrete Quantities (Logan Canyon Bridge)

Location	Phase 1	Phase 2
Deck (yd³)	68.6	124.9
Approach Slab (yd³)	44	80.3
Abut. Diaphragm (yd³)	18.1	35
Total	130.7	240.2

3.1.1. Deck Mix Design

The deck concrete was batched and transported by Jack B. Parson Companies. Concrete was delivered to the job site at 11:00 am on Monday September 26, 2005, where it was tested for slump, percent air and temperature. At the start of placement of the first section of concrete the outside air temperature was 57.2 degrees Fahrenheit. The concrete temperature was 67.5 degrees Fahrenheit. The concrete mix had a slump of 3.25 inches and an air content of 6.0%. Seventy-two total yards of concrete were ordered for the first section of the bridge deck.

Table 3.2 lists the concrete mix design weights that were targeted and the actual mix that was used for the bridge deck. These relate on to the first nine yards of the concrete pour. Looking at Table 3.2 it is determined that the actual design mix was very close to that of specified mix design. The concrete mix is divided into four main areas; aggregate, cement type; admixtures used, and amount of water added.

Table 3-2 Target and Actual Mix Design Weights

Element	Quantity	
	Target	Actual
Cement (Hol. II/V), Lb.	4500	4470
RIG. #57 (Aggregate), Lb.	16065	16040
RIG. SND (Aggregate), Lb.	10519	10560
Bridger (Type F Fly Ash), Lb.	1116	1120
Water, Gal./Yard	29	29
Micro-AE (Air Admixture), Oz.	66	67
P-200N (Water Reducer), Oz.	171	172

3.2 Sandy Bridge

The Sandy Bridge was designed as a simple span prestressed concrete (AASHTO type VI) girder bridge with a total of 14 girders, spaced at 7 feet, and composite with the slab. The bridge has a total length of 149' and a total width of 96' 10". Class AA(AE) cast-in-place concrete ($f'c = 4,000$ Psi) was used for the deck. The total volume of concrete used for the construction of the bridge deck was of 831 cubic yards. Grade 60 reinforcing steel was placed, and a 2" concrete cover was provided. The prestressed concrete used had a 28-day compressive strength of 7,500 Psi and a compressive strength at release of 6,500 Psi. Grade 270, low-relaxation prestressing strands with a 0.6 in. diameter were utilized. Half an inch of concrete is provided as wearing surface, and the bridge was designed for a future wearing surface of 35 PSF. The bridge has a design speed of 45 m.p.h.



Figure 3-2 Reinforcing Steel (Sandy Bridge)

3.2.1 Deck Mix Design

Concrete was delivered to the job site around 4:00 a.m. on Monday July 07, 2006. The concrete mix had a slump of 4.00 inches, a water/cement ratio of 0.44, an air content of 6.3%, and a concrete unit weight of 137.4 pcf. The components of the concrete mix, expressed in weights per cubic yard are shown on Table 3.3 below. Placement of the deck concrete is shown on Figure 3.3.

Table 3-3 Sandy Bridge Deck Mix Design

Element	Quantity
Cement, ASTM C-150 Type II, Lb.	489
Fly Ash, ASTM C-618 Type F, Lb.	122
Point C-33 Sand (Aggregate), Lb.	1144
Point # 67 Rock (Aggregate), Lb.	1683
Water, Lb. (GAL-US)	271
Water Reducer / WRDA 64, Oz.	18



Figure 3-3 Deck Placement

3.3 Provo Canyon Bridge

The Provo Canyon Bridge is a steel I beam girder bridge, with a total of 6 steel plate girders, spaced at 14.5 ft on center, and composite with a cast in place concrete deck. The width of the bridge is 83'2". Class 3A(AE) cast-in-place concrete ($f'c = 4,000$ Psi) was used for the deck, Class 4A(AE) cast-in-place concrete ($f'c = 4,500$ Psi) was used for footings, columns, pier caps, and abutments; and Class AA(AE) cast-in-place concrete ($f'c = 3,650$ Psi) was used for parapets and approach slabs. Grade 50 and 70 reinforcing steel was used, and a 2" concrete cover was provided. The bridge deck has a slope of 6.00% and the required thickness for the deck slab is 8 1/2". A 3/8" polymer epoxy overlay concrete was provided as wearing surface, and designed for a future wearing surface of 35 Psf. The bridge has a design speed of 50 m.p.h. The situation and layout for the Provo Canyon Bridge can be seen in Appendix C. Figure 3.4 shows the reinforcing steel prior to concrete placement.



Figure 3-4 Reinforcing Steel (Provo Canyon Bridge)

3.3.1 Deck Mix Design

Concrete was delivered to the job site around 5:00 a.m. on Monday July 12, 2006, where it was tested for slump, percent air and temperature. At the start of placement of the first section of concrete, the temperature was 52.0 degrees Fahrenheit. The concrete temperature was 76.0 degrees Fahrenheit. The concrete mix had a slump of 4.00 inches and an air content of 7.4%. The density of the concrete was 139.24 lb/ft³. The actual values of the concrete mix relate for the first ten yards of the concrete pour are shown on Table 3.4, and a picture of the deck placement is shown in Figure 3.5.

Table 3-4 Provo Canyon Deck Mix Design

Element	Quantity (Lb.)
Cement	5,230
Coarse Aggregate	17,600
Intermediate Aggregate	0
Fine Aggregate	11,400
Fly Ash	1,310
Water	2,070
Air Entrainment Admixture	4
Water Reducer Admixture	15



Figure 3.5. Deck Placement (Provo Canyon Bridge).

4.0 TEST DESCRIPTION AND RESULTS OF EXISTING DECK MIX

Six different tests were selected for characterizing the mechanical and durability properties of concrete for the three bridges. These were:

1) Compressive Strength Tests (ASTM C 31 and ASTM C 39). These were performed at 1, 3, 14, 28 and 56 days. Two 4" x 8" cylinders were used on each test day.

2) Split Tensile Strength Tests (ASTM C 496). These were performed at 1, 3, 14, 28 and 56 days. Two 4" x 8" cylinders were used on each test day.

3) Modulus of Elasticity. These were performed at 1, 3, 14, 28 and 56 days. Two 6" x 12" cylinders were used on each test day.

4) Shrinkage (ASTM C-157/C-157M). Two concrete prisms 3" x 3" x 16" were cast, left in their concrete molds for about 24 hours, and kept completely submerged in water for a period of 14 days, prior to testing. Shrinkage was then measured at 1, 3, 7, 14, 28, 56 days, and once a week for 60 days, for a total of 116 days of testing.

5) Freeze-Thaw Resistance (ASTM C 666). Two concrete prisms of 3"x3"x16" were tested. Both specimens were cast and cured from the original concrete pours. At 56 days, the specimens were placed in a freeze-and-thaw chamber where the temperature and cycles of freezing and thawing were controlled, and tested every 30 cycles until 300 cycles were completed.

6) Chloride Ion Penetration (ASTM C 1202). Two 2-inch thick slices of a 4" x 8" cylinder were isolated using a concrete chop saw. At 56 days the amount of electrical current passed through the slice over a 6-hour period was recorded. A potential difference of 60 Volts dc was maintained between a sodium chloride solution and a sodium hydroxide solution.

The importance of the characteristics tested, the test procedure and ultimately the results are presented below for each of the three bridges.

4.1. Compressive Strength

Strength is defined as the ability to resist stress without failure. In compression the test piece is considered to have failed even when no signs of external fracture are visible; however, the internal cracking has reached such an advanced state that the specimen is unable to carry a higher load.

The strength of concrete is the property most valued by designers and quality control engineers, and it is the property generally specified. This is because, compared to most other properties, testing of strength is relatively easy. Furthermore, many properties of concrete, such as elastic modulus, permeability, and resistance to weathering agents including aggressive waters, are believed to be a function of strength and may therefore be deduced from the strength data. Although in practice most concrete is subjected simultaneously to a combination of compressive, shearing, and tensile stresses in two or more directions, the uniaxial compression tests are the easiest to perform in laboratory, and the 28-day compressive strength of concrete determined by a standard uniaxial compression test is accepted universally as a general index of the concrete strength.

Although the actual response of concrete to applied stress is a result of complex interactions between various factors, to facilitate a clear understanding of these factors, they can be separately divided into three categories: (1) characteristics and proportions of materials, (2) curing conditions, and (3) testing parameters.

4.1.1 Characteristics and Proportions of Materials

The selection of proper material components and their proportions is the first step toward obtaining a product that would meet the specified strength.

4.1.1.1 Water-cement ratio

Duff Abrams found a relationship between water-cement ratio and concrete strength. This relation is represented by the expression:

$$f_c = \frac{k_1}{k_2^{w/c}} \quad (\text{Equation 4.1})$$

Where k_1 and k_2 are numerical constants and w/c represents the water-cement ratio. It can be concluded from the above expression that strength decreases as the water-cement ratio increases.

In low- and medium – strength concrete made with normal aggregate, both the interfacial zone transition zone porosity and the matrix porosity determine the strength of the concrete, and there is a direct relationship between the water-cement ratio and the concrete strength. In high-strength concrete, however, disproportionately high increases in the compressive strength can be achieved with very small reductions in the water-cement ratio.

4.1.1.2. Air Entrainment

Air voids, whether incorporated in concrete as a result of inadequate compaction or through the use of an air-entrainment admixture, also have the effect of increasing porosity and decreasing the strength of the system.

It has been observed, however, that the extent of strength loss as a result of entrained air depends not only on the water-cement ratio of the concrete mixture, but also on the cement content. By increasing the porosity of the matrix, entrained air will have an adverse effect on the strength of the composite material. On the other hand, by improving the workability and compactibility of the mixture, entrained air tends to improve the strength of the interfacial transition zone (especially in mixtures with very low water and cement contents) and thus improves the strength of concrete.

It is because of this, that at a given water-cement ratio, high-strength concretes (containing a high cement content) suffer a considerable strength loss with increasing amounts of entrained air,

whereas low-strength concretes (containing a low cement content) tend to suffer only a little strength loss or may actually gain some strength as a result of air entrainment.

4.1.1.3. Cement Type

The degree of cement hydration has a direct effect on porosity and consequently on strength. At early ages of hydration and a given water-cement ratio, a concrete containing Type III Portland cement (which has higher fineness) will hydrate more rapidly than the other types, will have lower porosity and correspondingly a higher strength up to about 28 days. However, this difference is minimized when different cement types achieve similar degrees of hydration.

4.1.1.4. Aggregate

Aggregate characteristics other than strength, such as the size, shape, surface texture, grading and mineralogy are known to affect concrete strength in varying degrees.

A change in the maximum size of well-graded coarse aggregate of a given mineralogy can have two opposing effects on the strength of concrete. With the same cement content and consistency, concrete mixtures containing larger aggregate particles require less mixing water than those containing smaller aggregate. On the contrary, larger aggregates tend to form weaker interfacial transition zone, containing more microcracks. The net effect is that increasing maximum aggregate size on the 28-day compressive strengths of the concrete was more pronounced with a high-strength (0.40 water-cement ratio) and a moderate-strength (0.55 water-cement ratio) concrete than with a low-strength concrete (0.7 water-cement ratio).

A change in the aggregate grading without any change in the maximum size of coarse aggregate, and with water-cement ratio held constant, can influence the concrete strength when this change causes a corresponding change in the consistency and bleeding characteristics of the concrete mixture.

The shape of the aggregate also has an effect on the compressive strength of concrete. A concrete mixture containing a rough-textured or crushed aggregate displays a higher strength than one of similar mineralogy containing a smooth surface. This is because there is a stronger physical bond between the aggregate and the cement paste. However, with a given cement content, usually more mixing water is needed to obtain the desired workability in a concrete mixture containing rough-textured aggregates. This is the reason why the small advantages in terms of concrete strength due to a better bonding is lost due to an increased amount of mixing water.

Differences in the mineralogical composition of aggregates are also responsible for affecting concrete strength. Reports show that the substitution of a calcareous for a siliceous aggregate, as well as a substitution of limestone for sandstone in a concrete mixture, can result in strength improvement.

4.1.1.5. Admixtures

Specifically, water-reducing admixtures, by their ability to reduce the water content of the concrete mixture, at a given consistency, the water-reducing admixtures can enhance both the early and ultimate strength of concrete.

4.1.2 Curing Conditions

The curing of concrete involves a combination of conditions that promote the cement hydration such as time, temperature, and humidity conditions, immediately after the placement of a concrete mixture into formwork.

4.1.2.1. Time

For a given water-cement ratio, the longer the moist curing period, the higher the strength, assuming that the hydration of the anhydrous cement particles is on going.

4.1.2.2 Humidity

The influence of the curing humidity on concrete strength is a very positive one. After 180 days at a given water-cement ratio, the strength of continuously moist-cured concrete is about three times greater than the strength of continuously air-cured concrete.

A minimum period of 7 days of moist-curing is generally recommended with concrete containing normal Portland cement. However with concrete mixtures containing either a blended Portland cement or a mineral admixture, a longer curing period is needed to ensure strength contribution from the pozzolanic reaction. Moist curing is provided by spraying, ponding, or covering the concrete surface with wet sand, sawdust, or cotton mats.

4.1.3 Testing parameters

4.1.3.1 Specimen Parameters

In the United States, the standard specimen for testing the compressive strength of concrete is a 4 x 8 in. cylinder (height/diameter ratio equal to 2). In general, the greater the height/diameter ratio, the lower the strength will be.

4.1.3.2 Loading Conditions

The compressive strength of concrete is measured in the laboratory by a uniaxial compression test (ASTM C 469) in which the load is progressively increased to fail the specimen within 2 to 3 min. It is evident that the actual loads (such as impact loads) and the loads under laboratory testing conditions vary. Therefore, it is important to have in mind that the loading condition has an important influence of the concrete strength.

For our project, 4" x 8" cylinders were cast in order to determine the concrete compressive strength. Each cylinder was submitted to the proper vibration, and finally placed in the fog room where it was allowed to cure. They were subsequently tested according to the ASTM C 31 and ASTM C 39, at each of the following days, from the day they were cast: 1, 3, 7, 14, 28, and 56 days.



Figure 4-5 Vibration of Concrete Specimens, onsite at Sandy Bridge

Two cylinders were tested on each of the testing days, from which an average compressive strength was determined. The compressive strength was calculated using the below equation.

$$f = \frac{P}{A}$$

(Equation 4.2)

Where:

f = the compressive stress at any desired test day, and ($f'c$) being specifically the 28 day compressive strength of tested specimens. (Psi)

P = failure load of the concrete specimen (Lb.)

A = the cross sectional area of the concrete specimen (in^2)



Figure 4-6 Compressive Strength Test

Test results for the compressive strength of the concrete from the three bridges are shown below:

Table 4-5 First Dam Bridge Compressive Strength Test Results

Cylinder	Days	Area (in2)	P (Lb.)	f (Psi)	Avg. f (Psi)
Test #1	3	12.57	36600	2912.54	2832.96
Test #2			34600	2753.38	
Test #1	7	12.57	35100	2793.17	2908.56
Test #2			38000	3023.94	
Test #1	14	12.57	41600	3310.42	3521.30
Test #2			46900	3732.18	
Test #1	28	12.57	63000	5013.38	4834.33
Test #2			58500	4655.28	
Test #1	56	12.57	69500	5530.63	5331.69
Test #2			64500	5132.75	

Table 4-6 Sandy Bridge Compressive Strength Test Results

Cylinder	Days	Area (in2)	P (Lb.)	f (Psi)	Avg. f (Psi)
Test #1	1	12.57	26185	2083.75	1923.63
Test #2			22161	1763.51	
Test #1	3	12.57	40331	3209.42	3129.58
Test #2			38324	3049.74	
Test #1	7	12.57	49769	3960.48	4013.28
Test #2			51096	4066.08	
Test #1	14	12.57	58200	4631.41	4543.87
Test #2			56000	4456.34	
Test #1	28	12.57	72500	5769.37	5888.73
Test #2			75500	6008.10	
Test #1	56	12.57	76256	6068.26	6479.99
Test #2			86604	6891.73	

Table 4-7 Provo Canyon Bridge Compressive Strength Test Results

Cylinder	Days	Area (in²)	P (Lb.)	f (Psi)	Avg. f (Psi)
Test #1	1	12.57	35557	2829.52	2940.07
Test #2			38335	3050.62	
Test #1	3	12.57	49868	3968.40	3862.65
Test #2			47211	3756.90	
Test #1	7	12.57	55125	4386.71	4779.62
Test #2			65000	5172.54	
Test #1	14	12.57	70000	5570.42	5371.48
Test #2			65000	5172.54	
Test #1	28	12.57	65000	5172.54	5570.42
Test #2			75000	5968.31	
Test #1	56	12.57	87862	6991.84	6778.01
Test #2			82488	6564.19	

As can be seen from tables 4.1 – 4.3, the 28 day compressive strength for the First Dam Bridge, Sandy Bridge, and Provo Canyon Bridge were, respectively: 4834.33 Psi, 5888.73 Psi, and 5570.42 Psi.

A plot of the Compressive Stress vs. Time for each of the three concrete mixes can be seen in Figure 4.1. A steady increase in compressive strength is experienced on average for each specimen.

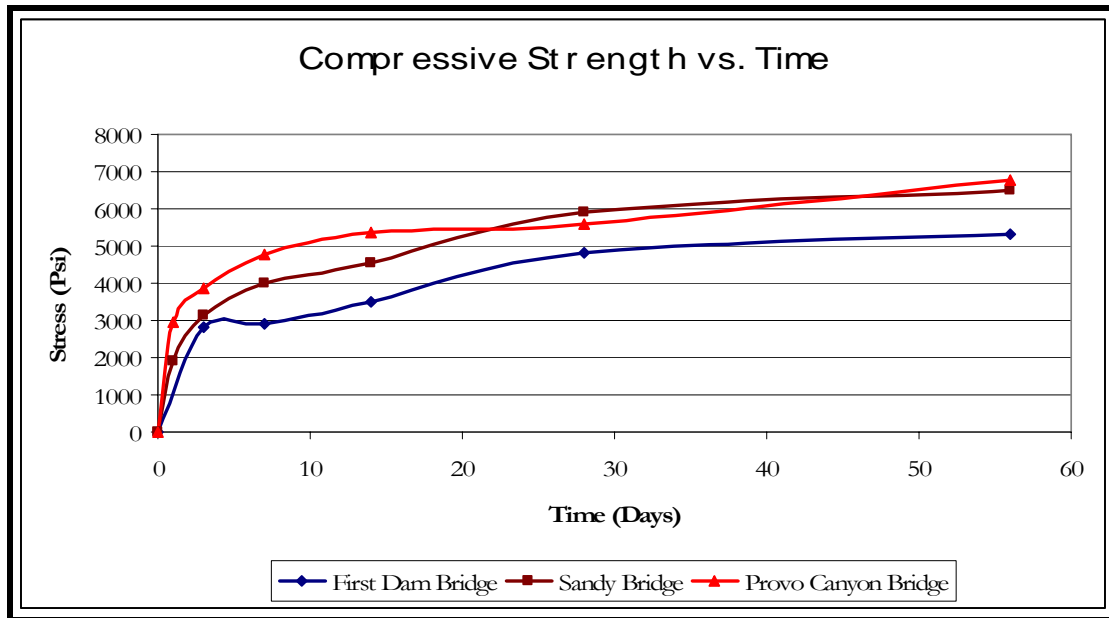


Figure 4-7 Compressive Strength vs. Time Results for Three Bridges

4.2. Tensile Strength

Although it is generally assumed that concrete performance is governed mostly by its compression capabilities, tensile strength and shear capacity are important with respect to the appearance and durability of concrete structural members. Variation of tensile strength with time is an important factor in concrete shear strength prediction at different curing times. Cracking has been reported in concrete early in its life, before its final set. Such undesirable cracking only occurs when the tensile strength of concrete has been exceeded; therefore a comprehensive knowledge of the time variation in magnitude of the tensile strength in concrete is very important, particularly at early ages, when concrete is first subjected to flexural actions due to construction load and when it may not have developed its specified strength.

Direct tension tests of concrete are seldom carried out, mainly because the specimen holding devices introduce secondary stresses that cannot be neglected. The most commonly used tests for estimating the tensile strength of concrete are the ASTM C 496 splitting tension test and the ASTM C 78 third-point flexural loading test. The one used for this project was the splitting tension test (ASTM C 496).

In the splitting tension test 4 x 8 in. concrete cylinders are subjected to compression loads along two diametrically opposite axial lines, producing a transverse tensile stress, which is uniform along the diameter. The load was to be applied within the splitting tension stress range of 0.7 to 1.3 MPa, until the specimen fails. Failure is regarded as a fracture of the test piece along its diameter.

For our project, we cast concrete in 4" x 8" cylinders. They were submitted to the proper vibration, and finally placed in the fog room and allowed to cure. They were subsequently tested according to the ASTM C 496, with a continuously applied load of 4,800 lbs/min (within the range of stress range of 0.7 to 1.3 MPa) until failure (Figure 4.4). This was done in the following days, from the day they were cast: 1, 3, 7, 14, 28, and 56 days.



Figure 4-8 Tensile Strength Test

Two cylinders were tested on each of the testing days, from which an average tensile strength was determined. The tensile strength was calculated using the equation below:

$$T = \frac{2P}{LD\pi} \quad \text{(Equation 4.3)}$$

Where:

T= Tensile Strength (Psi)

P = Failure Load (lbs)

L = Length of Concrete Specimen (in.)

A = Cross Sectional Area of Concrete Specimen (in.)

It is important to note that, compared to direct tension, the splitting tension test is known to overestimate the tensile strength of concrete by 10 to 15 percent.

Test results for the tensile strength of the concrete from the three bridges are shown in Tables 4.4 through 4.6.

Table 4-8 First Dam Bridge Tensile Strength Test Results

Cylinder	Days	Length (in.)	Diameter (in.)	P (lbs)	T(Psi)	Avg. T (Psi)
Test #1	3	12	6	8214	163.41	161.00
Test #2			6	7971	158.58	
Test #1	7	12	6	10342	205.74	262.22
Test #2			6	16020	318.70	
Test #1	14	12	6	15744	313.22	322.87
Test #2			6	16714	332.51	
Test #1	28	12	6	9700	192.98	207.90
Test #2			6	11200	222.82	
Test #1	56	12	6	13100	260.62	239.73
Test #2			6	11000	218.84	

Table 4-9 Sandy Bridge Tensile Strength Test Results

Cylinder	Days	Length (in.)	Diameter (in.)	P (lbs)	T (Psi)	Avg. T(Psi)
Test #1	1	8	4	11786	234.48	216.93
Test #2			4	10022	199.38	
Test #1	3	8	4	13418	266.94	245.33
Test #2			4	11246	223.73	
Test #1	7	8	4	10088	200.70	236.67
Test #2			4	13705	272.64	
Test #1	14	8	4	19800	393.91	380.98
Test #2			4	18500	368.05	
Test #1	28	8	4	15000	298.42	327.26
Test #2			4	17900	356.11	
Test #1	56	8	4	25049	498.33	430.89
Test #2			4	18269	363.45	

Table 4-10 Provo Canyon Bridge Tensile Strength Test Results

Cylinder	Days	Length (in.)	Diameter (in.)	P (lbs)	T(Psi)	Avg. T (Psi)
Test #1	1	8	4	8214	163.41	161.00
Test #2			4	7971	158.58	
Test #1	3	8	4	10342	205.74	262.22
Test #2			4	16020	318.70	
Test #1	7	8	4	15744	313.22	322.87
Test #2			4	16714	332.51	
Test #1	14	8	4	9700	192.98	207.90
Test #2			4	11200	222.82	
Test #1	28	8	4	13100	260.62	239.73
Test #2			4	11000	218.84	
Test #1	56	8	4	14310	284.69	305.42
Test #2			4	16394	326.15	

As can be seen from Tables 4.4 – 4.6, the 28 day tensile strength for the First Dam Bridge, Sandy Bridge, and Provo Canyon Bridge were, respectively: 208Psi, 327 Psi, and 294 Psi.

A plot of the Tensile Stress vs. Time for each of the three concrete mixes can be seen in Figure 4.5. A steady increase in tensile strength is experienced on average for each specimen. However, there was some decrease in the tensile strength of the specimens for all three bridges at 14 days or at 28 days.

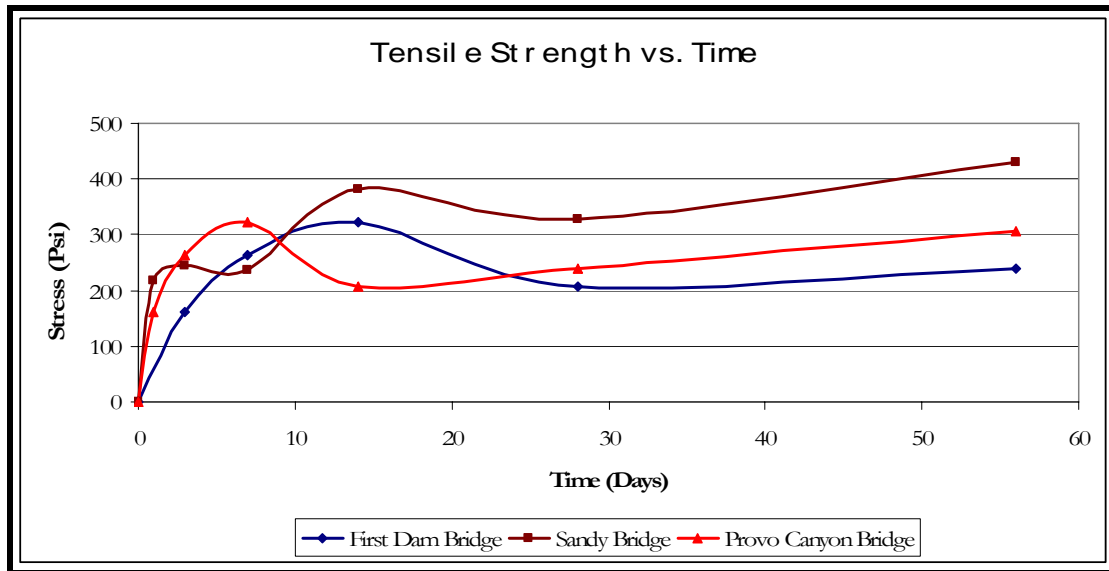


Figure 4-9 Tensile Strength vs. Time Results for Three Bridges

4.3. Elastic Modulus of Elasticity

Initially, when strain is proportional to the applied stress and is reversible on unloading the specimen, it is called the elastic strain. The modulus of elasticity is defined as the ratio between the stress and the reversible strain. The significance of the elastic limit lies in the fact that it represents the maximum allowable stress before the material undergoes permanent deformation. Therefore, the elastic modulus of the material influences the rigidity of a design.

For concrete, there is a direct relation between strength and elastic modulus, since both are affected by the porosity of the constituent phases, although not to the same degree. Several factors affect the modulus of elasticity of concrete. Among these are: aggregate, cement paste matrix, transition zone, and testing parameters.

The aggregate characteristic that most affects the elastic modulus of concrete is porosity. Dense aggregates have a high elastic modulus and the more of these aggregates in the concrete, the higher the elastic modulus of the mix. Aggregate size, shape, surface texture, grading, and mineralogical composition also have an effect on the modulus of elasticity, since they can influence micro cracking, thus affecting the shape of the stress-strain curve.

The elastic modulus of the cement paste is determined by its porosity, which is in turn controlled by the water-cement ratio, air content, mineral admixtures, and degree of cement hydration.

Regardless of mix proportions or curing age, concrete specimens that are tested in wet conditions show about 15 percent higher elastic modulus than the corresponding specimens tested in a dry condition.

The modulus of elasticity was measured from the deck concrete used in the initial phase of the first dam bridge constructed at the mouth of Logan Canyon. The concrete specimens for the elastic modulus tests were 6" x 12" cylinders. These cylinders were stored in a constant moisture and temperature room to achieve optimum curing conditions. The procedures according to ASTM C 469, a standard test method for measurement of the static modulus of elasticity, was followed (Figure 4.6).

The elastic modulus tests were performed at: 1, 3, 7, 14, 28, and 56 days after the time concrete samples. On each of the test days two specimens were tested. The compressive strength of the concrete was obtained on each testing day by using 4" x 8" cylinders, as previously described. The elastic modulus specimens (6" x 12") were then loaded to 40% of that compressive strength. By determining the slope of the resulting stress-strain curve, we were able to determine the modulus of elasticity of our concrete. Once the values of modulus of elasticity for each testing day were obtained a graph of modulus of elasticity vs. time was created.



Figure 4-10 Modulus of Elasticity Test

The ACI manual provides a commonly used equation to calculate the elastic modulus. This equation is used to compare our experimental results with what they should be, based on the ACI.

$$E = 57,000\sqrt{f'c} \quad \text{(Equation 4.4)}$$

Where:

E = Modulus of Elasticity (Psi)

f'c = Compressive Strength at each test day (Psi)

Test results for the modulus of elasticity of the concrete from the three bridges is shown below:

Table 4-11 First Dam Bridge Modulus of Elasticity

Cylinder	Days	E (psi)	Avg. E (Psi)
Test #1	3	3334900	3.3755E+06
Test #2		3416000	
Test #1	7	3935800	4.1399E+06
Test #2		4343900	
Test #1	14	4376400	4.1979E+06
Test #2		4019300	
Test #1	28	4601200	4.3734E+06
Test #2		4145500	
Test #1	56	4608100	4.3041E+06
Test #2		4000000	

Table 4-12 Sandy Bridge Modulus of Elasticity

Cylinder	Days	E (Psi)	Avg. E (Psi)
Test #1	1	3516721	3.6651E+06
Test #2		3813402	
Test #1	3	4656433	4.5701E+06
Test #2		4483729	
Test #1	7	5193638	5.0723E+06
Test #2		4950876	
Test #1	14	5028613	5.1268E+06
Test #2		5225078	
Test #1	28	5475521	5.4091E+06
Test #2		5342729	
Test #1	56	5455781	5.4107E+06
Test #2		5365667	

Table 4-13 Provo Canyon Modulus of Elasticity

Cylinder	Days	E (psi)	Avg. E (Psi)
Test #1	1	3416516	3.5854E+06
Test #2		3754326	
Test #1	3	4278101	4.4484E+06
Test #2		4618646	
Test #1	7	4940525	4.9485E+06
Test #2		4956550	
Test #1	14	4803505	5.0026E+06
Test #2		5201780	
Test #1	28	5513508	5.3368E+06
Test #2		5160036	
Test #1	56	5345545	5.4945E+06
Test #2		5643491	

The Stress vs. Strain plots from which the above values of Modulus of Elasticity were derived, is shown on Appendix B, for all three bridge samples.

A plot of Modulus of Elasticity vs. Time for each of the three concrete mixes can be seen in Figure 4.7. A steady increase in Modulus of Elasticity is experienced on average for each specimen. However, the rate of increase reduced dramatically after around 28 days.

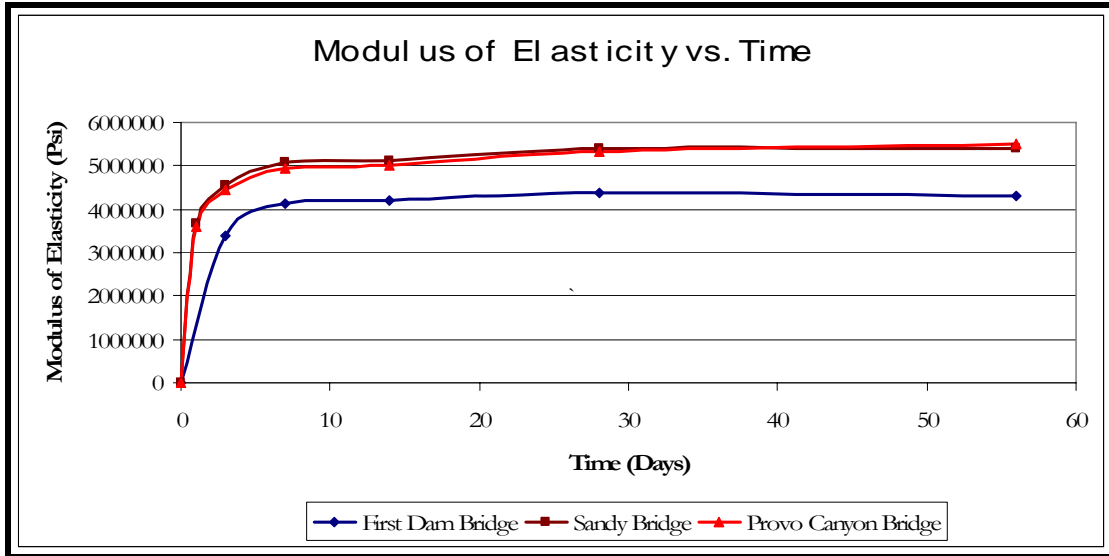


Figure 4-11 Modulus of Elasticity vs. Time Results for Three Bridges

We now compare our experimental results from the three bridges, to the previously stated ACI equation, based on the compressive strength of the specimens, determined for each day. This comparison is shown below, for each of the three bridges.

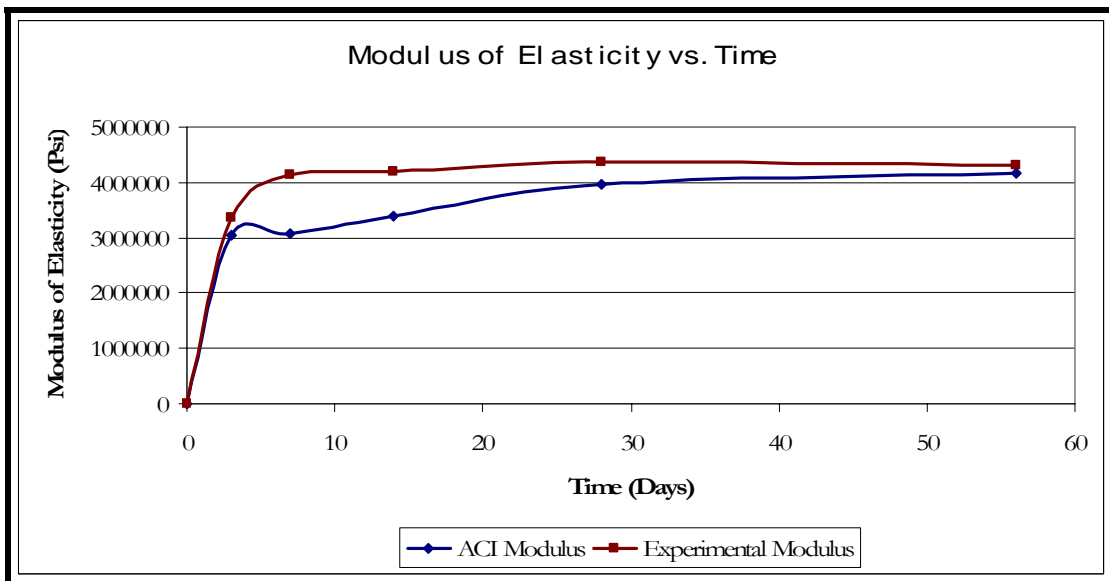


Figure 4-12 Experimental and ACI Modulus of Elasticity Comparison (First Dam Bridge)

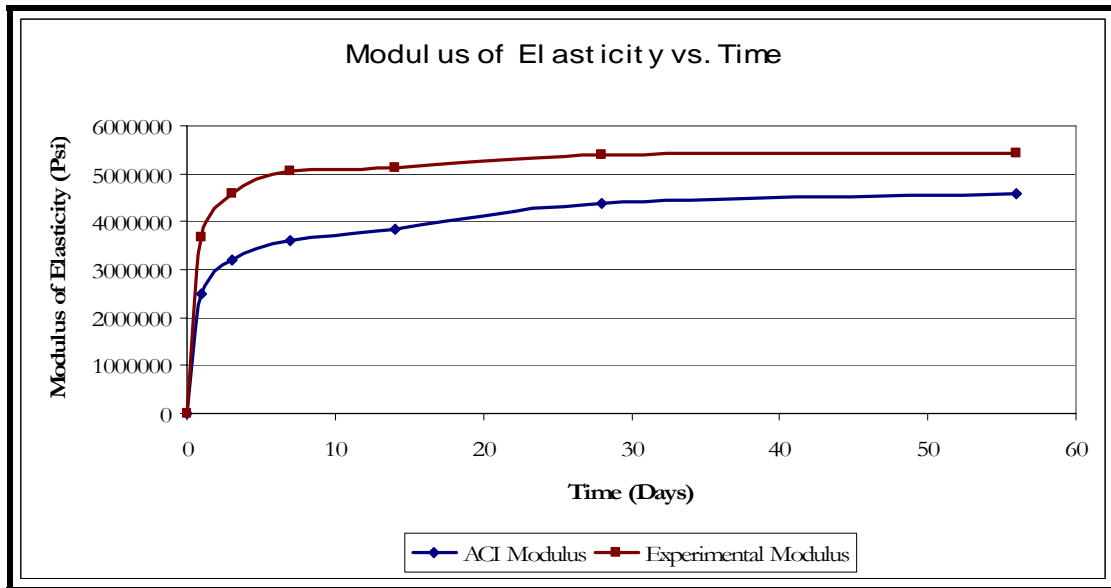


Figure 4-13 Experimental and ACI Modulus of Elasticity Comparison (Sandy Bridge)

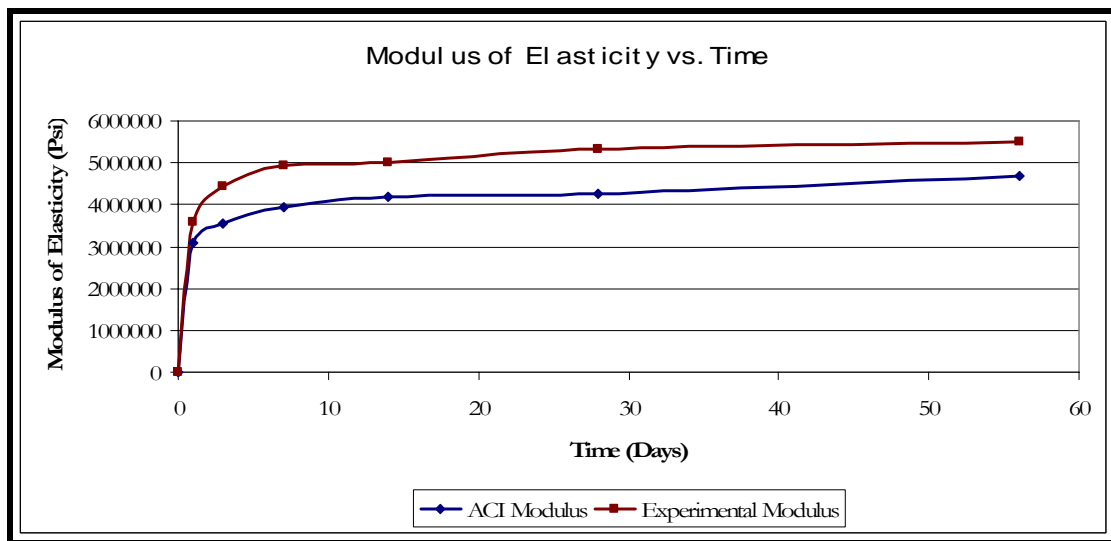


Figure 4-14 Experimental and ACI Modulus of Elasticity Comparison (Provo Canyon Bridge)

The ACI equation yields lower modulus of elasticity values for all cases. In the case of the First Dam Bridge, the ACI Modulus of Elasticity is on average 14% lower than the Experimental Modulus of Elasticity. In the case of the Sandy Bridge, the ACI Modulus of Elasticity is on

average 34% lower than the Experimental Modulus of Elasticity and 22% lower in the case of the Provo Canyon Bridge. This was expected since this equation is meant to be conservative.

4.4. Shrinkage

Shrinkage is the decrease (or swelling) of concrete when exposed to ambient humidity due to the removal of absorbed water (by evaporation) from the hydrated cement paste. Restraint to this shrinkage, provided by the reinforcement, or another part of the structure, causes tensile stresses to develop in the hardened concrete. Among the factors affecting shrinkage, researchers have found the following:

4.4.1. Cement Factor

The main source of moisture-related deformations in concrete is the hydrated cement paste. The greater the volume of hydrated cement to total volume of concrete, the higher the shrinkage.

4.4.2. Aggregate Properties

The grading, maximum size, shape, and texture of aggregate all influence drying shrinkage. It is generally agreed, however, that the modulus of elasticity of the aggregate is the most important characteristic influencing drying shrinkage. It influences the degree to which the aggregates restrain the shrinkage of the paste. The higher the elastic modulus of the aggregate, the lower the shrinkage of our element will be. This is why concrete containing dense limestone and quartz (high elastic modulus), have lower values of drying shrinkage than those containing sandstones and gravel (lower elastic modulus).

4.4.3. Water Content

High water content decreases the volume of the aggregate, which in turn decreases the restraint offered to the shrinkage of the paste. The higher the water content, the higher the drying shrinkage.

4.4.4. Type of Cement

The fineness of Portland cement affects the rate of hydration of the cement paste. Very fine cement has a greater surface area, and can therefore lose more water (in molecular layers) from around gel particles.

4.4.5 Curing and Storage

An increase in the atmospheric humidity is expected to slow down the relative rate of moisture flow from the interior to the outer surfaces of the concrete. Therefore, the lower the relative humidity, the higher the shrinkage will be.

4.4.6 Size Effects

As a specimen becomes larger, its ratio of surface area to volume decreases. This results in lower surface area for water to evaporate from, and more moist concrete to restrain shrinkage.

The ASTM C 157/C 157M testing procedures were used when testing the bridge deck concrete for shrinkage. The specimens were concrete prisms 3”x 3” x 16” in dimension. During casting, metal studs were placed in the ends of each specimen to assist in monitoring the change in length of each specimen. The specimens were placed and kept completely submerged in water for a period of 14 days, prior to testing.

Shrinkage readings were taken in the comparator (Figure 4.11) at 3, 7, 14, 28, 56, and once a week after the first initial reading. In total, changes in length of the two concrete specimens were monitored for 116 days.

Length change was calculated for each specimen at any age after the initial reading, the following equation:

$$\varepsilon = \frac{CR - IR}{G}$$

Equation (4-5)

Where:

ε = strain of the specimen at test age.

CR = Comparator reading at the test age.

IR = Initial reading.

G = Gage length.

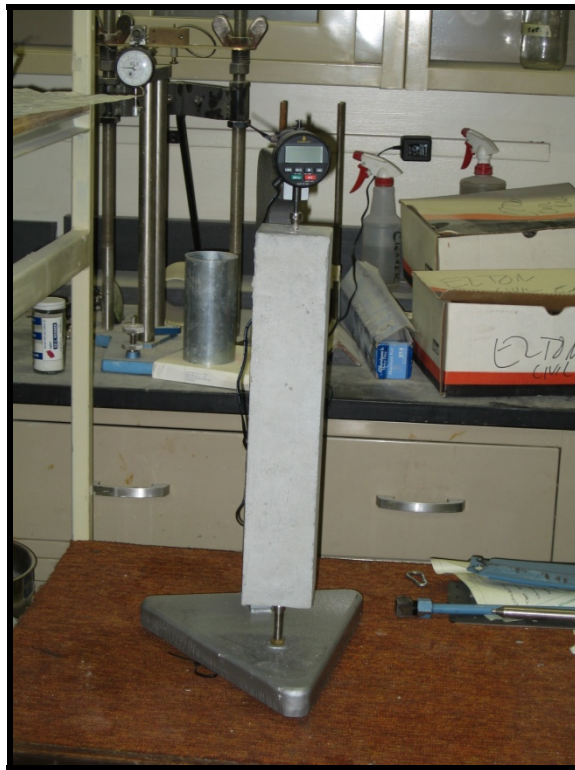


Figure 4-15 Shrinkage Test

Shrinkage test recordings for all three bridges are shown on the following figure:

Table 4-14 Shrinkage Test Recordings

Days	First Dam Bridge (Specimen #1) (in)	First Dam Bridge (Specimen #2) (in)	Provo Canyon Bridge (Specimen #1) (in)	Provo Canyon Bridge (Specimen #2) (in)	Sandy Bridge (in)
Initial	0.0685	0.0455	0.7519	0.6699	0.7519
3	0.0679	0.0443	0.7515	0.6695	0.7519
7	0.0660	0.0424	0.7513	0.6692	0.7513
14	0.0635	0.0398	0.7502	0.6683	0.7497
28	0.0605	0.0376	0.7491	0.6683	0.7491
56	0.0593	0.0364	0.7486	0.6661	0.7480
63	0.0588	0.0361	0.7477	0.6651	0.7471
70	0.0588	0.0359	0.7458	0.6633	0.7467
78	0.0582	0.0358	0.7454	0.6629	0.7465
84	0.0581	0.0357	0.7442	0.6622	0.7464
100	0.0583	0.0353	0.7436	0.6617	0.7458
108	0.0574	0.0355	0.7431	0.6611	0.7453
116	0.0591	0.0359	0.7414	0.6599	0.7433

Using equation 4.5, the length change was calculated for each specimen, with reference to the initial reading. The results are shown in Table 4.11.

Table 4-15 Length Change Calculations

Days	First Dam Bridge (Specimen #1) ΔL (in)	First Dam Bridge (Specimen #2) ΔL (in)	Provo Canyon Bridge (Specimen #1) ΔL (in)	Provo Canyon Bridge (Specimen #2) ΔL (in)	Sandy Bridge ΔL (in)
3	0.0006	0.0012	0.0003	0.0004	0.0000
7	0.0025	0.0031	0.0005	0.0007	0.0005
14	0.0050	0.0057	0.0016	0.0017	0.0022
28	0.0080	0.0079	0.0028	0.0017	0.0028
56	0.0092	0.0091	0.0033	0.0039	0.0038
63	0.0097	0.0094	0.0041	0.0048	0.0047
70	0.0097	0.0096	0.0060	0.0066	0.0051
78	0.0103	0.0097	0.0064	0.0070	0.0053
84	0.0104	0.0098	0.0077	0.0077	0.0055
100	0.0102	0.0102	0.0082	0.0082	0.0060
108	0.0111	0.0100	0.0088	0.0088	0.0066
116	0.0094	0.0096	0.0104	0.0100	0.0085

By dividing the results in Table 4.13 by the length of our specimen (16 in.), we obtain the strain of each of the specimens at each of the test days, expressed to the 10^{-6} .

Table 4-16 Strain (10^{-6})

Days	First Dam Bridge (Specimen #1)	First Dam Bridge (Specimen #2)	Provo Canyon Bridge (Specimen #1)	Provo Canyon Bridge (Specimen #2)	Sandy Bridge
3	0.0000	75.0000	21.8750	25.0000	0.0000
7	156.2500	193.7500	34.3750	43.7500	34.3750
14	312.5000	356.2500	103.1250	103.1250	137.5000
28	500.0000	493.7500	171.8750	103.1250	171.8750
56	575.0000	568.7500	206.2500	240.6250	240.6250
63	606.2500	587.5000	259.3750	300.0000	296.8750
70	606.2500	600.0000	378.1250	412.5000	321.8750
78	643.7500	606.2500	403.1250	437.5000	334.3750
84	650.0000	612.5000	481.2500	481.2500	343.7500
100	637.5000	637.5000	515.6250	515.6250	378.1250
108	693.7500	625.0000	550.0000	550.0000	412.5000
116	587.5000	600.0000	653.1250	625.0000	534.3750

Table 4.13 shows the average of the strains shown on the previous table.

Table 4.13. Average Strain (10^{-6})

Days	First Dam Bridge	Provo Bridge	Sandy Bridge
3	37.5000	23.4375	0.0000
7	175.0000	39.0625	34.3750
14	334.3750	103.1250	137.5000
28	496.8750	137.5000	171.8750
56	571.8750	223.4375	240.6250
63	596.8750	279.6875	240.6250
70	603.1250	395.3125	275.0000
78	625.0000	420.3125	309.3750
84	631.2500	481.2500	343.7500
100	637.5000	515.6250	378.1250
108	659.3750	550.0000	412.5000
116	593.7500	639.0625	618.7500

A plot of Strain vs. Time for each of the three concrete mixes is shown on Figure 4.14.

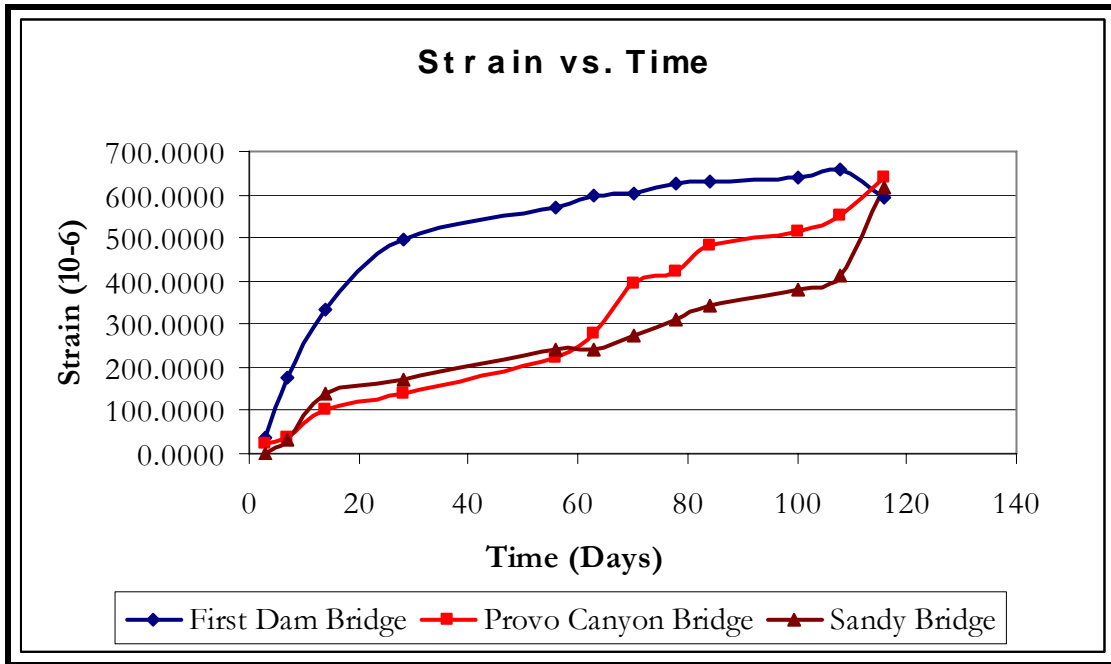


Figure 4-16 Strain vs. Time

4.5 Freeze/Thaw

When water freezes, it expands to about 9% of its volume. As the water in moist concrete freezes, it produces pressure in the pores of the concrete. If the pressure developed exceeds the tensile strength of the concrete, the cavity will dilate and rupture. The accumulative effect of successive freeze-thaw cycles and disruption of paste and aggregate can eventually cause expansion and cracking, scaling, and crumbling of the concrete.

Deicing chemicals used for snow and ice removal, such as sodium chloride, can aggravate freeze-thaw deterioration. Moisture tends to move towards zones with higher salt concentrations (by osmosis); thus, if salts are present in the pore solution, the osmotic pressure is increased. In

addition, the application of deicing salts increases the rate of cooling, increasing the potential for freeze-thaw deterioration at the concrete surface.

The resistance of concrete to freezing and thawing in a moist condition is significantly improved by the use of intentionally entrained air. The tiny entrained air voids act as empty chambers in the paste for the freezing and migrating water to enter, thus relieving the pressure in the pores and preventing damage to the concrete. Concrete with a low permeability (that is, a low water-cement ratio and adequate curing) is better able to resist freeze-thaw cycles.

ASTM C 666 describes the test method to determine the resistance of concrete specimens to rapidly repeated cycles of freezing and thawing in the laboratory by two different procedures: Procedure A, Rapid Freezing and Thawing in water, and Procedure B, Rapid Freezing in air and Thawing in water. This research was based on the freeze/thaw test of Procedure A. This procedure will help assist in determining the effects of variations in the properties of concrete on the resistance of the concrete to freezing-and-thawing cycles.



Figure 4-17 Concrete Specimens placed in Freeze-Thaw Machine

Two concrete specimens of 3"x3"x16" dimensions were tested. Both specimens were cast and cured from the original concrete deck pours. The specimens were placed in a freeze-and-thaw chamber where the temperature and cycles of freezing and thawing were controlled (Figure 4.13). Water was placed around both specimens not allowing the depth of the water over the specimen to exceed 1/8" and to become less than 1/32". After starting the freeze/thaw test the specimens were removed from the freeze/thaw apparatus in a thawed condition, at intervals not exceeding 36 cycles of exposure to the freezing-and-thawing cycles, and then tested for their fundamental longitudinal frequency, using an HP Dynamic Analyzer. Appendix A outlines the steps for performing this measurement using the HP Dynamic Analyzer.

The results of the Dynamic HP analyzer and the cycle at which the specimen was tested are listed in Table 4.13.

Frequencies Table 4-14 Longitudinal

No. of Cycles	First Dam Bridge Specimen 1 (KHz)	First Dam Bridge Specimen 2 (KHz)	Sandy Bridge Specimen 1 (KHz)	Sandy Bridge Specimen 2 (KHz)	Provo Bridge Specimen 1 (KHz)	Provo Bridge Specimen 2 (KHz)
0	5.150	5.159	5.032	5.066	5.164	5.109
34	5.105	5.121	5.007	5.041	5.119	5.087
54	5.157	5.178	5.037	5.071	5.171	5.104
97	5.119	5.134	5.011	5.045	5.187	5.126
131	5.197	5.210	5.082	5.116	5.153	5.154
160	5.134	5.161	5.016	5.050	5.147	5.094
190	5.149	5.147	5.031	5.065	5.163	5.099
219	5.161	5.185	5.053	5.087	5.180	5.127
244	5.136	5.149	5.018	5.052	5.158	5.087
301	5.168	5.182	5.050	5.084	5.187	5.127

Based on the fundamental longitudinal frequencies, the Relative Dynamic Modulus of Elasticity can be calculated using equation 4.6.

$$P_c = 100 * \frac{n_1^2}{n^2} \quad \text{Equation (4-6)}$$

Where,

P_c = Relative Dynamic Modulus of Elasticity.

n_1 = Fundamental transverse natural frequency of the sample at time of testing.

n = Fundamental transverse natural frequency of the sample at the initial time.

The Relative Dynamic Moduli of Elasticity, based on the average value of the longitudinal frequencies for each of the bridges, are shown on Table 4.14.

Table 4-15 Relative Dynamic Moduli

# cycles	First Dam Bridge Relative Dynamic Modulus	Sandy Bridge Relative Dynamic Modulus	Provo Canyon Bridge Relative Dynamic Modulus
0	100.00	100.00	100.00
34	101.63	101.01	101.33
54	99.50	99.80	99.96
97	101.10	100.85	99.22
131	98.13	98.05	99.33
160	100.27	100.62	100.61
190	100.25	100.04	100.21
219	99.29	99.18	99.34
244	100.47	100.55	100.54
301	99.21	99.30	99.20

The durability factor for each of the cycles is shown in Table 4.15 below. In each case the concrete show high durability characteristics with the lowest durability factor reaching only 0.98.

Table 4-16 Durability Factors

# cycles	First Dam Bridge DF	Sandy Bridge DF	Provo Canyon Bridge DF
0	1.00	1.00	1.00
34	1.02	1.01	1.01
54	1.00	1.00	1.00
97	1.01	1.01	0.99
131	0.98	0.98	0.99
160	1.00	1.01	1.01
190	1.00	1.00	1.00
219	0.99	0.99	0.99
244	1.00	1.01	1.01
301	0.99	0.99	0.99

4.6 Chloride Ion Penetration

Because chloride ions play an important role in the corrosion of reinforcing steel and eventually the cracking of concrete, the permeability of concrete is a key to preventing this from happening. Concrete mixture parameters such as, a low water-cement ratio, adequate cement content, control of aggregate size and grading, and use of mineral admixtures can help lower the permeability of our concrete.

The repair and replacement costs associated with concrete bridge decks damaged by the corrosion of reinforcing steel have become a major maintenance expense. This hints at the importance of the measure of chloride ion penetration in our concrete.

ASTM International C 1202 (2002) describes the chloride penetration test by monitoring the amount of electrical current passed through a 2-inch thick slice of a given diameter of concrete cylinders over a 6-hour period. A potential difference of 60 Volts dc is maintained across a sodium chloride solution, with the other attached to a sodium hydroxide solution. The total charge passed as a result of this potential difference in coulombs, has been found to be related to the resistance of the specimen to chloride ion penetration.

Two samples from each bridge deck concrete was used in the chloride penetration test. Cylinders 4" x 8" in dimensions were stored in a wet room from the day it was cast until preparation for the chloride penetration test which commenced 56 days later. A 2-inch thick slice from the middle of the cylinder was isolated using a concrete chop saw. After isolating the specimen, it was allowed to surface dry in air for at least 1-hour. This 2-inch specimen then had an epoxy coating placed around its side surface. Following the drying of the surface epoxy, the specimen was placed in vacuum desiccators where both ends of the specimen were exposed. The desiccators were sealed and the vacuum pump was started. The specimen was left in this vacuum state for the next 3-hours after which de-aerated water was placed in the vacuum that completely covered the specimen. As soon as enough water was in the vacuum the stopcock was closed and the vacuum pump was allowed to run for one more hour. The vacuum was then shut off and air was allowed back into the desiccators and the specimen was left to soak for the next 18 + or - 2 hours. Each cell was filled with either a sodium chloride (NaCl) solution or a sodium hydroxide solution (NaOH). Three grams of NaCl was used to every 100 grams of water, with the actual concentration equaling 18 grams of NaCl to 600 grams of water. Twelve grams of NaOH was used to every 1 liter of water, which is the actual concentration for NaOH. At which point an electrical connections were made and the current was applied to the specimen with the voltage being read in mili Amperes. Current was read and recorded at least every 30 minutes. Each half of the test cell remained filled with the appropriate solution for the entire period of the test.



Figure 4-18 Chloride-Ion Penetration Test

Plotting the current (in amperes) vs. time (in seconds) and integrating under the curve will allow us to obtain the ampere-seconds, or coulombs, passed during the chloride penetration test. ASTM C 1202 Note 5 states that for current recorded at 30 minute intervals, the following formula (based on the trapezoidal rule) applies:

$$Q = 900(I_0 + 2I_{30} + 2I_{60} \dots + 2I_{300} + 2I_{330} + I_{360}) \quad \text{Equation (4-7)}$$

Where:

Q = Charge passed (coulombs).

I_0 = Current (amperes) immediately after voltage is applied.

I_t = Current (amperes) at t min after voltage is applied.

If the test specimen diameter is anything other than 3.75 inches (which was our case), then an adjustment is applied to the total calculated charge passed using the following equation:

$$Q_s = Q \left(\frac{3.75}{x} \right)^2$$

Equation (4-8)

Where,

Q_s = Charge passed (coulombs) through a 3.75-in. (95-mm) diameter specimen,

Q = Charge passed (coulombs) through x in. diameter specimen.

x = Diameter (in.) of the nonstandard specimen.

Table 4.16 is from the ASTM C 1202. It lists a numerical breakdown of how to rate the tested concrete. The larger the number of coulombs passed, the less resistant that the concrete is to chloride migration.

Table 4-17 Chloride Ion Permeability Based on Charge Passed

Charge Passed (Coulombs)	Chloride Ion Permeability
> 4,000	High
2,000 - 4,000	Moderate
1,000 - 2,000	Low
100 - 1,000	Very Low
< 100	Negligible

Table 4.16 shows the recorded current every 30 minutes for each of the samples of the three bridges.

Table 4-18 Recorded Current (Chloride Ion Penetration Test)

Minutes Elapsed	Current (Mili Amps)				
	First Dam Bridge	Sandy		Provo Canyon	
		Sample #1	Sample #2	Sample #1	Sample #2
0	45.3	88	85.2	94.8	76
30	45.6	86.8	81.6	82.4	70
60	46.2	86	79.6	80	60.4
90	47	85	75.6	73.6	60.4
120	47.7	84.6	74.8	73.6	59.2
150	48.4	84.4	72.8	68.8	52.4
180	49	84	70.8	72.8	58.8
210	49.5	83.8	70	68	58.4
240	49.8	83.6	69.2	67.6	58
270	50.1	83.4	70.8	70.4	57.6
300	50.4	83.4	70.8	71.2	57.2
330	50.1	83.2	71.2	70.4	56.8
360	50	83	70.8	68.4	56.4

By using Equation 4.7 and applying the adjustment suggested by Equation 4.8 we get The following calculated charges (in Coulombs) passing through each of the specimens, displayed below by Table 4.18.

Table 4-19 Calculated Coulombs.

	First Dam Bridge	Sandy Bridge	Provo Canyon Bridge
Q (Coulombs)	1,046.61	1,709.01	1,436.22
Qs (Coulombs)	919.87	1,502.06	1,262.30

Comparing our results from Table 4.18 to the chloride ion permeability values based on charge passed (Table 4.16) we find that the three bridges are rated the following way:

1) **First Dam Bridge:** Very Low Chloride Ion Permeability ($100 < Q_s = 919.87 < 1,000$).

2) **Sandy Bridge:** Low Chloride Ion Permeability ($1,000 < Q_s = 1,502.06 < 2,000$).

3) **Provo Canyon Bridge:** Low Chloride Ion Permeability ($1,000 < Q_s = 1,262.30 < 2,000$).

5.0 TEST DESCRIPTION AND RESULTS OF NEW DECK MIXES

Concrete tests are often specified with the purpose of having a strict quality control and to assure compliance with the contract documents specifications. In other cases, like ours, tests are prescribed in order to characterize the concrete subject to research. Thus, it can be comparable to the results of other concrete tests. In addition, if the results of different research projects are to be compared, the tests on what those research are based should be performed following certain standards and procedures. In this case, the concrete material tests were performed on concrete from three decks in which UDOT was investigating. This testing includes samples from a precast bridge deck fabricated at Eagle Precast and two representative bridges built on the Legacy Highway. Figures 1 and 2 show the two UDOT bridges that the cast-in-place concrete samples were obtained.



Figure 5.1 Bridge 668



Figure 5.2 Bridge 669

In order to characterize the mechanical and durability properties of the concrete used for this research, five different tests were selected. The tests and the ASTM standard to which they conform are summarized in Table 5-1.

Table 5-17 Summary of Performed Tests

Test	ASTM Standard(s)
3.1 Compressive Strength	C 31 & C 39
3.2 Modulus of Elasticity	C 469
3.3 Shrinkage	C 157
3.4 Freeze and Thaw Resistance	C 666
3.5 Chloride Ion Penetration	C 1202

A more detailed description of each test in Table 3-1 is presented below.

5.1 Compressive Strength

The compressive strength of concrete is the most specified property of concrete; it is the most commonly used design criteria specified by engineers in the design process. Various reasons make the compressive strength the most used property of concrete, one of the primary reasons is, the testing of the compressive strength is fairly easy. In addition research has been conducted to correlate compressive strength to all other major properties of concrete, such as, elastic modulus, tensile strength, permeability and resistance to weather agents.

The compressive strength of concrete is determined by loading the testing specimen to failure. Failure being the state of deformation or cracking such as the material is no longer able to sustain the applied load.

In order to attain a certain level of quality in the concrete mixing, three key aspects must be taken into consideration: selection and proportioning of the materials, curing conditions, and tests specifications.

5.1.1 Selection and Proportioning of the Materials

Since concrete is the product of mixing different materials, the interaction of these materials influence the compressive strength of concrete. Consequently the selection and proportioning of the materials is critical. In the following paragraphs, the most common materials and their importance in the compressive strength of concrete is presented.

5.1.1.1 Cement Type

The material that has most influence on the concrete properties, with respect to the other components, is the cement. As much as it is in quality, as it is in quantity. Neville (1996) describes the Portland cement as a cement obtained by intimately mixing together calcareous and

argillaceous, or other silica, alumina, and iron oxide-bearing materials, burning them at a clinkering temperature, and grinding the resulting clinker.

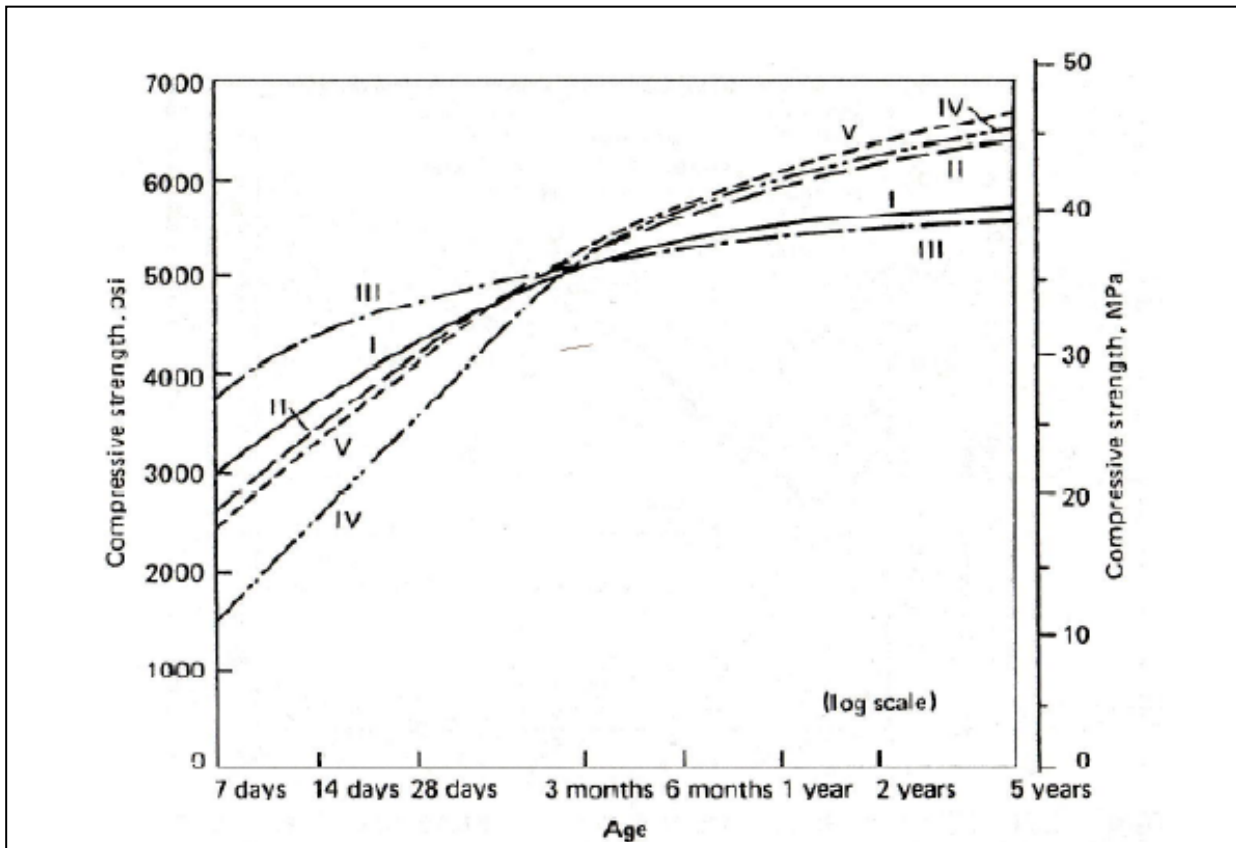


Figure 5.3 Effects of Type of Cement on Compressive Strength of Concrete (US Bureau of Reclamation, 1966)

The ASTM standard specification for Portland cement (ASTM C150) classifies the Portland cement into eight different types, manufactured to meet different chemical and physical requirements for specific purposes. The classification of the Portland cement given by the ASTM 150 is presented in Table 5-2.

Table 5-18 Classification of Portland Cement (ASTM 150)

Type	Use
I	When the special properties specified for any other type are not required
I A	Air-entraining cement for the same uses as Type I, where air-entrainment is desired
II	For general use, more specially where moderate sulfate resistance or moderate heat of hydration is desired.
II A	Air-entraining cement for the same uses as Type II, where air-entrainment is desired
III	For use when high early strength is desired
III A	Air-entraining cement for the same uses as Type III, where air-entrainment is desired
IV	For use when a low heat of hydration is desired
v	For use when high sulfate resistance is desired

When selecting the type of cement one particular property that affects the hydration of cement apart from its chemical composition, is the fineness of the cement ground. The finer the cement is ground, a direct increase in the hydration heat will occur, which results in early high strengths gains. A typical graph relating the cement fineness and the concrete strength at different ages is depicted in Figure 5-2.

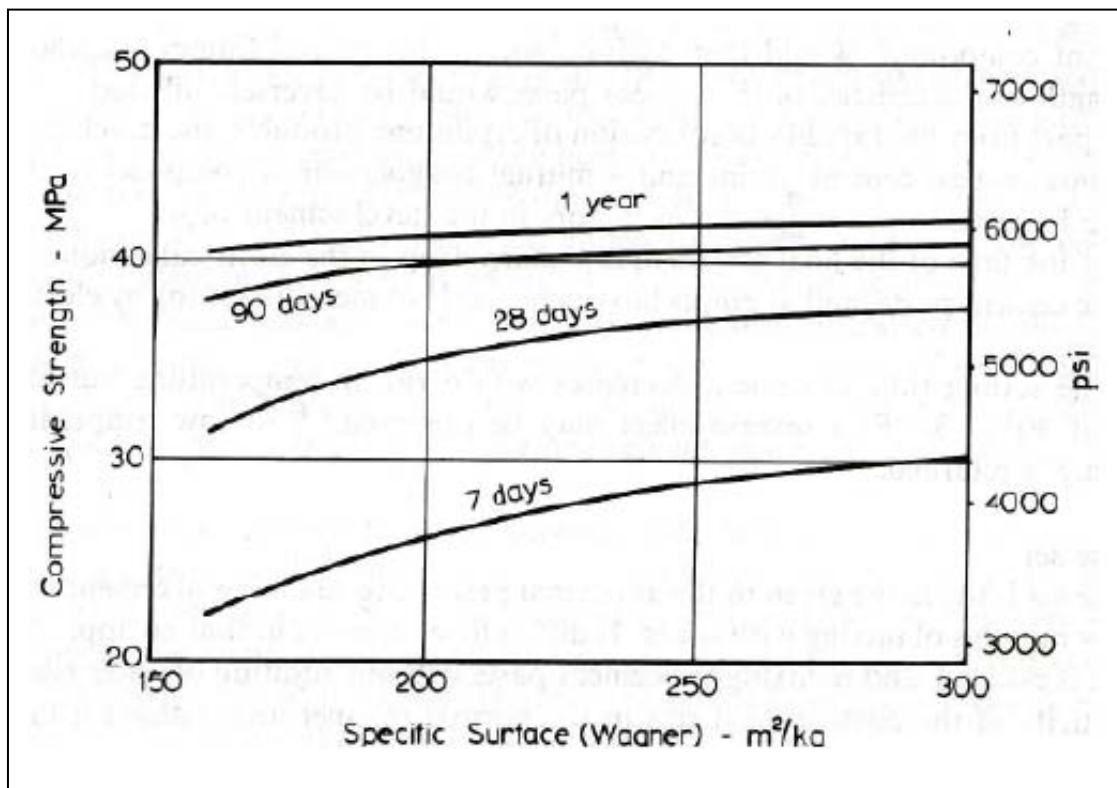


Figure 5.4 Relationship Between Fineness of Cement and Concrete Strength at Different Ages (Neville, 1996)

5.1.1.2 Water/Cement Ratio

The water cement ratio of any concrete mix should be selected considering two main factors, strength and workability. It has been vastly shown that the strength of concrete is conversely proportional to the water cement ratio. Therefore a lower w/c ratio results in a higher concrete strength. On the other hand, concrete mixes with too low of a w/c ratio lack of workability. Therefore, balance should be met between strength and workability.

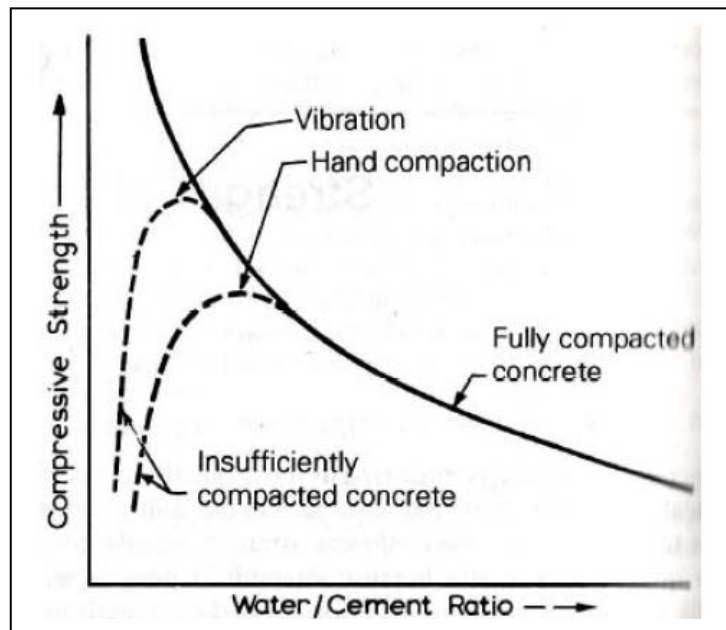


Figure 5.5 The Relation Between Strength and the Water/Cement Ratio of Concrete (Neville, 1996)

5.1.1.3 Aggregates

Since the aggregates occupy more than 60 percent of the concrete volume and are the strongest individual component, its properties influence the final compressive strength of the concrete. The fineness modulus and the maximum size of aggregate affects the fine to coarse aggregate proportion, as well as the water and cement quantities. Aggregate type also affects workability, economy and shrinkage tendencies.

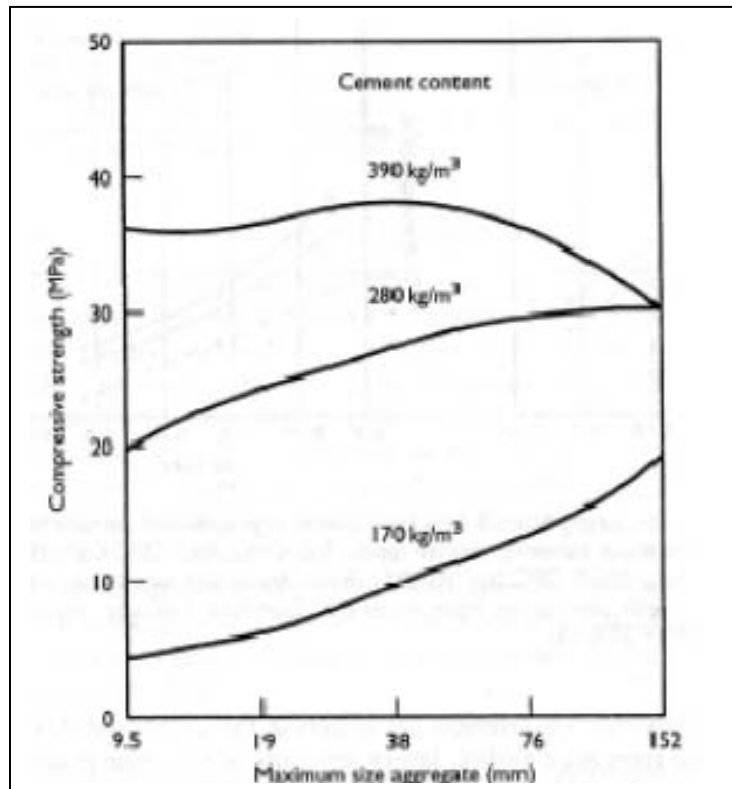


Figure 5.6. 28 day Compressive Strength of Concrete as Influenced by maximum size of aggregate and cement content (Higginson et al., 1963)

5.1.1.4 Admixtures

The concrete properties can be enhanced by the inclusion of admixtures. There are several types of admixtures, among them: water reducers, air entrainers, setting time retardants, etc. The most commonly used admixture to increase the compressive strength is the water reducer or superplasticizer, because they allow, for a given workability, less use of water, which traduces to a higher strength. The proportions of materials for the concrete mixes used for the scope of this research are listed in Table 5-3. For proprietary reasons, the mix design used in the Eagle Precast sample cannot be published in this research.

Table 5-19 Mix Designs

Materials	669 Bridge Deck	668 Bridge Deck
Cement (lbs/yd ³)	556	713
Fly Ash (lbs/yd ³)	103	178
Fine Aggregate (lbs/yd ³)	1604	1588
Coarse Aggregate (lbs/yd ³)	1355	1026
Water (lbs/yd ³)	270	348
w/cm	0.41	0.39

5.1.2 Curing Conditions

Since the concrete bleeds the excess water, and this water is evaporated due to the climate conditions, a humid environment should be provided to enhance the curing process. The proper concrete curing should start once the initial setting of the concrete has occurred, and common practice recommends that concrete should be cured for not less than seven days. The time of curing is directly proportional to the final strength of concrete; the longer the curing period, the higher the final strength of concrete.

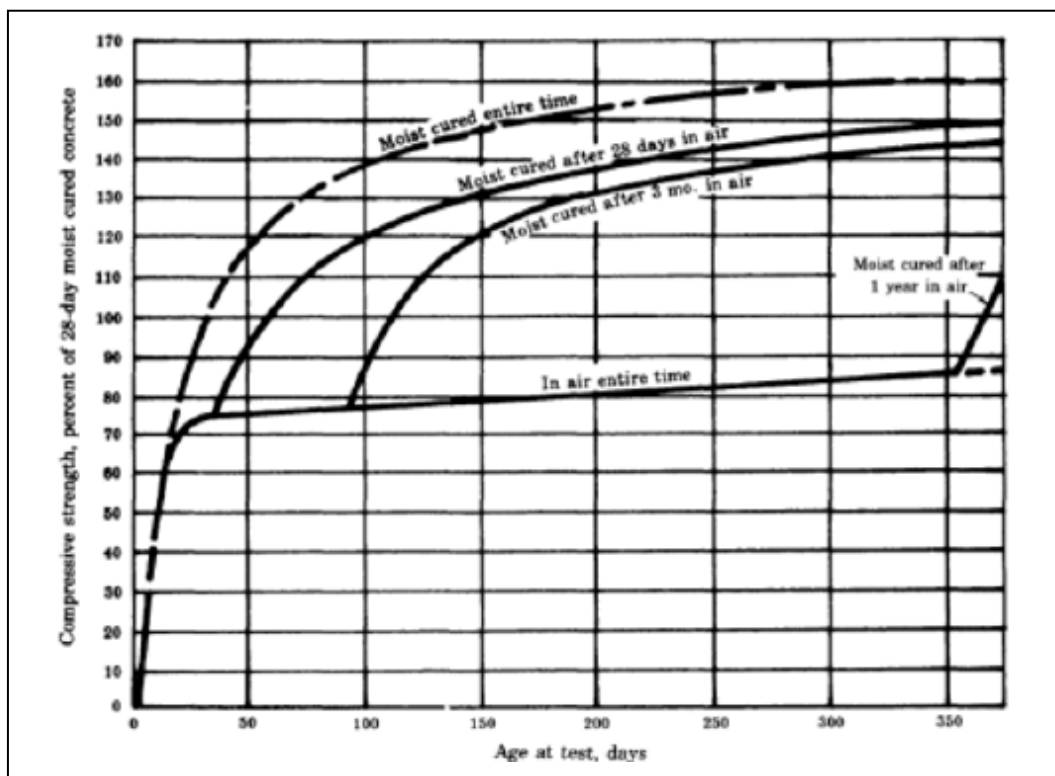


Figure 5.7. Curing on the Strength of Concrete (Portland Cement Association)

5.1.3 Test Specifications

All the compressive strength testing done for the scope of this research was made according to the provisions of the ASTM C39 Standard. The sampling of the concrete used in these tests conforms to the ASTM C31 Standard. The most common specimen used for the compressive strength testing was the 4 by 8 in. (diameter by height) cylinder.

For this project, the test cylinders were cast at the time each of the decks were poured. For the compressive strength test, 4 by 8 in. cylinders were cast. Proper curing conditions were provided for the testing cylinders. The standard ages for testing the compressive strength of concrete are: 1, 3, 7, 14, 28 and 56 days. Two cylinders were tested on each of testing days. The two cylinders were average to obtain the measured compressive strength. In order to calculate the compressive strength of the concrete Equation 4.2 was used.

The compressive strength tests results for the Eagle Precast Samples, the 669 Bridge Deck and the 668 Bridge Deck, are presented in Table 5-4, Table 5-5 and Table 5-6 respectively.

Table 5-20 Eagle Precast Compressive Strength Test Results

Days after Casting	Cylinder	Load (lb.)	σ (psi)	Avg. σ (psi)
1	4 x 8 (1)	77169	6141	6048
1	4 x 8 (2)	74825	5954	
3	4 x 8 (3)	105223	8373	9666
3	4 x 8 (4)	137702	10958	
7	4 x 8 (5)	122474	9746	9945
7	4 x 8 (6)	127473	10144	
14	4 x 8 (9)	138246	11001	11043
14	4 x 8 (10)	139284	11084	
28	4 x 8 (11)	151423	12050	12280
28	4 x 8 (12)	157200	12510	
56	4 x 8 (13)	161375	12842	12698
56	4 x 8 (14)	157762	12554	

Table 5-21 669 Bridge Deck Compressive Strength Test Results

Days after Casting	Cylinder	Load (lb.)	σ (psi)	Avg. σ (psi)
1	4 x 8 (1)	22712	1807	1834
1	4 x 8 (2)	23373	1860	
3	4 x 8 (3)	41576	3309	3162
3	4 x 8 (4)	37883	3015	
7	4 x 8 (5)	49790	3962	3960
7	4 x 8 (6)	49724	3957	
14	4 x 8 (9)	61922	4928	4828
14	4 x 8 (10)	59412	4728	
28	4 x 8 (11)	70006	5571	5796
28	4 x 8 (12)	75657	6021	
56	4 x 8 (13)	80580	6412	6388
56	4 x 8 (14)	79980	6365	

Table 5-22 668 Bridge Deck Compressive Strength Test Results

Days after Casting	Cylinder	Load (lb.)	σ (psi)	Avg. σ (psi)
11	4 x 8 (1)	57564	4581	4777
11	4 x 8 (2)	62496	4973	
19	4 x 8 (3)	69032	5493	5399
19	4 x 8 (4)	66655	5304	
28	4 x 8 (5)	75181	5983	5973
28	4 x 8 (6)	74948	5964	
56	4 x 8 (9)	85648	6816	6597
56	4 x 8 (10)	80158	6379	

It is shown in Tables 5-3 through 5-5, that the respective 28 compressive strength (f'_c) for the Eagle Precast, 669 Bridge Deck and 668 Bridge Deck, were 12,280 psi, 5,796 psi and 5,973 psi. It is important to mention that the Eagle Precast sample corresponds to the Self Consolidated High Performance Concrete used in the casting of the precast bridge decks. Each of the mix designs exceeded the required compressive stress of 4,000 psi according to the UDOT Bridge deck standards.

Figure 5-6 shows a plot of the compressive strength versus time for all three concrete samples.

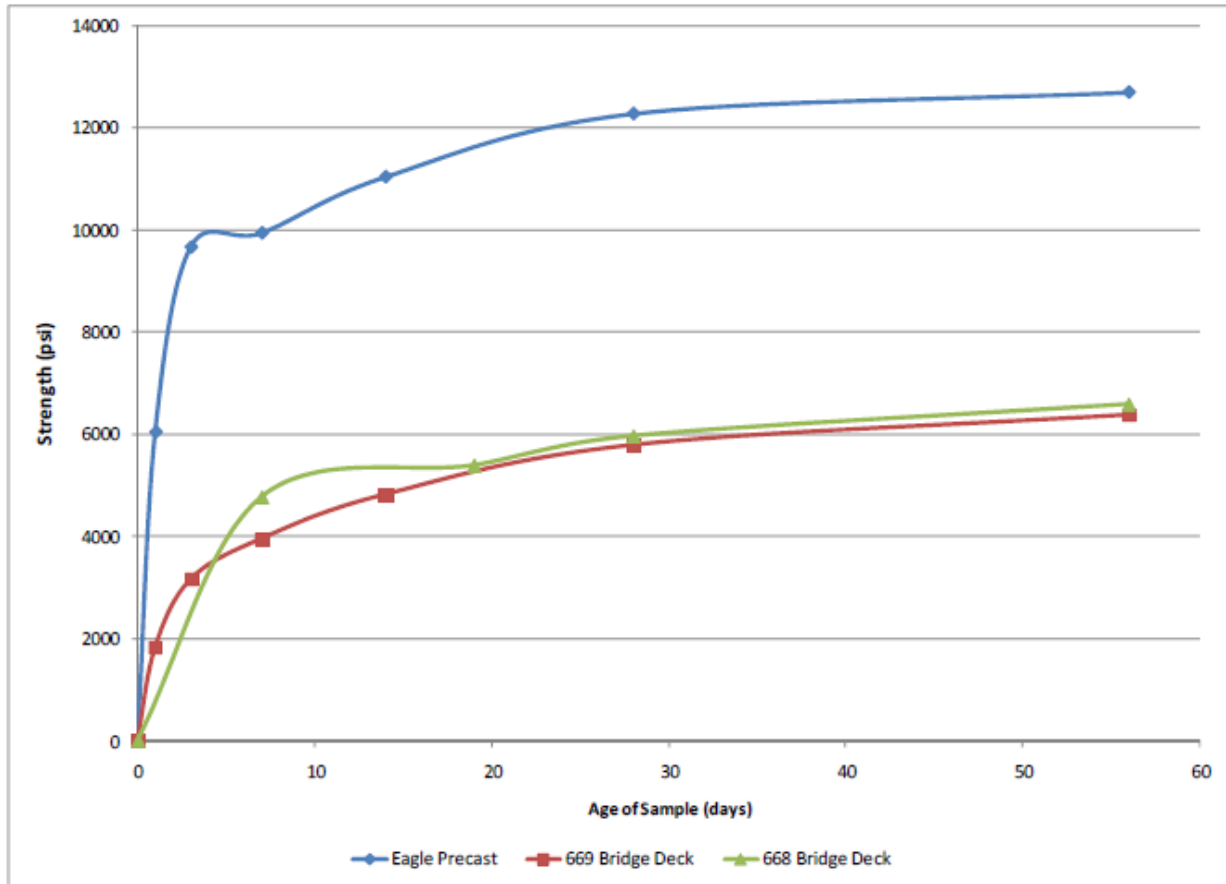


Figure 5.8. Compressive Strength vs. Time for all three Concrete Samples

5.2 Modulus of Elasticity

When the concrete is loaded within its elastic region, it is assumed that the stress is directly proportional to the strain. Taking advantage of this property, a concrete specimen can be axially loaded, and the shortening of the cylinder in the direction of the load is measured. Knowing the cross-sectional area of the cylinder and the length of the gauge, measuring the deformation the stress and strain can be calculated and then plotted on a curve. The slope of that curve in the elastic region is a measure of the modulus of elasticity.

For this research the procedures followed to perform the Modulus of Elasticity test were those contained in the ASTM C469 Standard. The concrete sample used for these tests consisted in 6 by 12 in. cylinders.

When conducting a Modulus of Elasticity test, two aspects must be taken into consideration: 1) the loading speed and 2) the maximum load applied.

For the first aspect, the ASTM standard states that the rate of loading is to be in the range of 35 ± 5 psi/s (in our case 59,000 lbs/min), and this loading rate must remain constant throughout the duration of the test. The reason for having a loading range is because at slower rates of loading additional creep can be developed in the specimen. This creep effect can be reduced by a more rapid rate of loading. For the second aspect, the ASTM procedure mandates that the maximum load applied to the specimen shall not exceed 40 percent of the tested ultimate load. The justification for this limit is due to micro cracks that develops at higher loads and propagates throughout the specimen negatively affecting the curvature of the stress – strain curve.

Two 6 by 12 in. specimens were tested at the ages of: 1, 3, 7, 14, 28 and 56 days. For each day, an average modulus of elasticity was calculated for each set of samples. The testing procedure was as follows: first a 4 by 8 in. cylinder was tested in order to determine the ultimate compressive strength of the concrete sample. Second, the 6 by 12 in. cylinders were loaded to the equivalent load that produces 40 percent of the ultimate strength. During the test the deflections were monitored with an electronic LVDT. The loading was registered in the data acquisition system and use to calculate the modulus of elasticity using the Eq. 5-1.

$$E = \frac{\sigma_1 - \sigma_2}{\varepsilon_2 - 0.000050} \quad \text{(Equation 5-1)}$$

Where:

E= Chord or Secant Modulus of Elasticity (psi).

σ_2 = Stress at 40 percent of the failure load (psi).

σ_1 = Stress at a longitudinal strain of 0.000050.

ε_2 = Strain corresponding to stress σ_2 .

The results of the modulus of elasticity tests performed to the Eagle Precast concrete samples are shown in Table 5-7.

Table 5-23 Eagle Precast Sample Modulus of Elasticity

Test Age (d)	Average E (psi)
1	3.318E+06
3	4.017E+06
7	4.460E+06
14	4.991E+06
28	4.815E+06
56	5.074E+06

The results of the modulus of elasticity tests performed to the 669 Bridge Deck concrete are shown in Table 5-8.

Table 5-24 669 Bridge Deck Sample Modulus of Elasticity

Test Age (d)	Average E (psi)
1	2.580E+06
3	3.191E+06
7	3.751E+06
14	3.872E+06
28	4.389E+06

The results of the modulus of elasticity tests performed to the 668 Bridge Deck concrete are shown in Table 5-9.

Table 5-25 668 Bridge Deck Sample Modulus of Elasticity

Test Age (d)	Average E (psi)
11	4.210E+06
18	4.117E+06
28	4.407E+06
60	4.447E+06

A plot of Modulus of Elasticity vs. time is depicted in Figure 5-7. As expected the modulus of elasticity reduces its rate of increasing after 28 days. The higher modulus of elasticity was observed in the concrete of the Eagle Precast sample, with a modulus of elasticity of 4,815 ksi., this was expected, since the modulus of elasticity is dependent on the concrete strength, and this is the concrete with the highest specified strength.

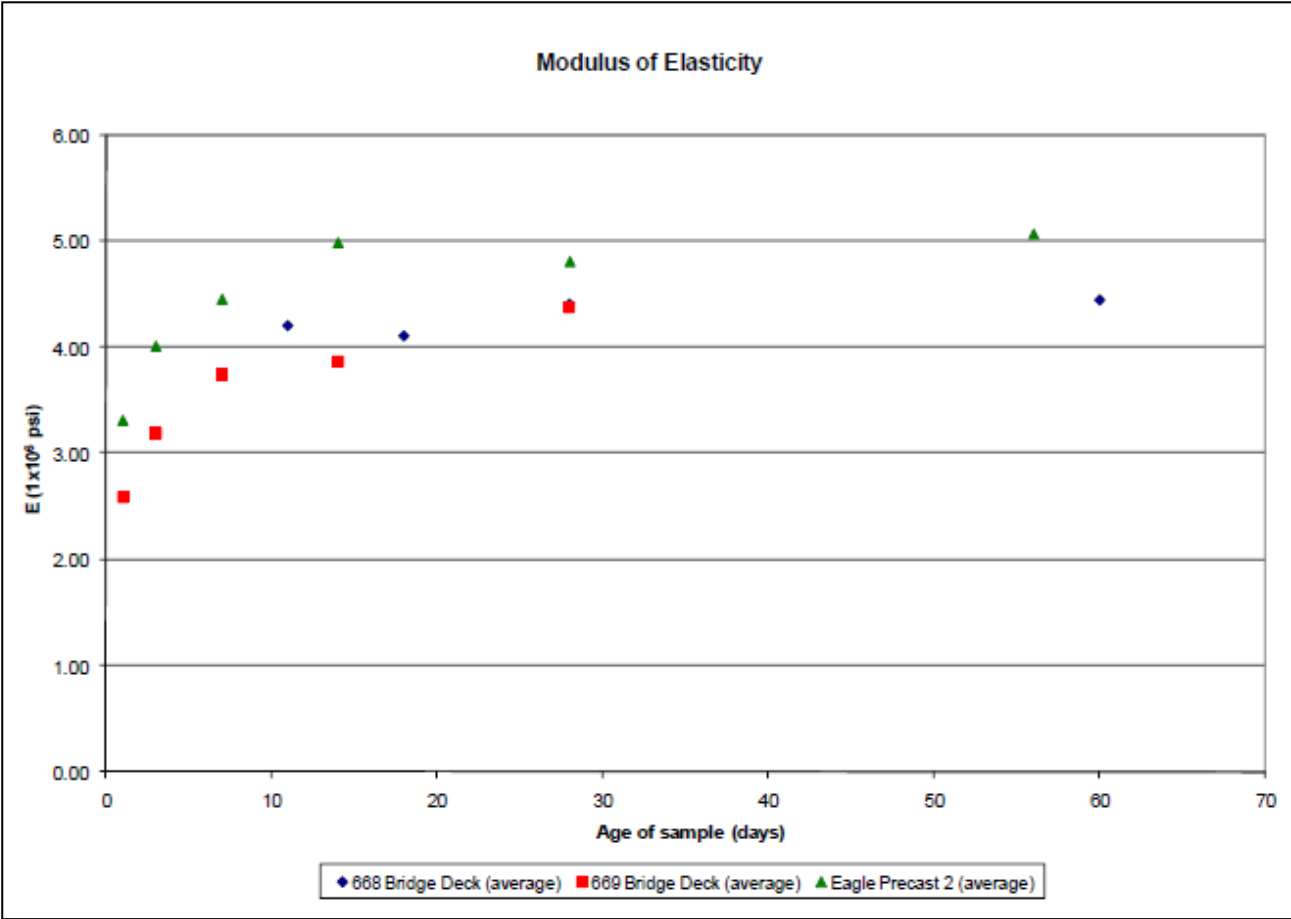


Figure 5.9. Summary of the Modulus of Elasticity vs. Time for all Three Samples

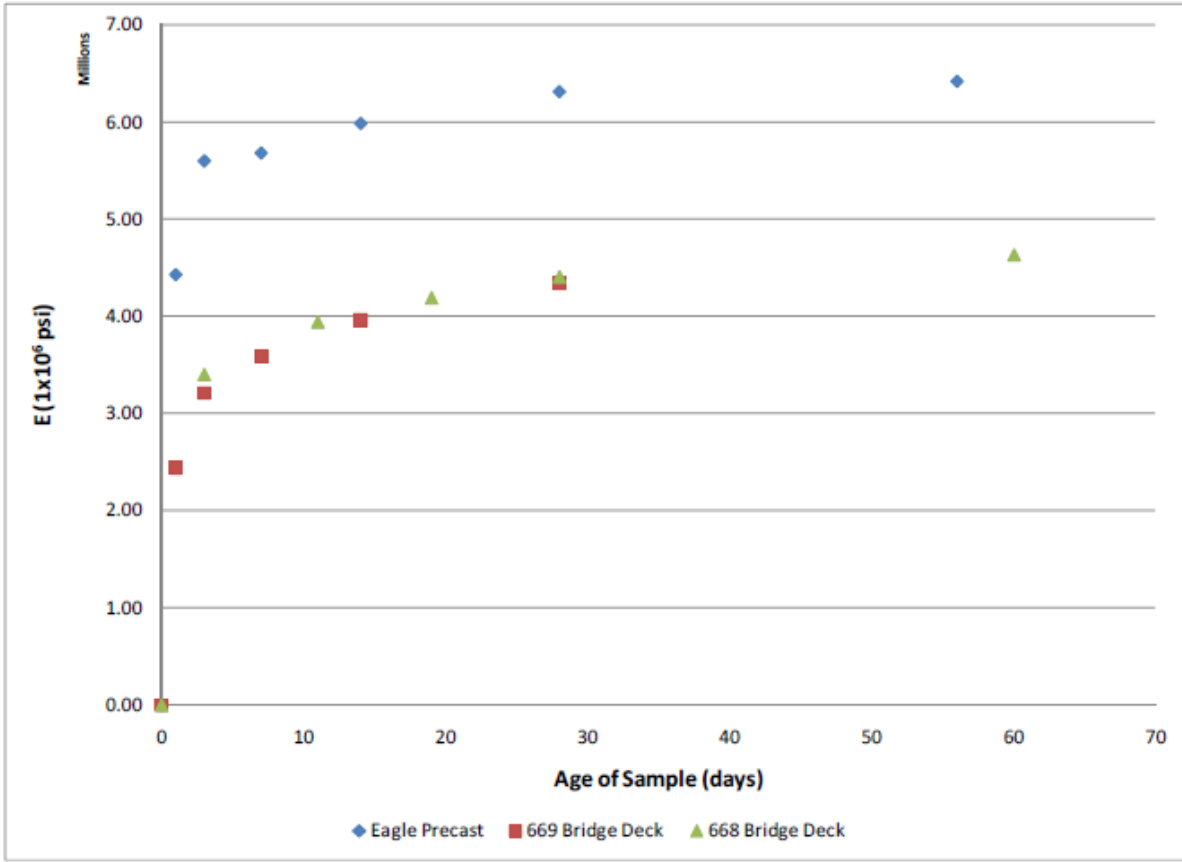


Figure 5.10. Modulus of Elasticity Calculated using Equation 4-4

Figure 5-8 shows a plot of the modulus of elasticity calculated using equation 4-4 given by the ACI 318 §8.5.1 and the measured values of average σ (psi) on Tables 5-3, 5-4 and 5-5 for the different concrete samples.

It can be observed that the Equation 4-4 overestimates the values of modulus of elasticity for the higher strength concrete (Eagle Precast) with a ratio of the calculated over the measured of 1.31 at 28 days of age. For the samples pertaining to the 669 Bridge Deck and 668 Bridge Deck, the Equation 3-3 gives a very accurate results with a ratio of the calculated over the measured of 0.98 and 0.99 respectively at 28 days of age.

5.3 Shrinkage

Since the concrete is a porous solid, it shares a property common to most porous solids in that it shrinks as a result of a reduction of its water content. Since the most common use of concrete is in the making of reinforced concrete structures, the restraint imposed to the concrete by the inclusion of reinforcing steel causes induced stresses to develop in the structure. If these stresses are higher than the tensile strength of concrete, cracks will form, compromising the structural integrity of the structure.

The shrinkage of the concrete is influenced by the elastic properties of the cement paste and aggregates and their shrinkage. In addition to the influence of the restraint imposed by the aggregates and the unhydrated cement, the relative humidity of the environment, drying time and water cement ratio also influence the magnitude of the shrinkage. Because shrinkage is affected by so many different factors, accurate predictions are difficult to determine.

The shrinkage tests performed on the concrete deck samples for this research were made following the provisions in the ASTM C157 standard. The test specimens consisted of concrete prisms with dimensions equal to 3" x 3" x 16". Metal studs were embedded at both ends of the specimen, in order to fit the reading apparatus. The specimens were kept out of the moisture room, in order to simulate field curing conditions.

An electronic gage comparator system was used to take readings at the ages of: 3, 7, 14, 28, 56 and 118 days. Shrinkage strain at each test day was calculated using the Equation 4-5. The results are shown in Table 5-10, Table 5-11 and Table 5-12.

Table 5-10 Strain of Eagle Precast Samples in $\mu\epsilon$

age (days)	Eagle Precast Samples			Average
	1	2	3	
1	0.0	0.0	0.0	0.0
7	162.3	215.5	324.6	234.1
14	220.3	268.1	314.5	267.6
28	353.6	307.2	394.2	351.7
56	394.2	365.2	452.2	403.9
118	426.7	401.6	492.3	440.2

Table 5-26 Strain of 669 Bridge Deck Samples in $\mu\epsilon$

age (days)	669 Bridge Deck (15% replacement)			Average
	1	2	3	
1	0.0	0.0	0.0	0.0
7	272.5	220.3	208.7	233.8
14	440.6	353.6	481.2	425.1
28	539.1	452.2	608.7	533.3
118	581.3	493.6	626.7	567.2

Table 5-27 Strain of 668 Bridge Deck Samples in $\mu\epsilon$

age (days)	668 Representative Deck (25% replacement)			Average
	1	2	3	
1	0.0	0.0	0.0	0.0
19	219.3	255.1	0.0	237.2
28	413.0	401.1	0.0	407.1
60	488.4	494.2	0.0	491.3
118	568.7	575.6	0.0	572.2

A plot of the strain of all three samples vs. time is shown in Figure 5-9.

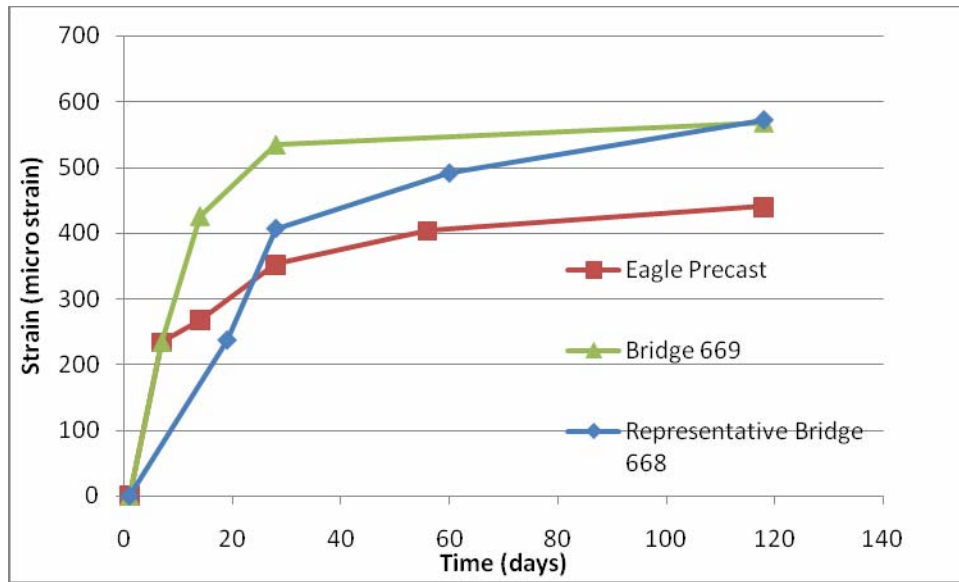


Figure 5.11. Strain vs. Time

5.4 Freeze & Thaw

Most concrete decks are exposed to climate changes. When the structure is subjected to some degree of saturation, a problem arises; this problem is the freezing of the water entrained in the concrete. Since water increases in volume by approximately 9 percent, this expansion translates in pressurizing the water in the concrete pores, and if this pressure exceeds the concrete capacity in tension, a crack will form. In addition, concrete subjected to repeated cycles of freezing and thawing deteriorates over time.



Figure 5.12. Freeze Thaw Chamber

This problem is aggravated when thawing occurs. Thawed water migrates to other parts of the structure, resulting in different cracks. When the structure is subjected to various cycles of freezing and thawing different parts of the structure begin to crack. In the beginning this could express as surface scaling, but in advanced stages this could become in permanent damage to the concrete deck.

The resistance of the concrete to these freeze-thaw cycles is dependant of many factors, such as the strength of the hardened cement paste, air entrained in the concrete and its porosity. A concrete with a low water to cement ratio will be less likely to be affected by the freeze and thaw cycles, due to its relatively low porosity.



Figure 5.13. Concrete Samples for the Freeze-Thaw Test

In order to simulate this freeze-thaw condition in the lab, 3" x 3" x 16" samples of concrete were made (Figure 3-11) from each of the deck concretes. The procedure followed to perform this test was the one described in the ASTM C666 Standard, Procedure A. The test specimens were placed in a freeze/thaw chamber submerged in water (Figure 3-10), the water above the surface of the test specimens couldn't be lower than 1/32" and couldn't surpass 1/8". The test specimens remained in the freeze-thaw chamber for approximately 300 cycles. Every 30 cycles the test was stopped, and then the fundamental transverse natural frequency of the test specimen was measured using a Dynamic Signal Analyzer (Figure 3-12).



Figure 5.14. Dynamic Signal Analyzer

With these values of fundamental natural frequency, the Relative Dynamic Modulus of Elasticity can be calculated using Eq.4.6.

The values of the fundamental transverse natural frequency collected from each of the deck samples are listed in the Table 5-14.

Table 5-28 Fundamental Transverse Natural Frequencies

No. Cycles	Frequency (KHz)							
	Eagle Precast 2			669 Bridge Deck			668 Bridge Deck	
	Sample 1	Sample 2	Sample 3	Sample 1	Sample 2	Sample 3	Sample 1	Sample 3
0	4.82	4.90	4.64	4.82	4.79	4.78	4.78	4.75
68	4.63	4.74	4.12	4.75	4.83	4.84	4.72	4.76
108	4.67	4.74	N/A	N/A	4.84	N/A	4.92	4.91
138	4.98	5.06	N/A	4.95	5.07	5.07	5.06	5.02
168	4.90	5.05	N/A	4.70	4.85	4.92	5.02	5.01
198	4.89	5.01	N/A	4.85	4.86	4.90	5.05	5.04
228	4.78	5.04	N/A	4.81	4.81	4.98	5.09	5.07
258	4.90	5.05	N/A	4.72	4.87	4.93	5.10	5.06
288	4.88	5.00	N/A	4.88	4.92	4.95	5.13	5.01
318	4.92	5.02	N/A	4.89	4.96	5.01	5.10	5.10

From Table 5-14, it can be seen that no data could be acquired from the Eagle Precast sample 3 due to excessive deterioration of the sample as can be seen in Figure 5-13.



Figure 5.15. Eagle Precast Sample 3

Using Eq. 5-5, and the fundamental natural frequencies data contained in Table 5-14, the Relative Dynamic Modulus of Elasticity was calculated, the results are in Table 5-15.

Table 5-29 Relative Dynamic Modulus of Elasticity

No. Cycles	Frequency (KHz)							
	Eagle Precast 2			669 Bridge Deck			668 Bridge Deck	
	Sample 1	Sample 2	Sample 3	Sample 1	Sample 2	Sample 3	Sample 1	Sample 3
0	100.00	100.00	100.00	100.00	100.00	100.00	100.00	100.00
68	96.16	96.73	88.79	98.55	100.84	101.26	98.64	100.11
108	96.99	96.73	N/A	N/A	4.84	N/A	102.76	103.22
138	103.39	103.31	N/A	102.61	105.76	106.11	105.73	105.58
168	101.77	103.06	N/A	97.51	101.25	102.93	104.96	105.43
198	101.56	102.24	N/A	100.62	101.46	102.51	105.58	105.96
228	99.27	102.86	N/A	99.79	100.42	104.18	106.42	106.59
258	101.77	103.06	N/A	97.93	101.67	103.14	106.61	106.44
288	101.35	102.04	N/A	101.24	102.71	103.56	107.25	105.43
318	102.18	102.45	N/A	101.45	103.55	104.81	106.52	107.32

Table 5-16 shows the durability factors calculated for every sample. From the results it can be seen that the lowest durability factor for either sample was no lower than 0.96.

Table 5-30 Durability Factors

No. Cycles	Frequency (KHz)							
	Eagle Precast 2			669 Bridge Deck			668 Bridge Deck	
	Sample 1	Sample 2	Sample 3	Sample 1	Sample 2	Sample 3	Sample 1	Sample 3
0	1.00	1.00	1.00	1.00	1.00	1.00	1.00	1.00
68	0.96	0.97	0.89	0.99	1.01	1.01	0.99	1.00
108	0.97	0.97	N/A	N/A	1.01	N/A	1.03	1.03
138	1.03	1.03	N/A	1.03	1.06	1.06	1.06	1.06
168	1.02	1.03	N/A	0.98	1.01	1.03	1.05	1.05
198	1.02	1.02	N/A	1.01	1.01	1.03	1.06	1.06
228	0.99	1.03	N/A	1.00	1.00	1.04	1.06	1.07
258	1.02	1.03	N/A	0.98	1.02	1.03	1.07	1.06
288	1.01	1.02	N/A	1.01	1.03	1.04	1.07	1.05
318	1.02	1.02	N/A	1.01	1.04	1.05	1.07	1.07

5.5 Chloride Ion Penetration

The chlorides do not attack the concrete directly; they attack the reinforcing steel, being a major cause of corrosion of the rebar. Once corrosion commences, the rebar expands, subsequently cracking the concrete. This is why the study of the chloride ion penetration through the deck concrete cover is important.

The chlorides ions can be present in the concrete from different sources; one of the major causes of the presence of chloride ions in bridge decks is the deicing salt. Other important source of chloride ions is the sea water in contact with concrete structures, airborne sea water drops that travels from the sea shore into the main land. Submerged structures are subject to a deeper penetration of the chloride ions, but since oxygen is not present in the cathode corrosion of the steel is not a problem.



Figure 5.16. Chloride Ion Penetration Apparatus

The procedure followed in this research for investigating the ability of the concrete deck samples to resist the chloride ion penetration is the one described in the ASTM C1202 standard. For this test, two samples of each concrete deck were prepared. The preparation of the samples was as follows: first two slices of two inches in thickness were cut from a 4 by 8 in. concrete cylinder; the concrete was then covered in the side surface by a concrete water sealant, in order to prevent water migrating from the inside. After that the samples were placed in a vacuum desiccator (Figure 5-15) and the air was removed over a 3-hour period. After which, the specimen was left to soak in distilled water for 18 hours.



Figure 5.17. Vacuum Desiccator Apparatus

Subsequently, the specimen was removed from the water, the excess water was blotted off, and the specimen was transferred to the testing apparatus. The contact surface between the specimen and the testing apparatus was sealed with a special silicone sealer. Then the cell that is connected to the negative terminal of the power supply was filled with a 3.0 percent NaCl solution, the other cell (the one that is connected to the positive terminal of the power supply) with a 0.3 N NaOH solution. Connections were made through a voltage power supply. The power was turned on then the voltage was set to $60.0 \text{ V} \pm 0.1 \text{ V}$ and the initial current was then registered. For a period of 6 hours, the current was read and recorded every 30 minutes.

According to the ASTM C1202, the total charge passed through the 2-inch specimen is a measure of the conductance of the concrete during the period of the test. Since the current was recorded every 30 minutes, the standard recommends using Equation 4.7 for calculating the charge passed by the specimen:

This test is standardized for specimens with a diameter of 3.75 inches. Since our specimens were 4 inches in diameter a correction shall be made according to the ASTM, using the Equation 4.8.

Table 5-17 shows the recorded current readings for all of the three samples.

Table 5-31 Recorded Current Readings

Minutes elapsed	Current (miliamp)					
	Eagle Precast		669 Bridge Deck		668 Bridge Deck	
	1	2	1	2	1	2
0	13.6	16.5	37.4	40.0	42.1	38.2
30	11.5	16.3	35.4	40.0	44.3	38.1
60	10.8	15.2	35.1	38.2	46.8	38.0
90	10.3	15.0	34.8	38.1	49.0	37.5
120	10.0	15.0	34.5	37.8	50.3	37.3
150	9.4	14.8	34.5	37.6	51.0	37.2
180	9.1	14.7	33.8	37.5	51.9	37.3
210	8.9	14.5	33.7	37.1	52.3	36.9
240	8.7	14.1	33.6	37.1	53.0	36.8
270	8.6	14.0	33.3	36.5	53.1	36.7
300	8.5	14.0	33.0	36.4	53.3	36.8
330	8.4	13.9	33.0	36.7	53.5	36.3
360	8.2	13.9	33.1	36.4	54.0	36.1

Using these recorded readings and with the aid of Eq. (4-6) the charge passed was calculated and the results are given in the Table 5-18.

Table 5-32 Charge Passed Through the Specimens (coulombs)

	Eagle Precast	669 Bridge Deck	668 Bridge Deck
Q(coulombs)	262.6	775.0	947.3
Q _s (coulombs)	230.8	681.2	832.6

The ASTM C1202 gives some guidelines for comparing the results obtained in this test. These guidelines are presented in Table 3-19 excerpted for the standard.

Table 5-33 Chloride Ion Permeability Based on Charged Passed

Charge Passed (coulombs)	Chloride Ion Penetrability
>4,000	High
2,000–4,000	Moderate
1,000–2,000	Low
100–1,000	Very Low
<100	Negligible

Judging by the results presented in Table 5-18, and comparing with the guidelines

in Table 5-19, all three concretes have very low chloride ion

6.0 CONCLUSION

In an effort to improve the Utah Department of Transportation concrete deck mix design, experimental testing performed and curing practices were observed on three UDOT bridge decks. Each of the three bridges were located in different regions and the concrete was supplied by different contractors. The material test results and observed curing practices from these three bridges were used to establish a baseline of the current state-of-practice. After the baseline properties of the current UDOT mix design was obtained, three additional proposed mix designs were evaluated. A comparison of the results led to the following conclusions::

6.1 Test Results for Current UDOT Mix Design

The following results are based on the material testing based on concrete deck samples from the existing UDOT mix design standards.

▪ **Compressive Strength tests** showed the following for each of the bridges:

- For the **First Dam Bridge (Logan)**, a 28 day compressive strength of 4,834 Psi and a 56 day compressive strength of 5,332 Psi.

- For the **Bridge in Sandy**, a 28 day compressive strength of 5,889 Psi and a 56 day compressive strength of 6,480 Psi.

- For the **Bridge in Provo Canyon**, a 28 day compressive strength of 5,570 Psi and a 56 day compressive strength of 6,778 Psi.

It can be stated, therefore, that 28 day compressive strength for all three bridges was in the range of 4,500 – 6,000 Psi.

▪ **Tensile Strength tests** showed the following for each of the bridges:

- For the **First Dam Bridge (Logan)**, a 28 day tensile strength of 208 Psi and a 56 day tensile strength of 240 Psi.

- For the **Bridge in Sandy**, a 28 day tensile strength of 327 Psi and a 56 day tensile strength of 431 Psi.

- For the **Bridge in Provo Canyon**, a 28 day tensile strength of 240 Psi and a 56 day tensile strength of 305 Psi.

It can be stated, therefore, that 28 day tensile strength for all three bridges was in the range of 200 – 350 Psi.

▪ **Modulus of Elasticity tests** showed the following for each of the bridges:

- For the **First Dam Bridge (Logan)**, a 28 day modulus of elasticity of 4.37×10^6 Psi and a 56 day modulus of elasticity of 4.30×10^6 Psi

- For the **Bridge in Sandy**, a 28 day modulus of elasticity of 5.41×10^6 Psi and a 56 day modulus of elasticity of 5.41×10^6 Psi.

- For the **Bridge in Provo Canyon**, a 28 modulus of elasticity of 5.34×10^6 Psi and a 56 day modulus of elasticity of 5.34×10^6 Psi.

It can be stated, therefore, that the 28 day modulus of elasticity for all three bridges was in the range of 4.30×10^6 Psi – 5.50×10^6 Psi.

▪ **Shrinkage tests** showed the following for each of the bridges at 116 days:

- For the **First Dam Bridge (Logan)**, the strain at 116 days reached a value of: 5.440×10^{-4} .

- For the **Bridge in Sandy**, the strain at 116 days reached a value of: 0.969×10^{-4} .
- For the **Bridge in Provo**, the strain at 116 days reached a value of: 0.687×10^{-4} .
- **Freeze-Thaw durability tests** showed a durability factor (DF) staying pretty much around 1.00 throughout the 300 cycles of the test.
- **Chloride-Ion permeability tests** showed the following for each of the bridges:
 - For the **First Dam Bridge (Logan)**, Very Low Chloride Ion Permeability ($100 < Q_s = 919.87 < 1,000$).
 - For the **Bridge in Sandy**, Moderate Chloride Ion Permeability ($1,000 < Q_s = 1,502.06 < 2,000$).
 - For the **Bridge in Provo Canyon**, Low Chloride Ion Permeability ($1,000 < Q_s = 1,262.30 < 2,000$).

Because there is a lack of correlation between field conditions and laboratory performance, these results are only guidelines as to what the long-term durability and strength performance of the in-situ bridge. Other factors, such as the adequate placement and curing of concrete and the existence or absence of early loading, will ultimately dictate what the actual durability and strength of the bridge.

6.2 Summary of Current Curing Practices

None of the three bridge decks that were observed after casting were most cured for the required 14 days. All decks were cover after casting and kept moist initially, but after as few as three days the decks were allowed to dry out. The moist cure for the Region 1 bridge was all but eliminated after 5 days. Similarly, the curing of the Region 2 and Region 3 bridges after 6 and 8 days respectively.

6.3 Test Results for Variations to UDOT Mix Design

- The 28 day compressive strength for the Eagle precast sample was 12,280 psi, for the 669 Bridge deck sample was 5,796 psi and for the 668 Bridge Deck sample was 5,973 psi.
- The Secant modulus of elasticity for the Eagle Precast sample at the age of 28 days was 4.85×10^6 psi, for the 669 Bridge deck was 4.389×10^6 psi at the same age and for the 668 Bridge deck was 4.407×10^6 psi.
- The shrinkage tests performed showed that the strain at 28 days for the Eagle precast concrete reached a value of 351.7×10^{-6} $\mu\epsilon$, for the 669 Bridge deck concrete the strain at 28 days was 533.3×10^{-6} $\mu\epsilon$ and for the 668 Bridge deck concrete, at the same age, was 307.2×10^{-6} $\mu\epsilon$.
- Freeze and thaw test showed very consistent results for all three samples, consisting of Durability Factors around 1 for all three concrete samples.
- Chloride Ion penetration test showed that the total charge passed through the Eagle precast concrete specimens was 230.8 coulombs, for the 669 Bridge deck concrete specimens was 681.2 coulombs and for the 668 Bridge deck concrete was 832.6 coulombs. Having all three concrete samples very low chloride ion permeability.

REFERENCES

Mehta, P. Kumar and Monteiro, Paulo J.M. *Concrete: Microstructure, Properties, and Materials*. McGraw Hill, Third Edition, 2006, p 49-128.

Mehta, P. Kumar and Monteiro, Paulo J.M. *Concrete: Microstructure, Properties, and Materials*. McGraw Hill, Third Edition, 2006, p 49-128.

Salem, R. and Burdette, E. *Development of an Optimal High-Performance Concrete Mixture for Tennessee Bridge Decks*. High Performance Structures and Materials, v 7, High Performance Structures and Materials II, 2004, p 361-369.

Streeter, Donald A. *Developing High – Performance Concrete Mix for New York State Bridges*. Transportation Research Record, n 1532, Sep, 1996, p 60-65.

Tikalsky, P.J. and Carrasquillo, R.L. *Influence of Fly Ash on the Sulfate Resistance of Concrete*. ACI Materials Journal (American Concrete Institute), v 89, n 1, Jan-Feb, 1992, p 69-75.

Waszczuk, Christopher M. and Juliano, Michelle L. *Application of High Performance Concrete (HPC) in a New Hampshire Bridge*. Concrete International, v 21, n 2, Feb, 1999, p 61-62.

Yunping Xi, Benson Shing, and Zhaohui Xie. *Development of Optimal Concrete Mix Designs for Bridge Decks*. Report No. CDOT-DTD-R-2001-11. Department of Civil, Environmental, and Architectural Engineering, University of Colorado, Boulder, CO, 2001.

APPENDIX A
SIGNAL ANALYZER SETUP FOR FREE-FREE RESONANT
COLUMN TEST

The following steps outline the setup of the analyzer required to begin a free-free resonant column test, as well as the steps required to measure the resonant frequency taking an average of measurements.

I. Setup

- a. Turn on the power to the analyzer by pushing in the power key in the lower left hand corner.
- b. Touch the Save / Recall button.
- c. Touch the Default Disk soft key.
- d. Touch the Non-Vol Ram Disk soft key.
- e. Key the Catalog soft key to Catalog On.
- f. Using the turn-wheel scroll to FFRC.sta
- g. Touch the Save / Recall button.
- h. Touch the Recall State soft key.
- i. Touch the Enter soft key.
- j. Key the Catalog soft key to Catalog Off.
- k. When the accelerometer is set on the specimen and you are ready to begin recording data touch the Start Button.

II. Measuring Resonant Frequency

- a. Strike the specimen.
- b. Touch the Avg. button.
- c. Touch the Avg. Preview soft key.

- d. Touch the Accept Time Record soft key (if the time record shows a considerable amount of noise, touch the Reject Time Record soft key and try again).
- e. Using the touch-wheel scroll the marker the peak frequency. Record this response.
- f. Touch the Freq. button.
- g. Touch the Center soft key.
- h. Enter the recorded peak frequency.
- i. Touch the Span soft key.
- j. Enter an appropriate span.
 - i. Aluminum – 300 Hz
 - ii. Concrete – 800 Hz
 - iii. Steel – 300 Hz
 - iv. Wood – 1 kHz
- k. Touch the Start Button.
- l. Repeat steps a. – d. until the 5 measurements have been taken.
- m. Touch the Pause / Cont. Button.
- n. Take one more measurement by repeating steps a. – d. once.
- o. Touch the Pause / Cont. Button.
- p. Using the touch-wheel, scroll the marker to the peak amplitude response.
- q. Record this peak response and resonant frequency.

III. Saving and Recalling Data

- a. After performing all of the steps of Section 3.4.III touch the Save / Recall button.
- b. Touch the Default Disk soft key.
- c. Touch the Internal Disk soft key.
- d. Insert a 3.5" floppy disk into the disk drive.
- e. Touch the Save / Recall button.
- f. Touch the Save Data soft key.
- g. Key the Format soft key to ASCII.

- h. Touch the Save Trace soft key.
- i. Touch the Into File soft key.
- j. Name the file an appropriate name (Aluminum – ALUM.TXT, etc.)
- k. Touch the Enter soft key.
- l. The data is saved as four files. The user should only be concerned with the two text files. One is designated as the x-axis data and the other is designated simply by the name chosen in step j. of this section.
- m. Open the text files and paste the values into Microsoft Excel. Using the values create a plot of the frequency response curve.

APPENDIX B

STRESS VS. STRAIN PLOTS, MODULUS OF ELASTICITY TESTS

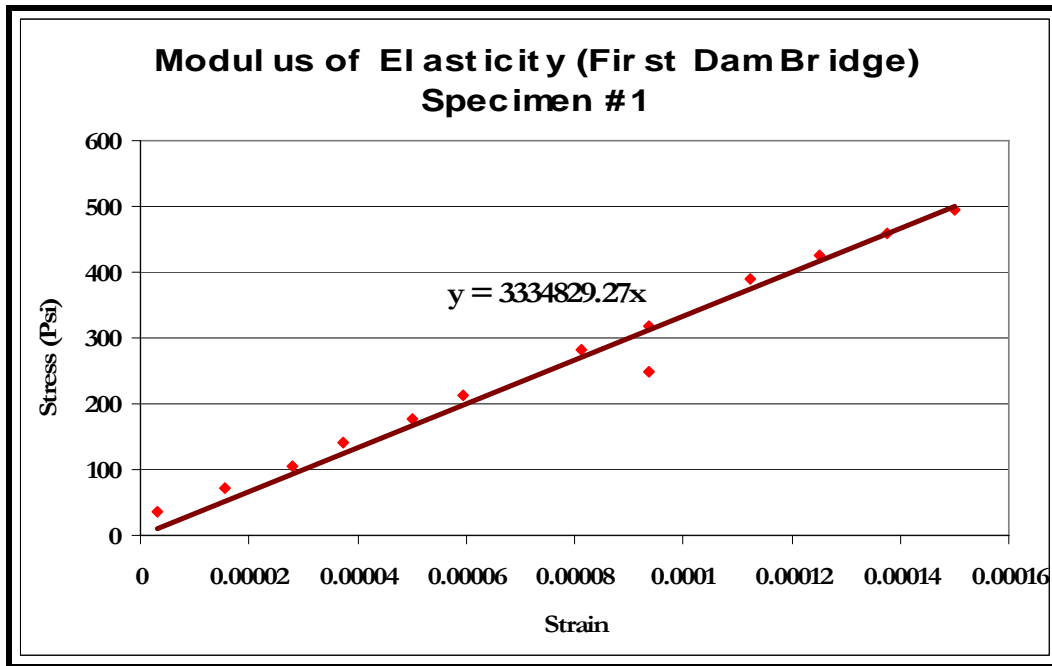


Figure B. 1 M.O.E First Dam Bridge Day 3

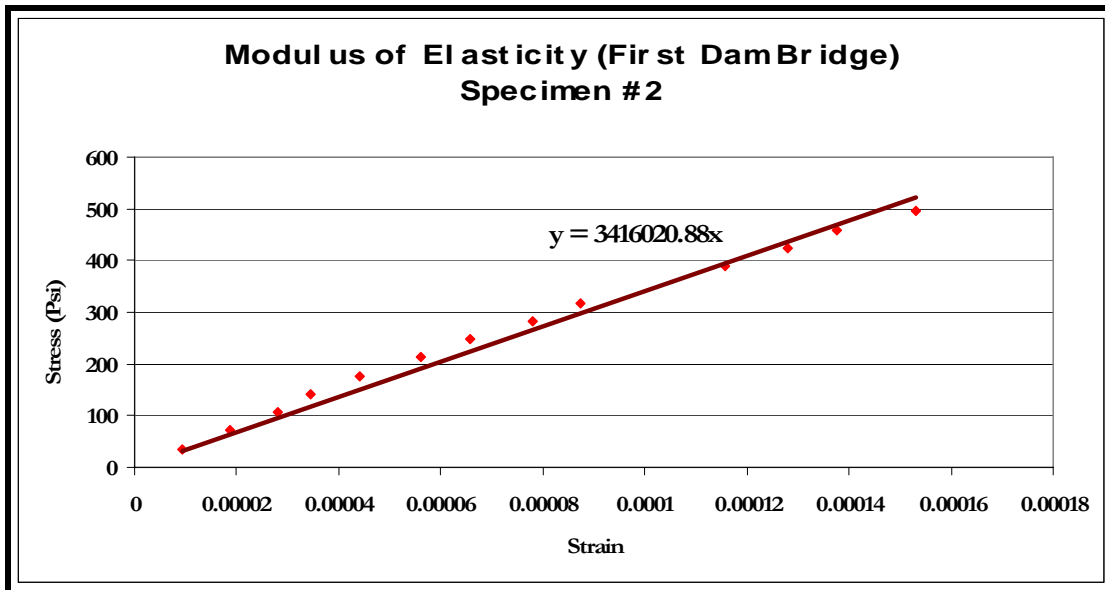


Figure B. 2 M.O.E First Dam Bridge Day 3.

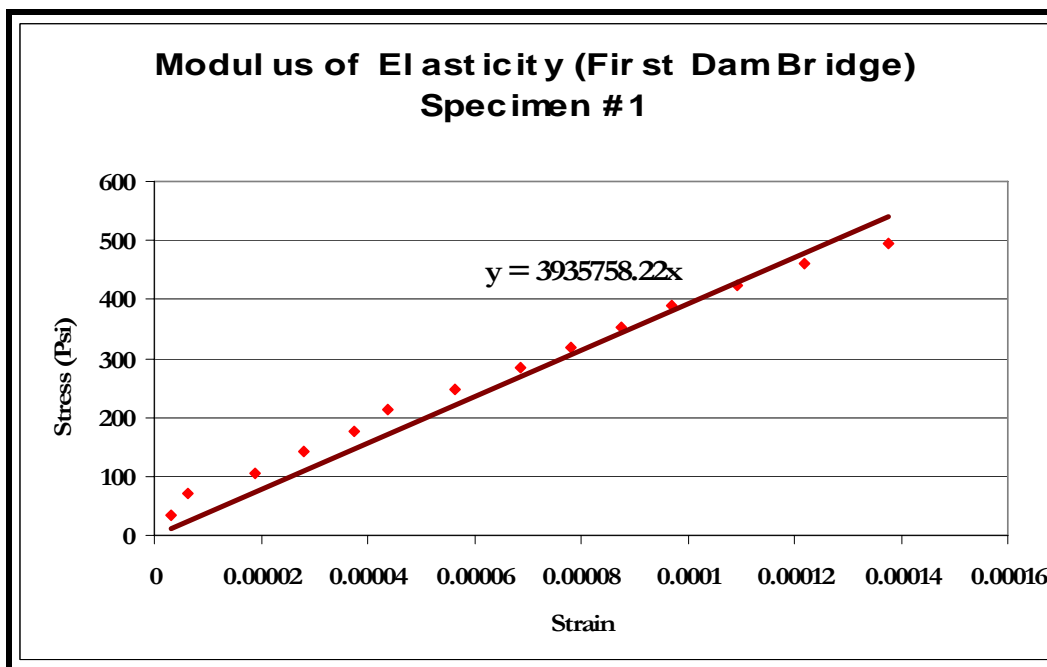


Figure B. 3 M.O.E First Dam Bridge Day 7.

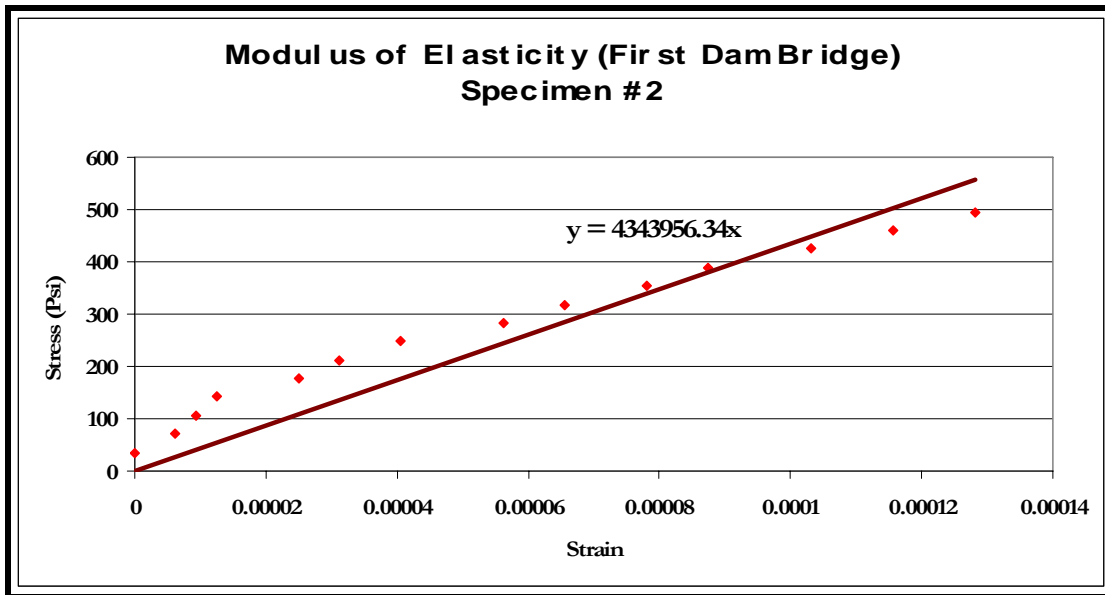


Figure B. 4 M.O.E First Dam Bridge Day 7

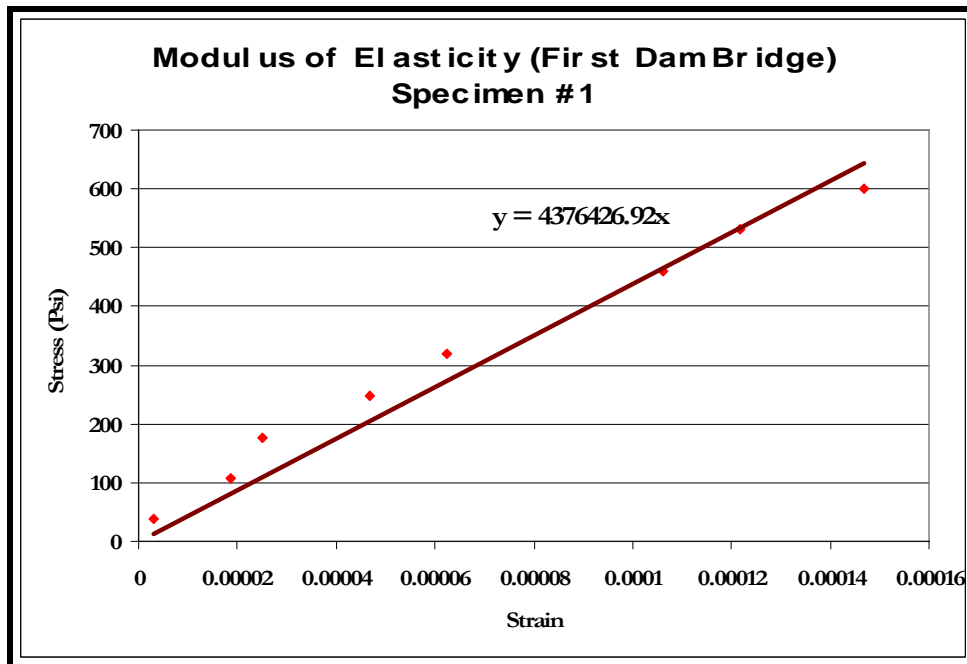


Figure B. 5 M.O.E First Dam Bridge Day 14.

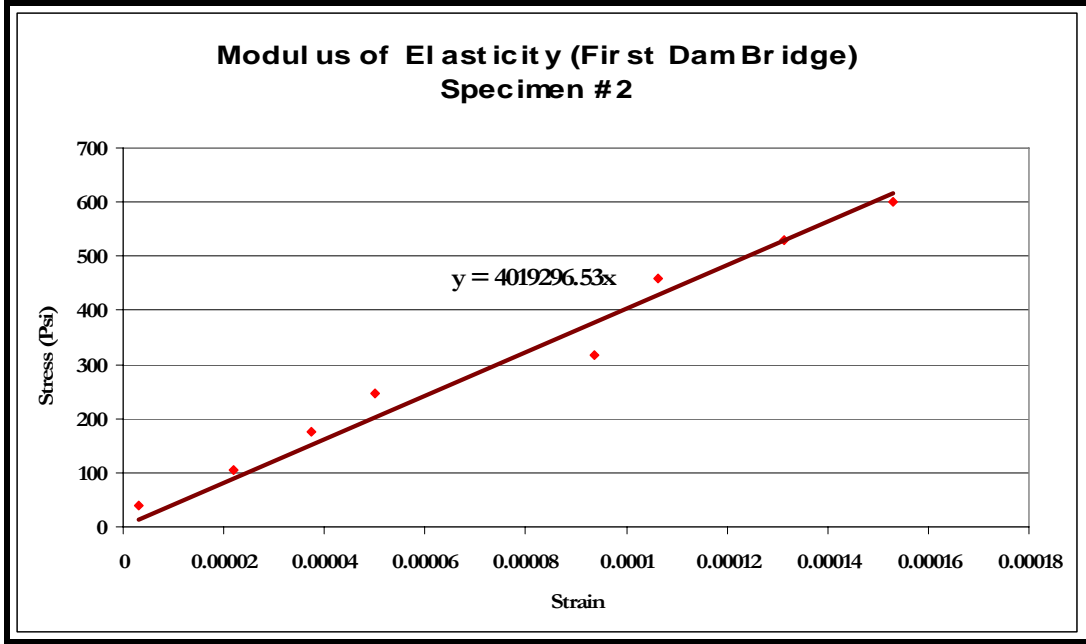


Figure B. 6 M.O.E First Dam Bridge Day 14.

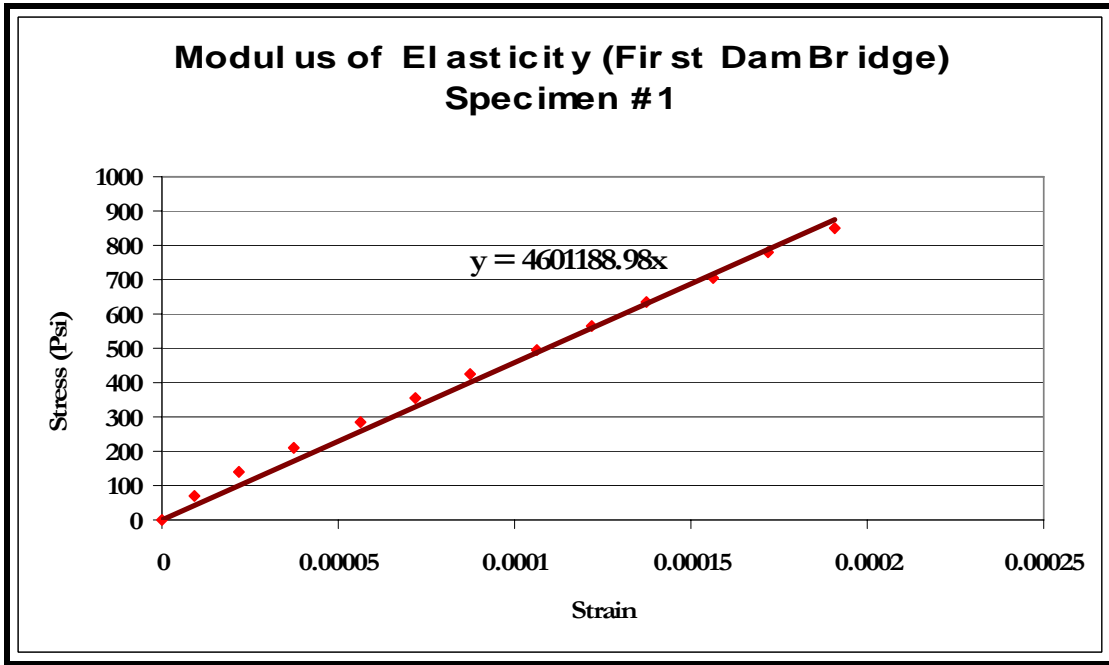


Figure B. 7 M.O.E First Dam Bridge Day 28.

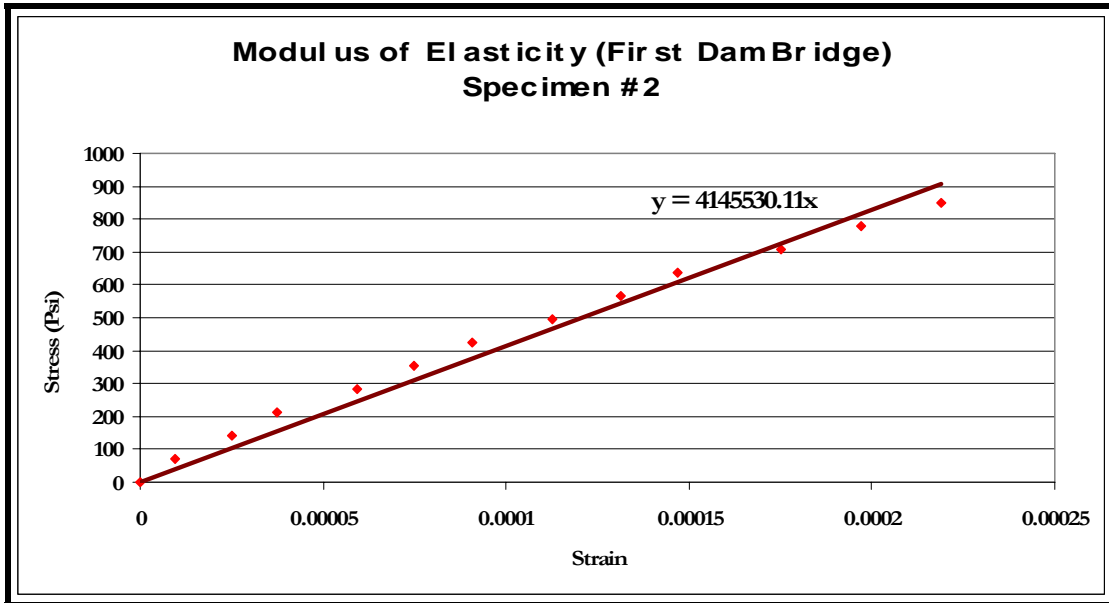


Figure B. 8 M.O.E First Dam Bridge Day 28.

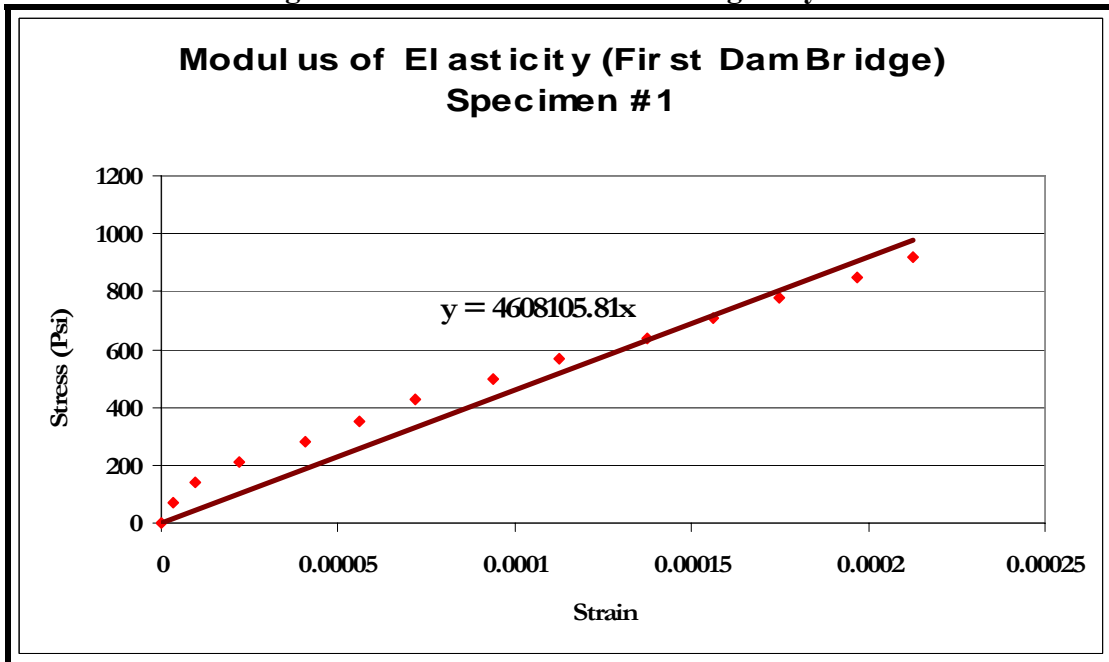


Figure B. 9 M.O.E First Dam Bridge Day 56.

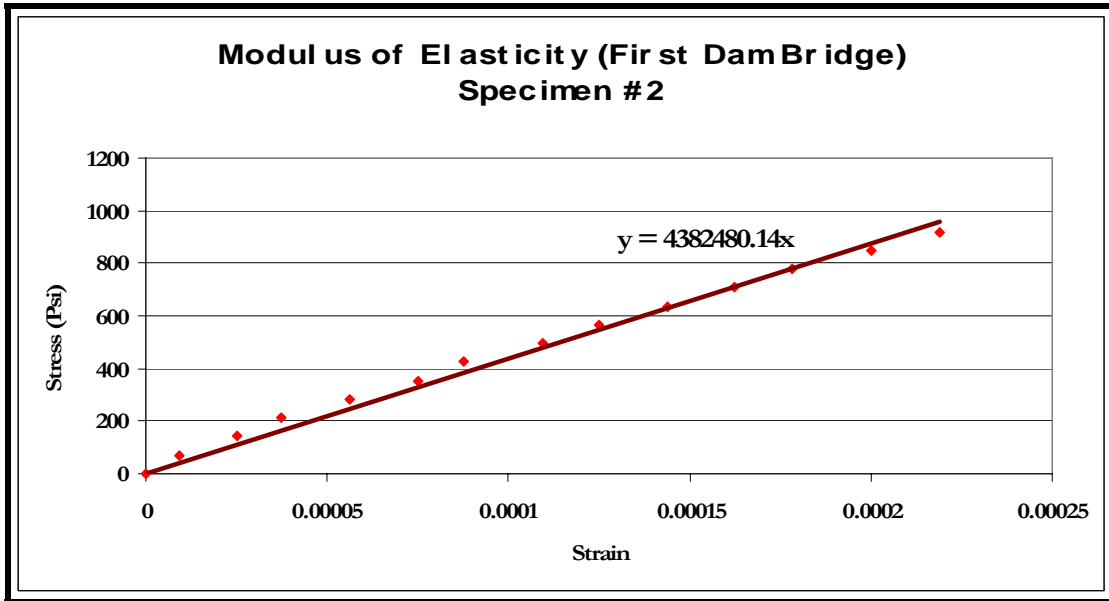


Figure B. 10 M.O.E First Dam Bridge Day 56.

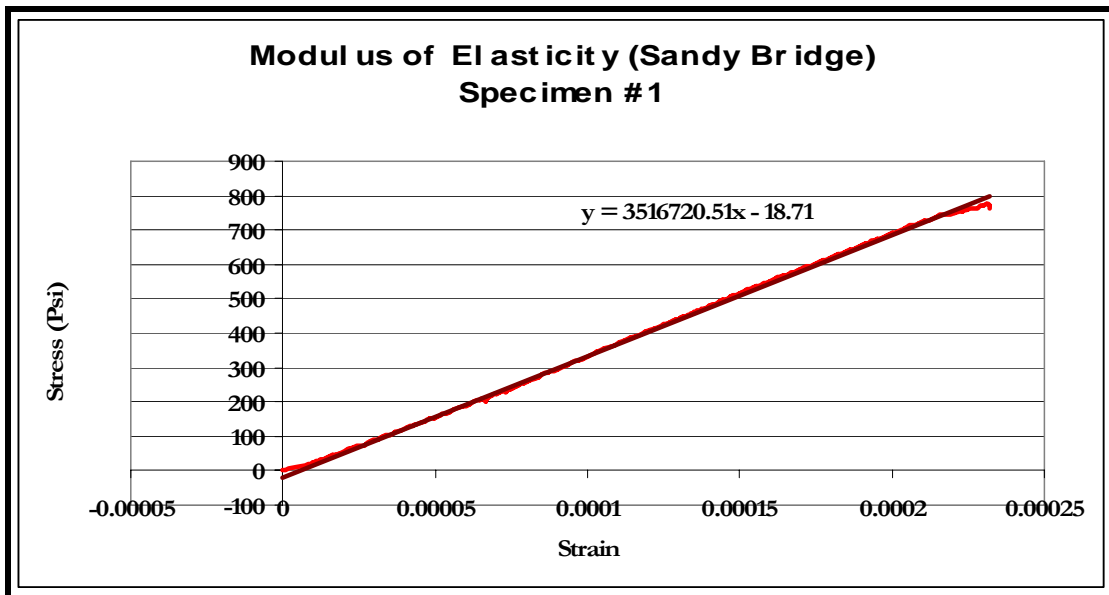


Figure B. 11 M.O.E Sandy Bridge Day 1.

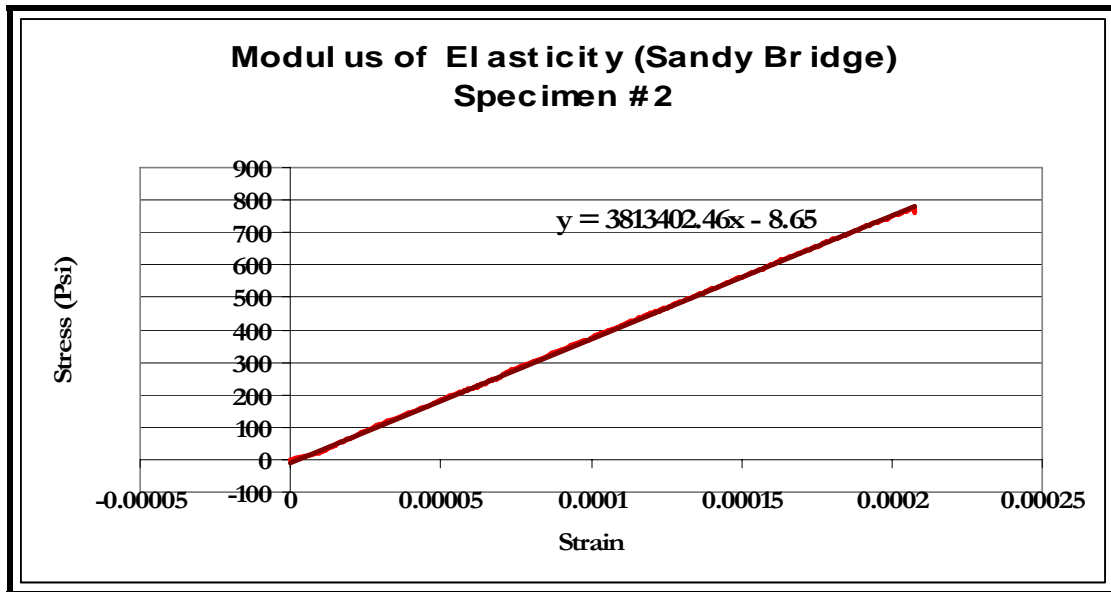


Figure B. 12 M.O.E Sandy Bridge Day 1.

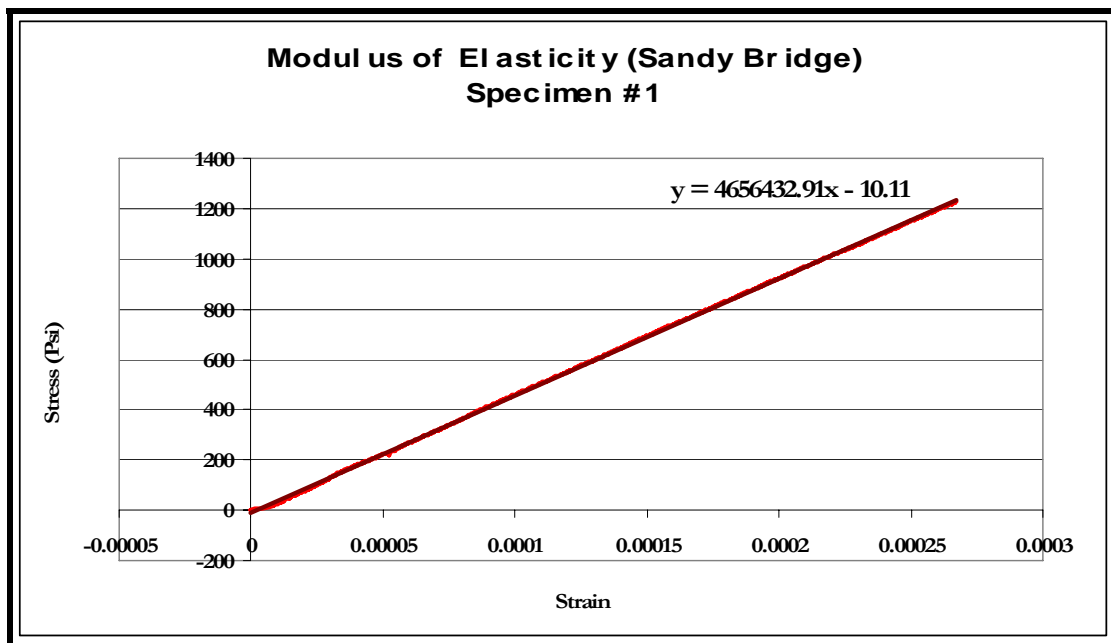


Figure B. 13 M.O.E Sandy Bridge Day 3.

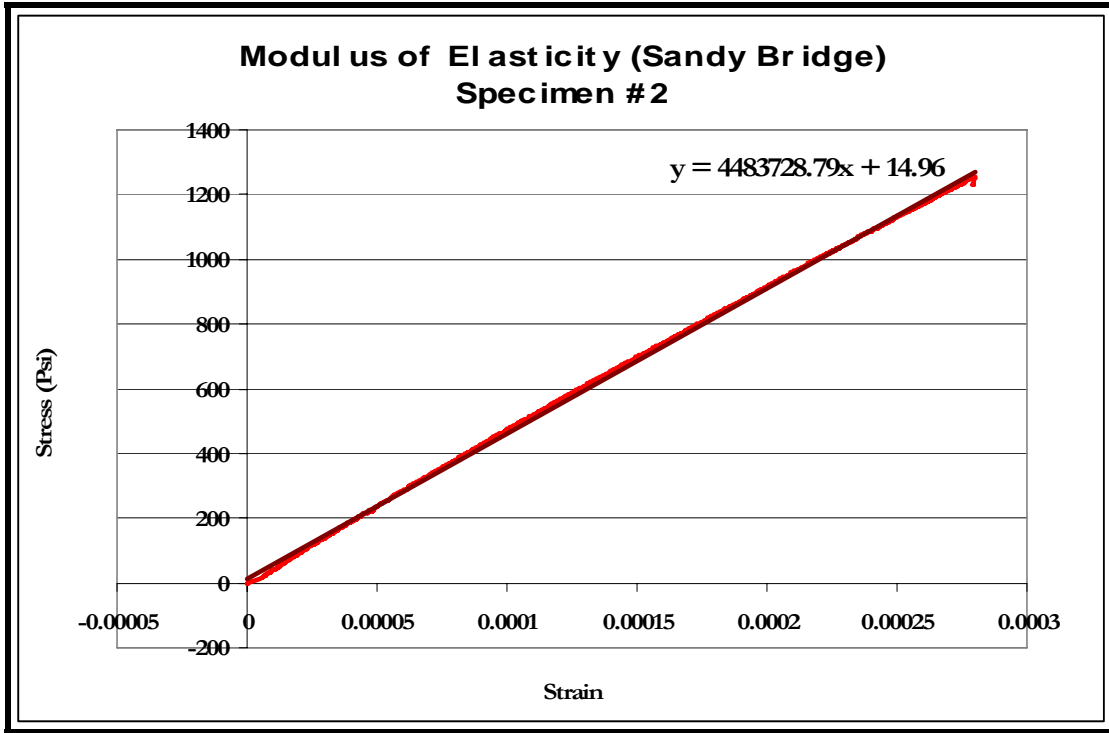


Figure B. 14 M.O.E Sandy Bridge Day 3.

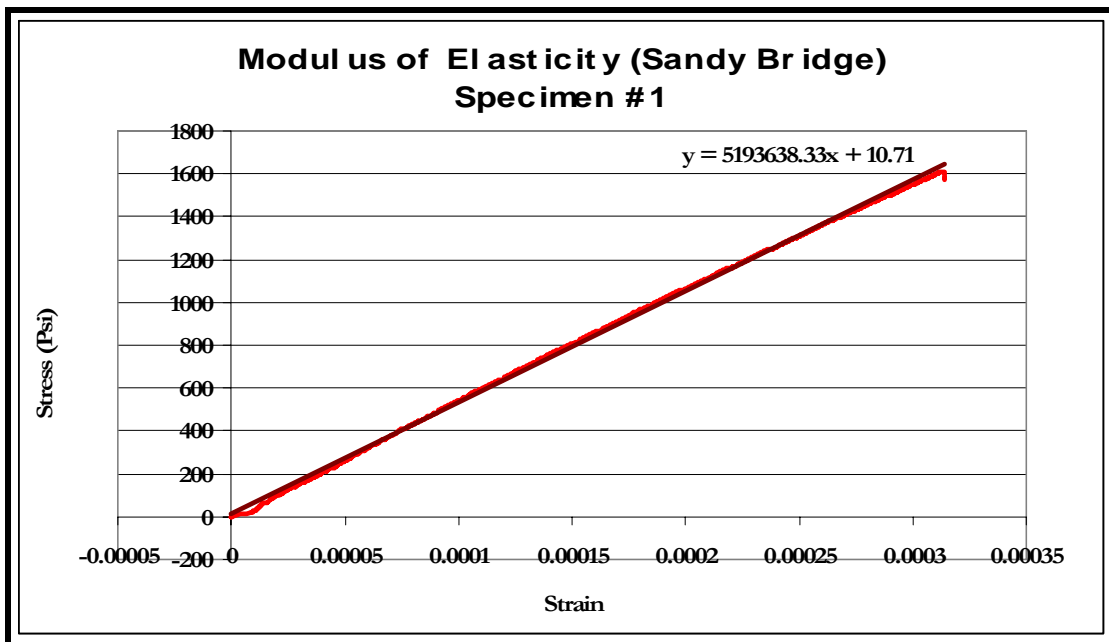


Figure B. 15 M.O.E Sandy Bridge Day 7.

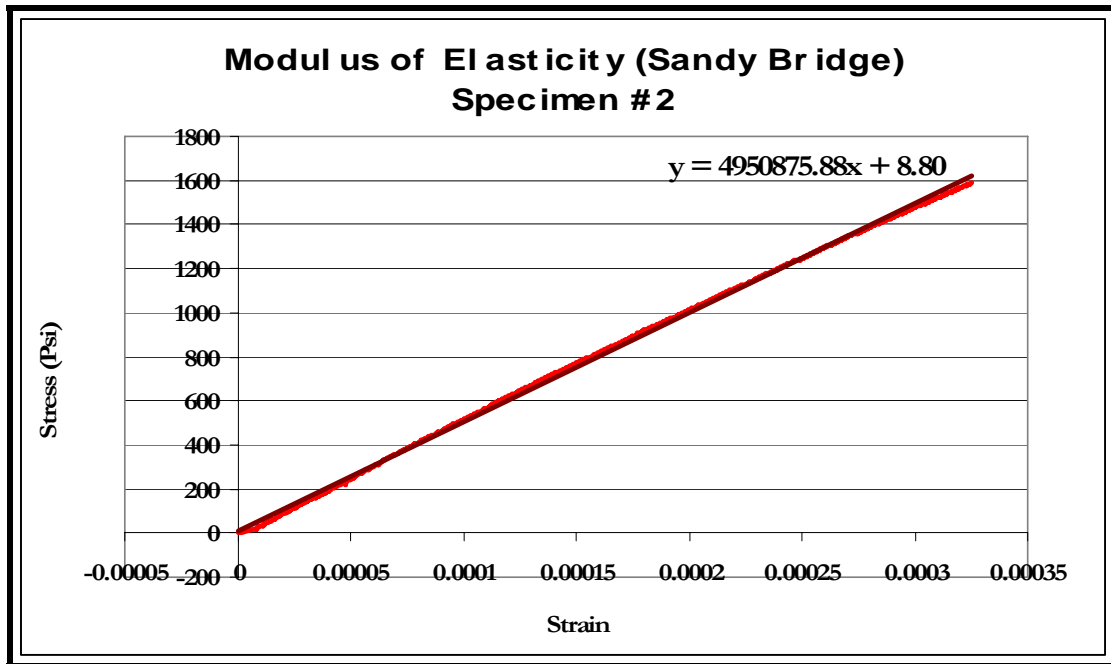


Figure B. 16 M.O.E Sandy Bridge Day 7.

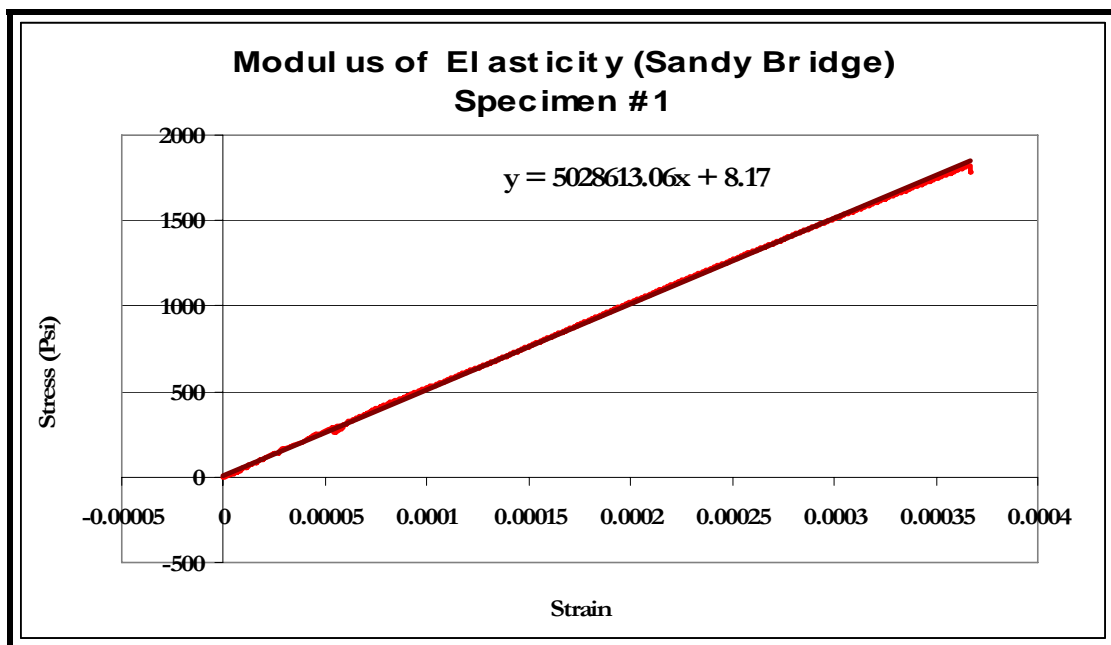


Figure B. 17 M.O.E Sandy Bridge Day 14.

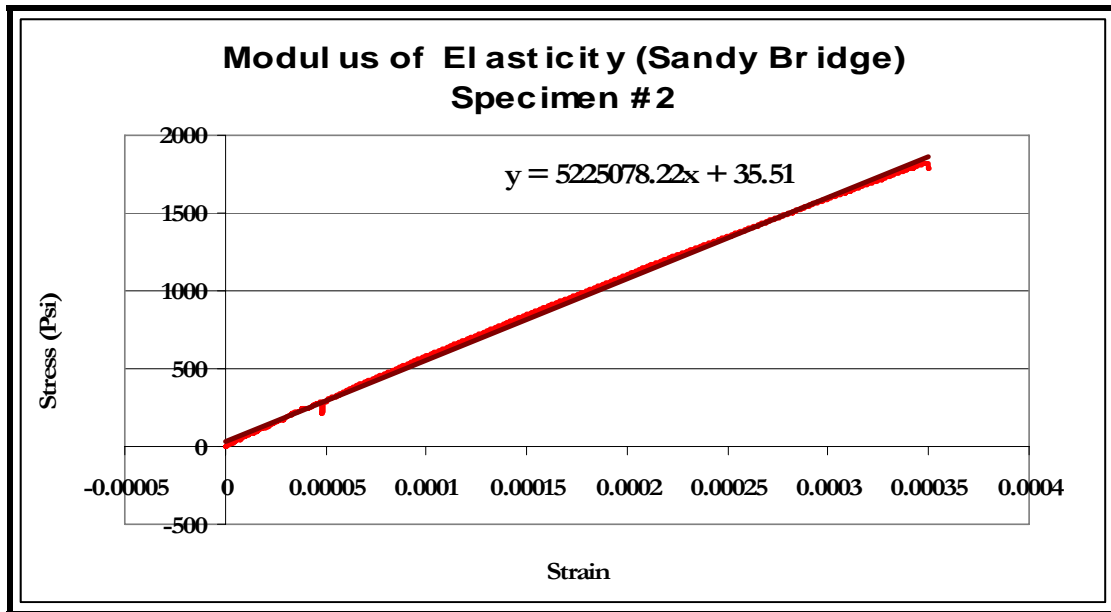


Figure B. 18 M.O.E Sandy Bridge Day 14.

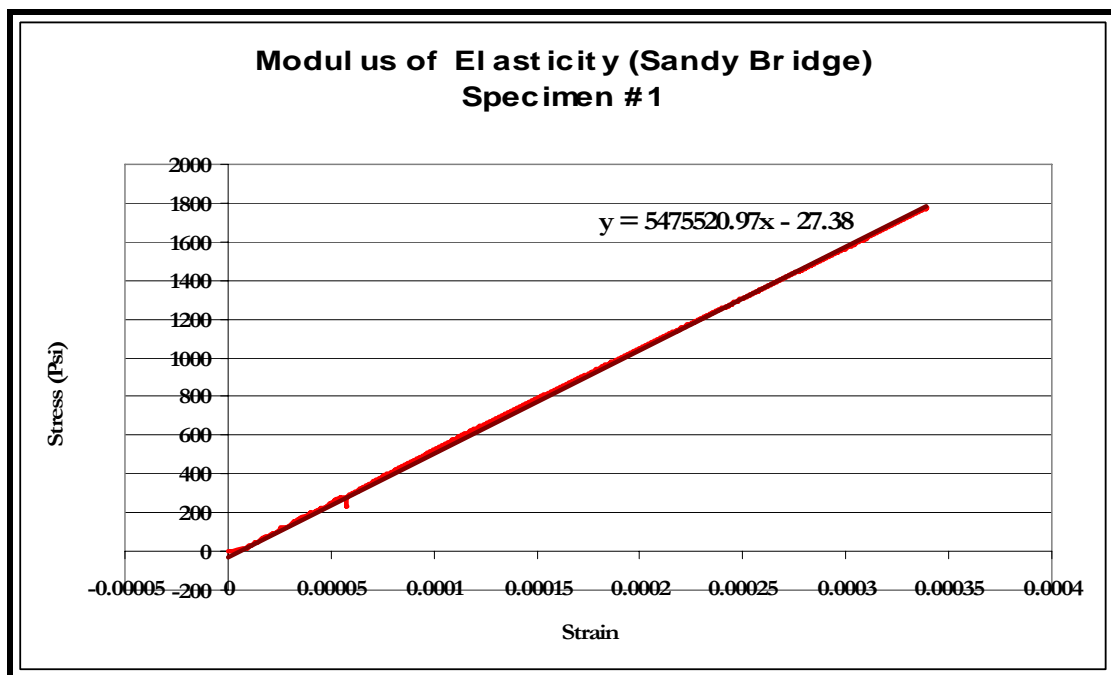


Figure B. 19 M.O.E Sandy Bridge Day 28.

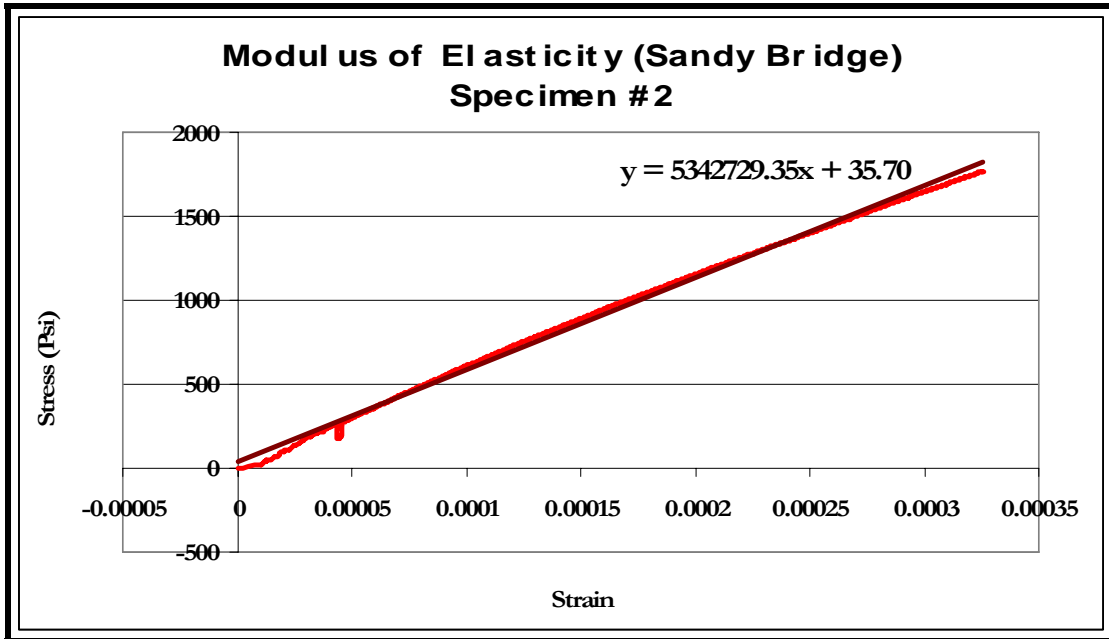


Figure B. 20 M.O.E Sandy Bridge Day 28.

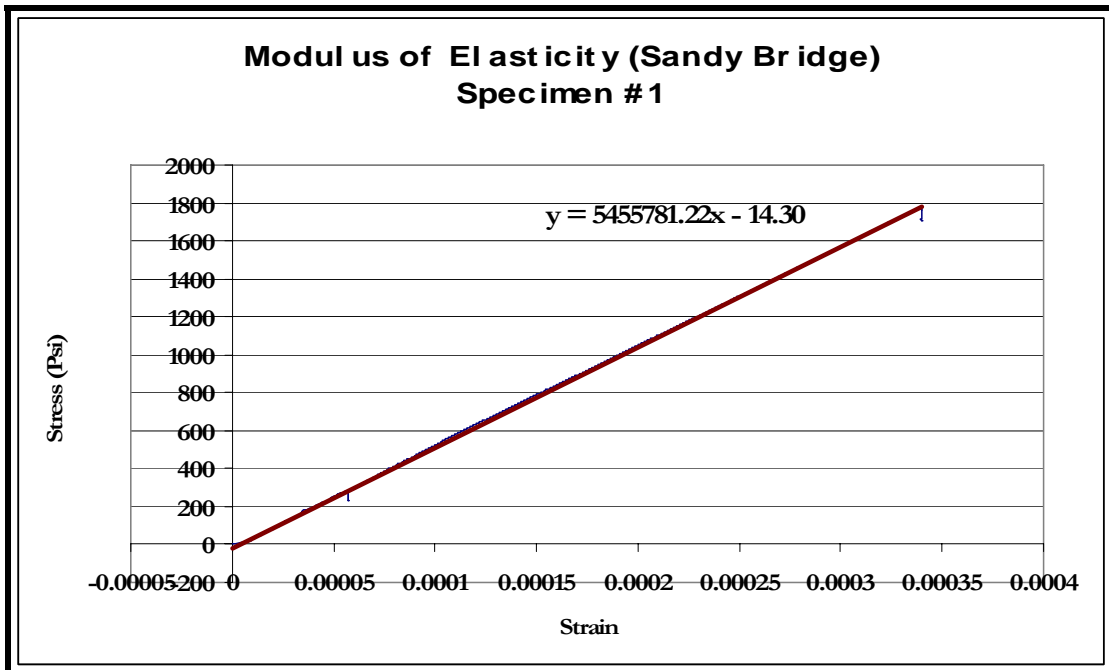


Figure B. 21 M.O.E Sandy Bridge Day 56.

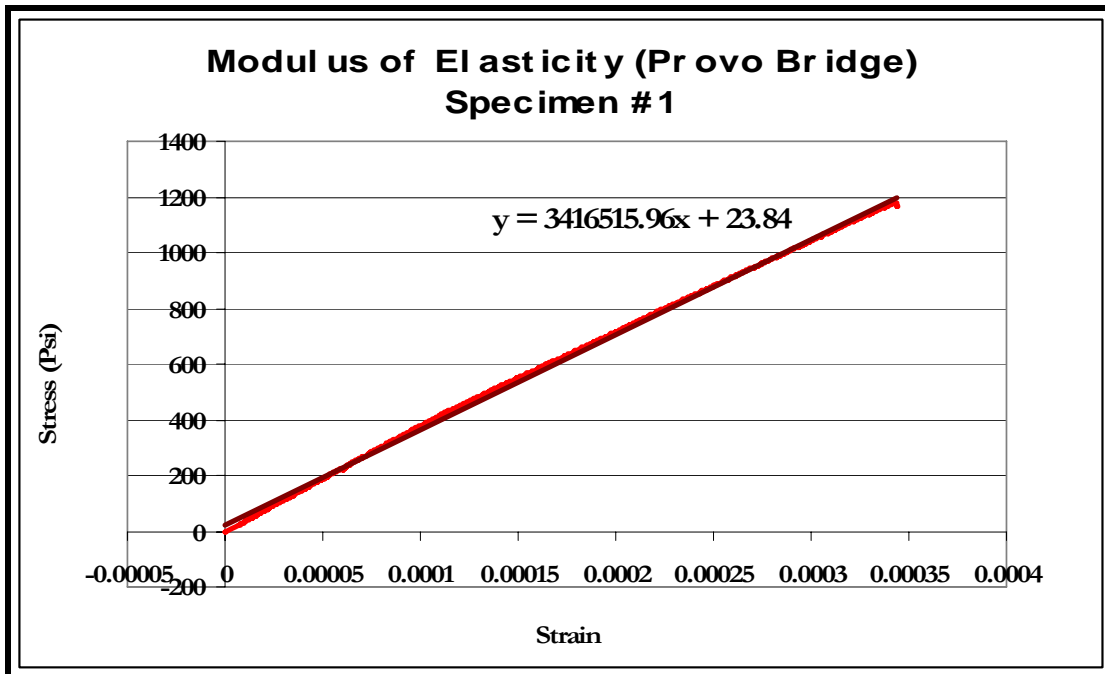


Figure B. 22 M.O.E Provo Canyon Bridge Day 1.

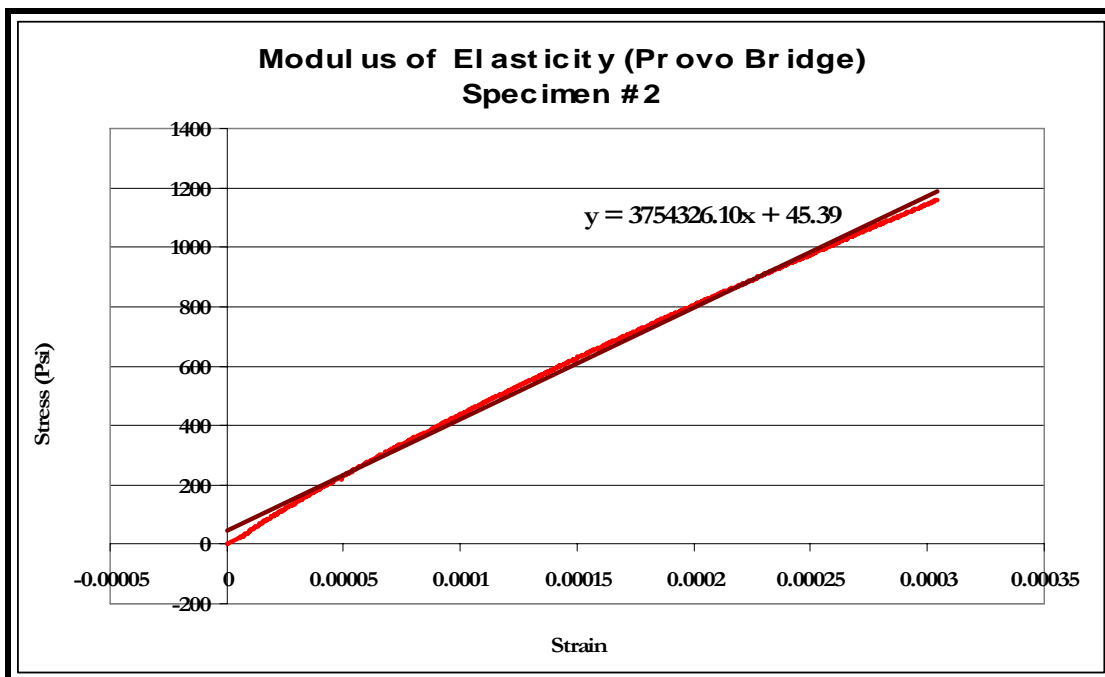


Figure B. 23 M.O.E Provo Canyon Bridge Day 1.

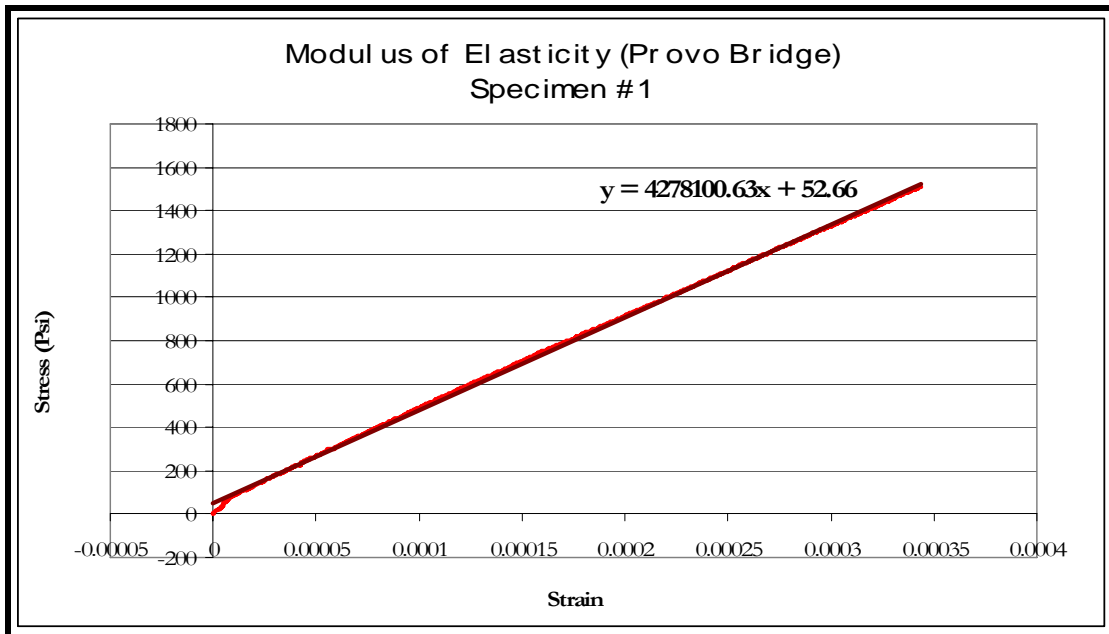


Figure B. 24 M.O.E Provo Canyon Bridge Day 3.

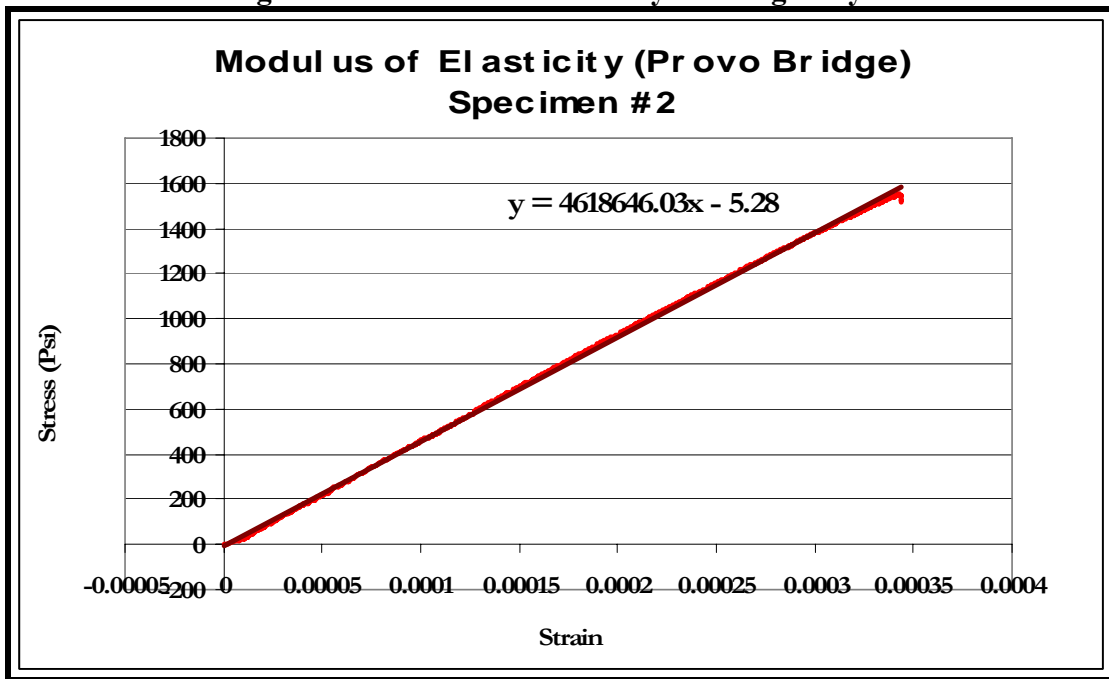


Figure B. 25 M.O.E Provo Canyon Bridge Day 3.

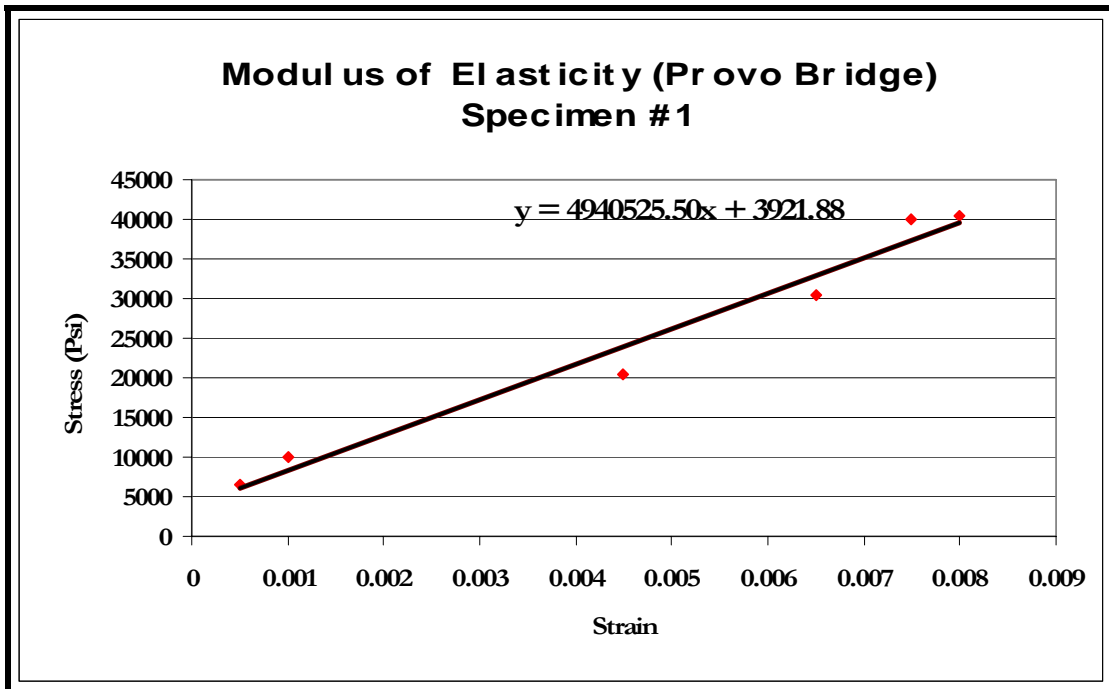


Figure B. 26 M.O.E Provo Canyon Bridge Day 7.

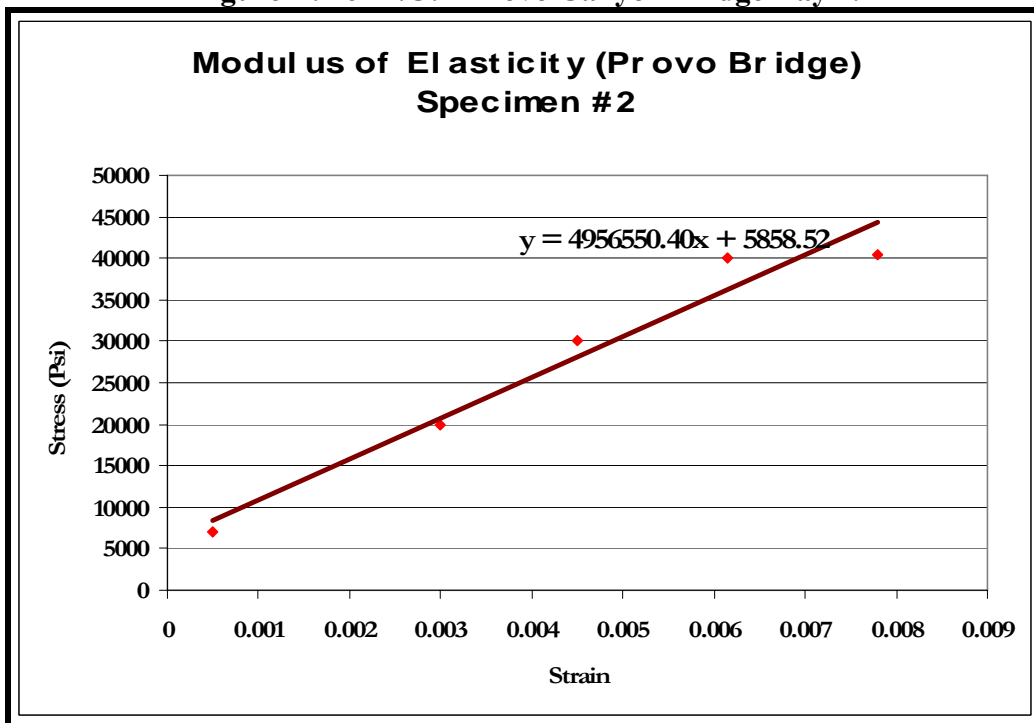


Figure B. 27 M.O.E Provo Canyon Bridge Day 7.

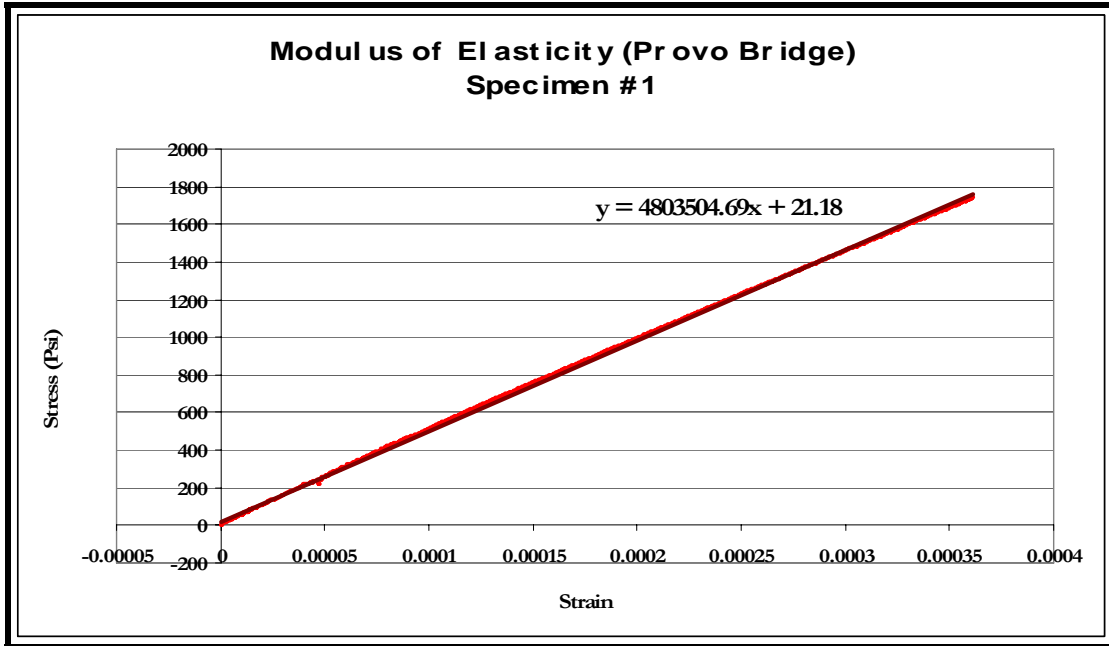


Figure B. 28 M.O.E Provo Canyon Bridge Day 14.

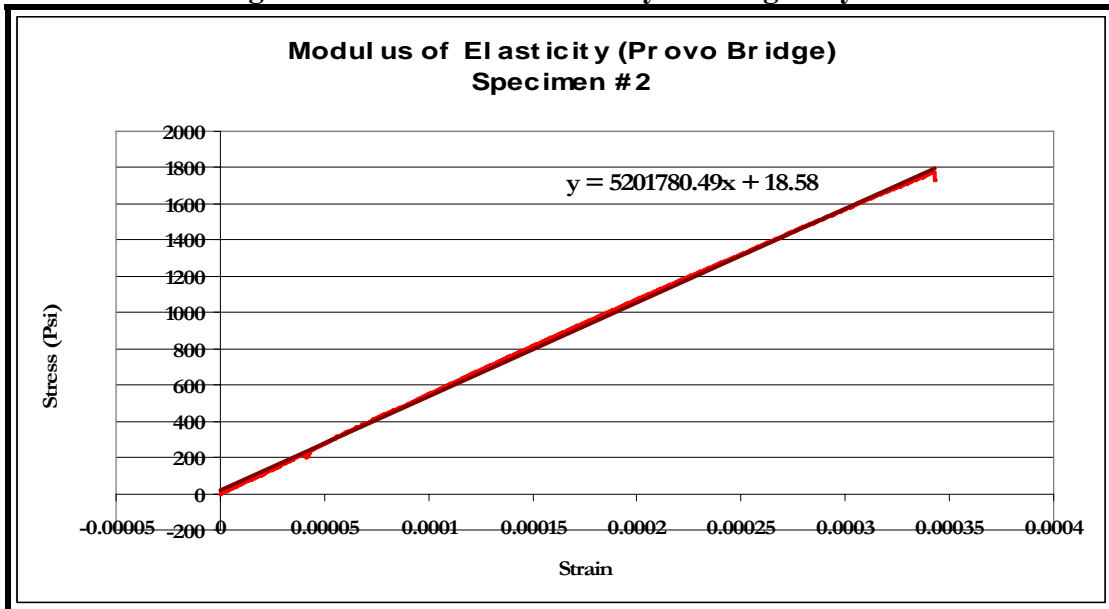


Figure B. 29 M.O.E Provo Canyon Bridge Day 14.

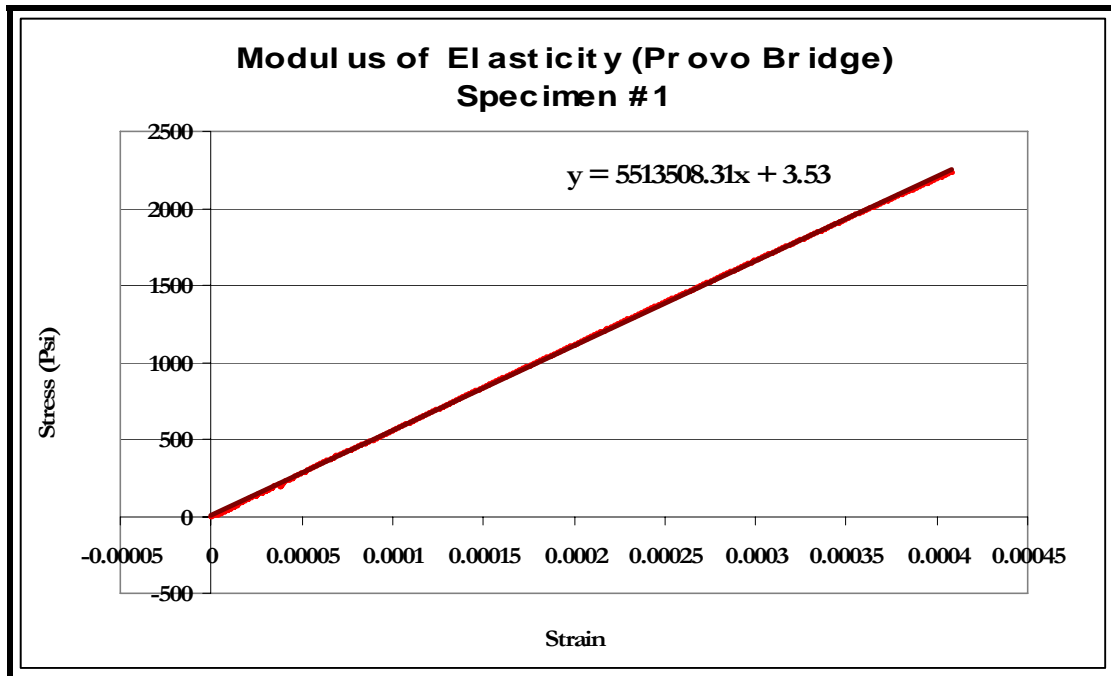


Figure B. 30 M.O.E Provo Canyon Bridge Day 28.

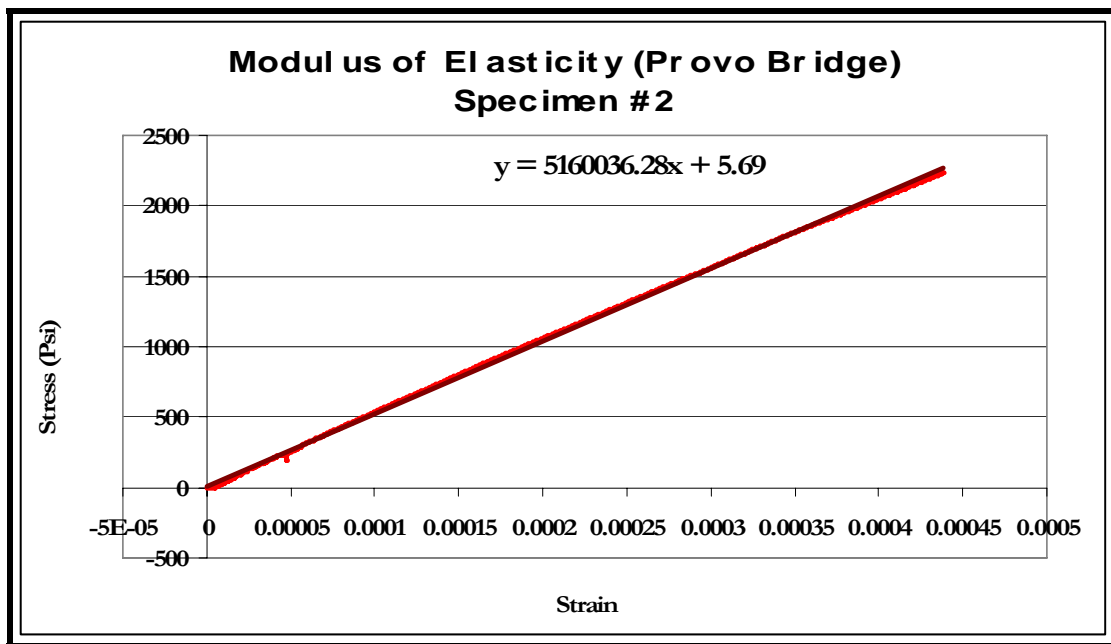


Figure B. 31 M.O.E Provo Canyon Bridge Day 28.

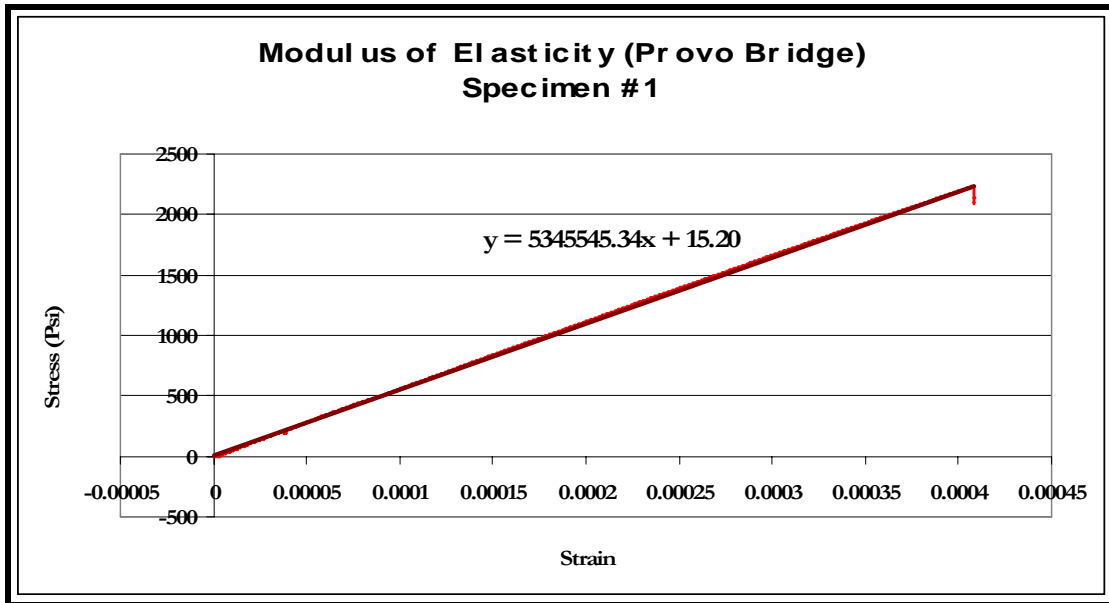


Figure B. 32 M.O.E Provo Canyon Bridge Day 56.